

VOLUMETRIC MUSCLE LOSS: CHARACTERIZATION OF ACUTE  
PATHOPHYSIOLOGY AND REGENERATIVE REHABILITATION APPROACHES

by

JENNIFER MCFALINE-FIGUEROA

(Under the Direction of Jarrod A. Call)

ABSTRACT

Volumetric muscle loss (VML) injury is a type of orthopedic trauma characterized by a severe loss of tissue, ultimately leading to long-lasting functional deficits. Patients suffering from VML often suffer from a poor range of motion, limb stiffness, and decreased strength. Despite these debilitating effects, there are no standard practices in the clinic to address soft tissue damage. This therapeutic desert means that patients are more likely to suffer decreasing mobility, which, combined with lean muscle mass loss, contributes to disability and the development of whole-body metabolic disease. The failure to create a standard clinical treatment to improve muscle function following VML partly stems from the lack of understanding of disease progression and how this affects contractility and metabolism. I designed and executed three studies with the purpose of providing an in-depth analysis of metabolic dysfunction following VML injury that could help dictate the development of future therapies by taking the needs of the recovering muscle into consideration. Study 1 evaluated the changes in metabolic flexibility and substrate preference in the early stages following VML injury. Injured muscle presented suppressed response to carbohydrate-driven metabolism compared to healthy muscle, though there was less variability in lipid-driven metabolism. Study 2 tested the efficacy of four FDA-approved medication with

history of use in skeletal muscle disease models on rescuing contractile and oxidative function following VML. From these experiments, treatment with formoterol resulted in the partial rescue of muscle function over non-treatment. Study 3 combined the pharmacological adjuvant formoterol with rehabilitation and regenerative method approaches to improve the drug's effect. The combination of formoterol with rest and voluntary exercise offered an improvement in contractile and metabolic function of VML-injured tissue. Overall, the work included herein adds to the growing library of knowledge regarding VML injury pathophysiology and offers therapeutic targets and candidates for further development for in-clinic use.

**INDEX WORDS:** skeletal muscle, volumetric muscle loss, pathophysiology, mitochondrial physiology, functional recovery, formoterol, metabolic inflexibility

VOLUMETRIC MUSCLE LOSS: CHARACTERIZATION OF ACUTE  
PATHOPHYSIOLOGY AND REGENERATIVE REHABILITATION APPROACHES

by

JENNIFER MCFALINE-FIGUEROA

BS, Universidad de Puerto Rico – Mayaguez, 2013

MS, Georgia State University, 2018

A Dissertation Submitted to the Graduate Faculty of The University of Georgia in Partial  
Fulfillment of the Requirements for the Degree

DOCTOR OF PHILOSOPHY

ATHENS, GEORGIA

2022

© 2022

Jennifer McFaline-Figueroa

All Rights Reserved

VOLUMETRIC MUSCLE LOSS: CHARACTERIZATION OF ACUTE  
PATHOPHYSIOLOGY AND REGENERATIVE REHABILITATION APPROACHES

by

JENNIFER MCFALINE-FIGUEROA

Major Professor:	Jarrod A. Call
Committee:	Luke Mortensen
	Johnna Temenoff
	Hang Yin

Electronic Version Approved:

Ron Walcott  
Vice Provost for Graduate Education and Dean of the Graduate School  
The University of Georgia  
December 2022

## DEDICATION

To whatever it is that keeps me going, be it curiosity, caffeine, or the shadows that pass out of the corner of my eye. Whatever it is that pokes and prods my wanderlust for knowledge and builds stories in my mind—I owe you a debt of gratitude. I don't know why you exist or why I've taken a shine to nurturing your insistent calls for attention, but you've built me a career and I am forever grateful. Let's see where you intend to guide me next.

## ACKNOWLEDGEMENTS

The list of individuals who have impacted my career path is interminable. I can only offer a list of the people who made their marks so indelible that I couldn't dare forget them if I tried. My most sincere thanks to:

–Dr. Jarrod Call for being an excellent advisor, mentor, role model, and friend. You are who every Ph.D. advisor should aspire to be—brilliant scientist and all-around decent human being.

–Dr. Johnna Temenoff, for taking a skilled chemist, fresh out of her undergrad, and teaching her how to be an inquisitive, thorough researcher. More importantly, for being an excellent mentor and still having my back years after I've left your lab.

–Dr. Anna Nichenko, Jun-Won Heo, and Albi Schifino for being great lab mates and burning the midnight oil with me on harvest weeks. I couldn't have done this without you all.

Tate Hunda, Lizzie Winders, and Patricia Ni for being the best undergrads anyone could have ever wanted.

–My collaborators Dr. Sarah Greising, Dr. Christiana Raymond-Pope, Dr. Emily Noble, Jessica Hoffman, Magen Lord, and Denise Fahey for their support in my projects and for letting me play around with science outside of my field for a little while.

–My entire family (grandparents, in particular) for having no idea what I study but having no doubt that I would do a great job.

–The three idiots I call best friends, Stephanie, Rebecca, and Jorge—we met 27 years ago, and I've been trying to get rid of you every day since. You annoy the living hell out of me. I don't know what I'd do without you.

## TABLE OF CONTENTS

	Page
ACKNOWLEDGEMENTS .....	v
LIST OF TABLES .....	ix
LIST OF FIGURES .....	x
CHAPTER	
1 INTRODUCTION AND LITERATURE REVIEW .....	1
Volumetric Muscle Loss .....	2
Current Standards of Care .....	3
Pathophysiology .....	4
Regenerative Rehabilitation .....	11
Specific Aims and Hypothesis .....	13
References .....	15
2 CHARACTERIZATION OF EARLY METABOLIC PATHOPHYSIOLOGY	
AFTER VOLUMETRIC MUSCLE LOSS .....	18
Abstract .....	19
Introduction .....	20
Materials and Methods .....	21
Results .....	26
Discussion .....	31
References .....	35

3	PHARMACEUTICAL AGENTS FOR CONTRACTILE-METABOLIC DYSFUNCTION AFTER VOLUMETRIC MUSCLE LOSS .....	38
	Abstract.....	39
	Introduction.....	40
	Materials and Methods.....	44
	Results.....	50
	Discussion.....	57
	References.....	63
4	FORMOTEROL TREATMENT IMPROVES CONTRACTILE-METABOLIC FUNCTION AFTER VOLUMETRIC MUSCLE LOSS INDEPENDENT OF REHABILITATION .....	71
	Abstract.....	72
	Introduction.....	3
	Materials and Methods.....	75
	Results.....	82
	Discussion.....	88
	Supplemental materials.....	91
	References.....	93
5	DISCUSSION AND CONCLUSIONS .....	95
	Metabolic inflexibility in VML starts early after injury .....	95
	Calcium overload plays a role in VML pathology.....	96
	Formoterol improves contractile-metabolic function after VML injury.....	97
	Future Directions .....	97

Conclusion .....	98
COMPLETE REFERENCE LIST .....	100

## LIST OF TABLES

	Page
Table 2.1: Mouse body mass and gastrocnemius muscle mass .....	26
Table 2.2: Mitochondrial enzyme activity .....	29
Table 3.1: Mouse body mass and gastrocnemius muscle mass .....	50
Table 3.2: Contractile properties.....	52
Table 3.3: Mitochondrial enzyme activity .....	56
Table 3.4: Relative gene expression .....	57
Table 4.1: Mouse body mass and gastrocnemius muscle mass .....	83
Table 4.2: Contractile properties.....	84
Table 4.3: Mitochondrial enzyme activity .....	86

## LIST OF FIGURES

	Page
Figure 1.1: Pathophysiology of volumetric muscle loss.....	7
Figure 2.1: VML-injured tissue has suppressed carbohydrate but not lipid utilization.....	27
Figure 2.2: Total Ca <sup>2+</sup> concentration in VML muscle .....	30
Figure 2.3: <i>In vitro</i> modeling of Ca <sup>2+</sup> involvement in VML injury.....	31
Figure 3.1: VML-injured tissue has a contractile and metabolic deficit compared to uninjured control limbs .....	51
Figure 3.2: Effect of pharmacological adjuvant administration on the contractile function of VML-injured tissue.....	53
Figure 3.3: Drug treatments improved oxidative capacity following VML injury.....	54
Figure 4.1: Effect of regenerative rehabilitation strategies on contractile function of VML-injured limbs .....	84
Figure 4.2: Effect of regenerative rehabilitation strategies on mitochondrial metabolism.....	85
Figure 4.3: Histological analysis of best-faring regenerative rehabilitation treatment.....	87
Figure S4.1: Sizing distribution for gel particulate.....	91
Figure S4.2: Cumulative release of FOR from PEG-DA-BSA gels over 30 days .....	91
Figure S4.3: Injection protocol for biomaterial .....	92
Figure S4.4: Passive stiffness of limbs injected with biomaterial .....	92

## CHAPTER 1

### INTRODUCTION AND LITERATURE REVIEW

Skeletal muscle plays an essential role in movement and locomotion, postural control, respiratory activity, and heat production. Due to its mass, an estimated 40% of the body's total weight, it is also an important glucose sink and one of the major regulators of energy homeostasis (Gamboa et al., 2011). This tissue has a high capacity for regeneration, repair, and remodeling of injured or dysfunctional muscle fibers, which contribute to the maintenance of muscle mass, function, and homeostasis. These processes demand a significant use of energy, in the form of ATP, which is produced by the vast network of highly organized mitochondria within the muscle fibers. The mitochondrial network is tightly regulated by dynamic pathways of biogenesis, fusion, fission, and mitophagy to maintain homeostasis (Hood et al., 2019). Of these pathways, peroxisome proliferator-activated receptor gamma (PPAR $\gamma$ ) and its coactivator PPAR $\gamma$ -1 $\alpha$  (PGC-1 $\alpha$ ) drive expression of several genes responsible for ATP synthesis and mitochondrial biogenesis in the muscle (Mukund & Subramaniam, 2020).

Injury (eccentric-contraction induced, burn, freeze injury, volumetric muscle loss), disease (muscular dystrophies) and age can disrupt mitochondrial network, upset muscular homeostasis, and contribute to muscle mass loss (Call et al., 2013; Warren et al., 2007). This loss of muscle mass, in turn, can lead to adverse effects such as development of metabolic diseases, loss of strength and mobility, and an overall decrease in quality of life. The accumulation of comorbidities borne from muscle atrophy, loss, or wasting eventually becomes a burden on public health. Thus,

there is a critical need to develop treatment strategies for pathologies where normal muscle function is threatened.

### **Volumetric muscle loss<sup>1</sup>**

The clinically accepted definition for volumetric muscle loss (VML) injury is “the traumatic or surgical loss of skeletal muscle with resultant functional impairment”(Corona et al., 2016; Cross et al., 2011; Owens et al., 2007; Owens et al., 2008). Traumatic muscle injuries like VML often result from either blunt force trauma in which an object strikes the body, from penetrating traumas in which an object pierces the body creating an open wound, or controlled, surgical trauma in which an object is removed from the body. Although traumatic injuries often cross tissue boundaries such as bone, nerve, vascular, tendinous, ligamentous, and/or cartilaginous, this chapter will focus on skeletal muscle pathology and regenerative rehabilitation strategies to improve skeletal muscle function. Skeletal muscle makes up ~40% of the body’s mass and contributes to locomotion, thermoregulation, and whole-body metabolism. Any loss of skeletal muscle function can negatively affect mobility and increase an individual’s risk of all-cause morbidity and mortality.

VML injury can result secondary to any of the 150,000 open fractures or 30,000 gunshot wounds (trauma), 36,000 chainsaw accidents (industrial/farm), and 13,000 soft-tissue sarcomas (cancer) that occur annually in the United States. Approximately 77% of all military casualties are

---

<sup>1</sup>Sorensen, J.R., McFaline-Figueroa, J., Call, J.A. (2022). *Pathophysiology of Volumetric Muscle Loss and Targets for Regenerative Rehabilitation*. In: Greising, S.M., Call, J.A. (eds) *Regenerative Rehabilitation. Physiology in Health and Disease*. Springer, Cham. Republished here with permission of the publisher.

musculoskeletal injuries, many that have a component of debilitating VML injuries (Cross et al., 2011; Owens et al., 2007; Owens et al., 2008). Data from the United States trauma centers indicate that two-thirds of traumatic injuries occur to extremities with 32% and 40% to the upper and lower extremities, respectively. Collectively, the United States economic burden related to trauma and injury is \$400 billion yearly (Seifert, 2007).

This chapter will *i)* touch upon current standards of care for VML injuries, *ii)* describe the pathophysiology of VML injury, and *iii)* discuss rehabilitation and regenerative medicine approaches to improve VML, to highlight the need for regenerative rehabilitation studies with functionally relevant outcome measurements to advance evidence-based approaches for VML.

#### *Current standards of care*

The current practices for definitive care following VML injury and orthopedic injuries involving concomitant VML injury can be generalized into three phases: *i)* immediate field care, *ii)* acute surgical care, and *iii)* short-term rehabilitative care. Standardization within these phases is complicated by the site of the injury and poly-traumatic nature of the injury that can include damage to the bone, muscle, skin, nerve, and/or vascular network. Prioritization of care among the phases starts with patient survival, minimizing infection risk, limb salvage, and finally tissue rehabilitation. Immediate field care often takes place at the site of injury (e.g., field of play, battlefield) and involves fixation of the limb for emergency transport, field dressing to minimize infection risk, and possible tourniquets to reduce blood loss from the injury. These practices prioritize patient survival. Acute surgical care involves surgical procedures and post-operative procedures conducted at a trauma center. Standard practices include blood transfusion, bone union, muscle flaps, nerve allografts, and limb amputation if required for survival (e.g., infection). Evidence of rehabilitative approaches applied in the intensive care unit immediately following

acute surgical care is non-existent, although could involve neuromuscular stimulation and/or mobilization. Short-term rehabilitative care often prioritizes task rehabilitation, e.g., regaining mobility or ability to navigate stairs, as opposed to functional rehabilitation (i.e., improving strength) due to a lack of evidence showing robust improvements in muscle function with current strategies. To address this challenge, there is an urgent need to identify new or existing strategies in combination that can bolster functional recovery. One idea is to explore regenerative rehabilitation approaches.

Regenerative rehabilitation was broadly defined in Chapter 1, so here a more specific definition will be advanced for VML injury. *Regenerative rehabilitation for VML injury is a focused effort to improve skeletal muscle quality and overall muscle function, advance mobility, and quality of life for the patient by integrating regenerative technologies with rehabilitation clinical practices.* For the VML-injured patient, any functional gains beyond those achieved with rehabilitation is expected to have a considerable impact on quality of life and as such regenerative rehabilitation may be an ideal tool to accomplish this goal.

### *Pathophysiology*

In this section we highlight primary pathologies associated with VML injuries, and then summarize outcome measurement commonly used to evaluate the effectiveness of an intervention. VML injuries are idiosyncratic, and any one injury may not involve all of the pathologies discussed below. Additionally, investigators should consider the pros and cons of each technique in relation to their study design questions and anticipated outcomes. Throughout this section we will reference **Figure 1.1** that provides examples of common pathologies after VML injuries at four different regions of the VML-injured muscle. These four regions include: (1) the Defect, representing the area in which a volume of muscle was removed; (2) the Border, representing the tissue layer

between the Defect and remaining muscle; (3) the Near Defect, representing the remaining muscle in close proximity to the Defect; and (4) the Distant to Defect, representing the remaining muscle far enough from the Defect area that it was not injured by the initial VML injury. The pathologies taking place at these four muscle regions can all contribute to the long-lasting functional deficits observed after VML injury and the lack of full muscle restoration and are in contrast to the full muscle recovery capable after more common contraction-induced muscle injuries.

#### *-Loss of muscle function*

Skeletal muscle has many roles, perhaps the most important is to facilitate movement. Thus, the drastic loss of muscle function following a VML injury is considered the most consequential. Clinically, individuals that have some form of VML injury display a wide spectrum of functional deficits including strength loss, limited range of motion, and muscle stiffness. The gold standard for quantifying the extent of an injury or the efficacy of a regenerative or rehabilitative intervention is by testing the functional capacity of the muscle. Follow up assessments also show conflicting results related to the ability of the muscle to restore function several months post-injury. In some VML injuries, the limb may be completely void of any initial functional strength or intervention-induced strength gains, while other VML injuries, though limited, can show promise for a restoration of function over time. Overall, the loss of function is typically disproportionately greater than the size of muscle removed(Corona et al., 2016). The most unfortunate finding from clinical work is that muscle function may actually decline chronically, despite the use of rehabilitative and/or regenerative interventions(Mase et al., 2010; Tanaka et al., 2017).

### *-Loss of metabolic function*

The effects of VML injuries are not constrained to mobility deficits. Loss of functional muscle fibers is analogous to a stark reduction of metabolically active cells that, for example, contribute to basal metabolic rate and circulating glucose levels. At a cellular level, skeletal muscle's metabolic efficiency is regulated by the mitochondria. Within this organelle, several factors contribute to this metabolism, including enzyme kinetics of the components of the electron transport chain, oxygen consumption, and mitochondrial membrane polarization. Oxidative capacity has been shown to decrease by roughly 25% in VML-injured muscle when compared to uninjured muscle (Greising et al., 2018; Southern et al., 2019). This could have potential whole-body implications as VML-injured mice are reported to have a lower overall metabolic rate despite similar levels of physical activity (Dalske et al., 2021). Such whole-body changes can lead to metabolic deficits associated with an increased likelihood of developing diabetes, cardiovascular disease, and metabolic syndrome. The muscle-specific and whole-body characterization of metabolic changes after VML is relatively new and there is a large knowledge gap relating to clinical manifestations and cellular mechanisms.

### *-Loss of regenerative capacity*

Successful restoration of injured muscle tissue requires the repair and/or regeneration of muscle fibers, which are highly organized in bundles with specific structural and contractile properties. Typically, skeletal muscle has a robust endogenous regenerative response following acute injuries (exercise-induced, strains, contusions), which follow a canonical regenerative order that ultimately restores tissue structure and function to, or even above, pre-injury levels (**Figure 1.1**). This regenerative process occurs over the course of several days to weeks in mammals and follows a time dependent, energy demanding sequence characterized by robust infiltration and

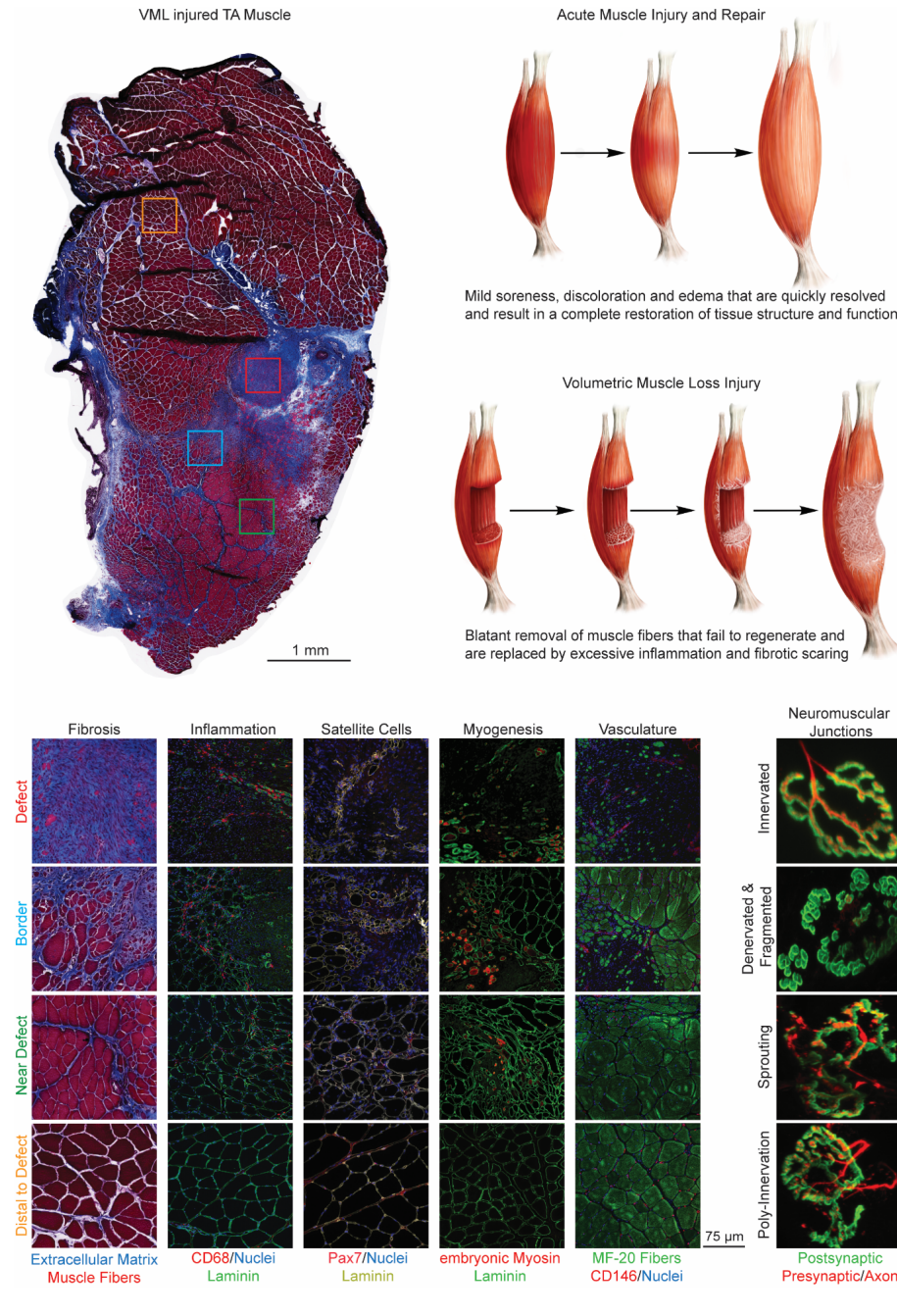


**Figure 1.1** Pathophysiology of volumetric muscle loss injury. Acute skeletal muscle injuries (e.g., strains, contusions, and exercise induced) follow a canonical sequence of cellular events that typically result in the successful restoration of the damaged tissue to its previously uninjured and functional state. Conversely, VML injuries are plagued with an irregular pathologic response that overwhelms the remaining tissue. The VML pathology is greatest in and around the defect area and gradually declines at the more distal regions of the injured tissue. Characteristics include excessive fibrosis, persistent and irregular inflammation, poor satellite cell migration, and activation, limited formation of new muscle fibers, changes in vascularity, and dysregulation of the

remaining neuromuscular junctions. Ultimately, VML-injured muscle fails to recover the structural and function components of healthy skeletal muscle tissue, often resulting in long-term disability. The images in this figure are representative of a VML injury at different locations in a rat tibialis anterior muscle 21 days following the surgical removal of a full thickness, 6 mm biopsy punch. Cell identification markers used in this figure include the colocalization of nuclei (DAPI) with CD68<sup>+</sup> macrophages, Pax7<sup>+</sup> satellite cells, or CD146<sup>+</sup> endothelial cells.

adaptation of immune cells, expansion, and migration of muscle progenitor cells (satellite cells,

**Figure 1.1**), and remodeling of the vasculature, motor units and extracellular matrix (ECM). Unfortunately, VML injuries do not follow the same regenerative time course and ultimately fail to restore functional muscle tissue to its original form (Pollot & Corona, 2016).

A number of preclinical VML studies do show an initial increase in muscle function following VML injury, suggesting that the endogenous regenerative repair response may be present in the early phase of the injury (Aguilar et al., 2018; Corona et al., 2018; Greising et al., 2017). Upon further inspection however, this response is characterized by irregular waves of inflammation, an absence of progenitor cell expansion and migration into the defect area and excessive formation of ECM collagens that fill the VML defect area with scar tissue (Greising et al., 2017). Thus, the early improvements in function may not indicate regeneration, but instead an unregulated cellular response with a passive increase in force transmitting collagens that ultimately overwhelm the tissues endogenous regenerative capacity.

*- Loss of functional ECM replaced with Pathologic Fibrosis*

The complex web-like structure that surrounds the muscle tissue is known as the extracellular matrix (ECM), which is an extension of the tendon, transmitting the contractile forces generated from muscle fiber contraction to the bone for movement. Beyond the ECM's contribution to movement, there is mounting evidence to support its critical role in the healing of injury muscle tissue (Gillies & Lieber, 2011; Hyldahl et al., 2015). Skeletal muscle ECM is composed of various collagen isoforms, proteoglycans, and glycosaminoglycans that serve as a scaffolding to provide structural support for the muscle fibers, vasculature, nerves, and the diverse cellular populations that reside within the tissue micro-environment. Healthy muscle has a relatively consistent ratio of ECM in comparison to myofiber cross-sectional area. As muscle fibers hypertrophy, there is a

corresponding increase and complex remodeling of ECM content (Mendias et al., 2017). However, muscle wasting conditions such as muscular dystrophies appear to disrupt this relationship, resulting in greater ECM accumulation with smaller muscle fibers. The unbalanced accumulation of ECM (fibrosis) results in deterioration of muscle quality and poor muscle function by reducing joint range of motion and maximal force production. Excessive ECM accumulation is one of the primary characteristics of VML injury. Following the blunt removal of muscle fibers, mononuclear cells infiltrate the defect area and deposit thick layers of ECM that create a ball of scar tissue to replace the muscle fibers.

Following acute injuries (i.e., strains, or exercise induced) the ECM undergoes a remodeling phase that is vastly important for healthy regeneration and repair of the damaged myofibers. This transient remodeling phase is referred to as the transitional ECM and includes the enzymatic breakdown and cellular upregulation of collagens and adhesion related proteoglycans (i.e., tenascin-c, fibronectin, hyaluronic acid) (Calve et al., 2010). The transitional ECM acts as a highway for cells to migrate towards the injury sight and facilitate the repair/regeneration process. The disappearance of a transitional matrix can lead to widespread fibrogenesis, as is observed in other skeletal muscle disorders (i.e., muscular dystrophy) and aging (Sorensen et al., 2018). There appears to be a tipping point in more severe pathologies, where muscle regeneration is repressed, and ECM deposition progresses uninhibited (**Figure 1.1**). For example, the blunt removal of muscle fibers, resident mononuclear cells and ECM components following VML injuries results in the aggressive formation of highly cross-linked or dense collagens (Hoffman et al., 2021). Indeed, the loss of functional ECM appears to limit the regenerative potential of the muscle, likely contributing to failed migration of satellite cells from the remaining tissue into the defect area. Notably, the frank removal of the existing ECM eliminates the structural support system that is

needed for new muscle fibers to grow and survive. Therefore, regenerative medicine interventions have attempted to address these issues with an approach of inserting various biomimetic scaffolds into the VML defect area to establish a physical support system for angiogenesis, myogenesis and reinnervation(Aurora et al., 2015; Haas et al., 2019). This approach has had varying levels of success, specifically in the ability to restore function. Going forward, it will be critical to find a balance between functional ECM remodeling and inhibition of fibrogenesis.

#### *-Extensive and irregular inflammation*

The extent of damage caused by VML injuries is typically beyond the muscle's natural ability to regenerate. Regeneration takes place under complex inflammatory conditions, entailing the activation of the innate immune system and recruitment of effector immune cells (**Figure 1**). Early stages of healing involve a pro-inflammatory environment, where resident macrophages are polarized towards the M1 phenotype and, along with other recruited immune cells, facilitate the repair process by breaking down cellular debris. This process is also important for the activation and migration of muscle satellite cells to the area of injury. Under normal conditions, this pro-inflammatory milieu subsides as damaged cells and extracellular matrices are cleared away. Macrophages will then polarize toward the M2 or anti-inflammatory phenotype which will stimulate satellite cell differentiation and myofiber repair.

VML injured muscle maintains an increased expression of chemotactic, inflammatory, and immune cell infiltration gene transcripts (Greising et al., 2016; Greising et al., 2017). Where other muscle injuries see a decrease in inflammatory signaling a few days after injury, VML has been shown to maintain this sustained expression even 28 days following injury(Aguilar et al., 2018). Similar to other models of severe muscle trauma, VML presents with an inflammatory profile, producing an abundance of COX1/2, CSF2, IL6, MIF, and STAT3. Moreover, immune pathways,

such as complement activation, and fibrosis-inducing pathways, like TGF- $\beta$ 1 and Wnt, remain constantly activated after injury. This is important because TGF- $\beta$ 1 and Wnt control the behavior of multipotent fibro-adipogenic precursors living in the cellular niche of the muscle, which are thought to be responsible for the increased fibrosis in the VML defect area and the suppression of muscle satellite cell activation respectively.

Increased fibrosis in the muscle defect creates a myogenesis-inhibitive feedback loop, as fibrotic tissue secretes cytokines that block myogenic differentiation factors such as MyoD, MyoG, and Mef2. Fibrosis, prolonged immune cell infiltration and action create an unfavorable environment where remodeling enzymes are constantly activated to clear away extracellular matrix that is interfering with the growth of new myofibers, leading to further inflammation (Shayan & Huang, 2020). This environment is unreceptive to therapies and causes a degenerative phenotype in satellite, immune and fibro-adipogenic precursor cells (Larouche et al., 2018). Therefore, therapeutic candidates must be able to immunomodulate the cell niche to usher in the anti-inflammatory stages of repair, when appropriate, stave off fibrosis and adipogenesis, preserve the remaining muscle, and positively influence satellite cells.

### *Regenerative Rehabilitation*

The status quo as it pertains to treatment strategies for VML is: i) various regenerative medicine approaches that modestly improve function pre-clinically and require further maturation to achieve clinically meaningful functional improvement; ii) a dearth of VML studies that include reliable, clinically relevant outcome measurements of function, and iii) no standards of care for the patient. Regenerative rehabilitation offers a departure from the status quo by combining best practices of regenerative medicine and rehabilitation, especially if future studies incorporate clinically meaningful outcome measurements of muscle function. This provides context to discuss next steps

toward advancing regenerative rehabilitation for VML and pursuing standards of care for patients with VML injuries.

A systematic review and meta-analysis published in 2019 by Greising and colleagues (Greising et al., 2019) identified 2,312 studies (search ended January 2019); however, once those studies were screened for the inclusion of outcome measurements of muscle function only 44 studies remained for the meta-analysis (2%). The lack of VML studies including a clinically meaningful outcome measurement is a current challenge area for the field if providing standards of care is a goal for the future. Muscle represents ~40% of a typical individual's body mass, represents an important metabolic engine for basal metabolism, and collectively the primary job of muscle is to contract, produce force, and help move the body. Ultimately, some measurement of metabolism, contractility, and/or movement should be involved in VML studies validating a new approach to improve the pathology.

Regenerative rehabilitation seeks to take the best practices from rehabilitation and regenerative medicine alone and combine them to optimize restoration of muscle function after VML. To date, there have only been a few regenerative rehabilitation studies that included a clinically relevant outcome measurement of muscle function and a comparison to a non-intervention VML group. Beyond augmenting muscle function, these regenerative rehabilitation studies can also provide insight into the timing and/or absence of rehabilitation and the positive effects of combined approaches on other physiologically important outcomes.

## **Specific Aims and Hypothesis**

The development of effective strategies for treating VML injuries is contingent upon the cumulative knowledge of the state of the extracellular environment, activated signaling cascades, metabolic changes within the muscle fibers, and the relative plasticity of the affected muscle. Therefore, the overall objective is to contribute to the growing repository of knowledge concerning the pathophysiology of VML injury and possible treatment strategies to address these deficiencies. Specifically, my dissertation will be aimed at understanding the changes occurring in mitochondrial metabolism during the early stages of VML injury and determine how these contribute to the total decline of muscle quality. Additionally, I will use the current literature in the muscle injury field to select pharmaceutical agents and rehabilitation techniques and determine their efficacy at improving contractile-metabolic function after VML injury. For this purpose, my dissertation had the following specific aims and hypothesis:

Specific Aim 1: Characterization of mitochondrial metabolism decline as a function of acute VML injury progression. Wherein I will identify early metabolic pathology in the remaining muscle after VML injury by interrogating  $\text{Ca}^{2+}$  dysregulation in VML injuries and the metabolic processes thereby affected. I hypothesize that early metabolic inflexibility describes the metabolic challenges in VML.

Specific Aim 2: Pharmaceutical agents for the improvement of contractile-metabolic function following volumetric muscle loss. Wherein I will screen pharmaceutical agents with proven success in other muscle pathologies and apply them within the context of VML. I hypothesize that by selecting drugs shown to stimulate pathways of mitochondrial biogenesis, we can improve muscle mass and thus, muscle function, after VML.

Specific Aim 3: Regenerative rehabilitation approaches for the improvement of contractile-metabolic function following volumetric muscle loss. Wherein I will combine the use of the best candidate from Specific Aim 2 and combine it with a rehabilitation technique or different delivery system. I hypothesize that the combination of pharmaceutical agent with a separate rehabilitation will further improve muscle

function after VML. However, this aim will also offer an alternative to patients who may not be able to receive rehabilitation due to physical constraints.

## References:

- Aguilar, C. A., Greising, S. M., Watts, A., et al. (2018). Multiscale analysis of a regenerative therapy for treatment of volumetric muscle loss injury. *Cell Death Discov*, 4, 33. <https://doi.org/10.1038/s41420-018-0027-8>
- Aurora, A., Roe, J. L., Corona, B. T., & Walters, T. J. (2015). An acellular biologic scaffold does not regenerate appreciable de novo muscle tissue in rat models of volumetric muscle loss injury. *Biomaterials*, 67, 393-407. <https://doi.org/10.1016/j.biomaterials.2015.07.040>
- Call, J. A., Warren, G. L., Verma, M., & Lowe, D. A. (2013). Acute failure of action potential conduction in mdx muscle reveals new mechanism of contraction-induced force loss. *The Journal of physiology*, 591(15), 3765-3776.
- Calve, S., Odelberg, S. J., & Simon, H. G. (2010). A transitional extracellular matrix instructs cell behavior during muscle regeneration. *Dev Biol*, 344(1), 259-271. <https://doi.org/10.1016/j.ydbio.2010.05.007>
- Corona, B. T., Flanagan, K. E., Brininger, C. M., et al. (2018). Impact of volumetric muscle loss injury on persistent motoneuron axotomy. *Muscle Nerve*, 57(5), 799-807. <https://doi.org/10.1002/mus.26016>
- Corona, B. T., Wenke, J. C., & Ward, C. L. (2016). Pathophysiology of Volumetric Muscle Loss Injury. *Cells Tissues Organs*, 202(3-4), 180-188. <https://doi.org/10.1159/000443925>
- Cross, J. D., Ficke, J. R., Hsu, J. R., et al. (2011). Battlefield orthopaedic injuries cause the majority of long-term disabilities. *J Am Acad Orthop Surg*, 19 Suppl 1, S1-7. <https://doi.org/10.5435/00124635-201102001-00002>
- Dalske, K. A., Raymond-Pope, C. J., McFaline-Figueroa, J., et al. (2021). Independent of physical activity, volumetric muscle loss injury in a murine model impairs whole-body metabolism. *PLoS One*, 16(6), e0253629. <https://doi.org/10.1371/journal.pone.0253629>
- Gamboa, J. L., Garcia-Cazarin, M. L., & Andrade, F. H. (2011). Chronic hypoxia increases insulin-stimulated glucose uptake in mouse soleus muscle. *Am J Physiol Regul Integr Comp Physiol*, 300(1), R85-91. <https://doi.org/10.1152/ajpregu.00078.2010>
- Gillies, A. R., & Lieber, R. L. (2011). Structure and function of the skeletal muscle extracellular matrix. *Muscle Nerve*, 44(3), 318-331. <https://doi.org/10.1002/mus.22094>
- Greising, S. M., Corona, B. T., McGann, C., et al. (2019). Therapeutic Approaches for Volumetric Muscle Loss Injury: A Systematic Review and Meta-Analysis. *Tissue Eng Part B Rev*, 25(6), 510-525. <https://doi.org/10.1089/ten.TEB.2019.0207>
- Greising, S. M., Dearth, C. L., & Corona, B. T. (2016). Regenerative and Rehabilitative Medicine: A Necessary Synergy for Functional Recovery from Volumetric Muscle Loss Injury. *Cells Tissues Organs*, 202(3-4), 237-249. <https://doi.org/10.1159/000444673>
- Greising, S. M., Rivera, J. C., Goldman, S. M., et al. (2017). Unwavering Pathobiology of Volumetric Muscle Loss Injury. *Sci Rep*, 7(1), 13179. <https://doi.org/10.1038/s41598-017-13306-2>
- Greising, S. M., Warren, G. L., Southern, W. M., et al. (2018). Early rehabilitation for volumetric muscle loss injury augments endogenous regenerative aspects of muscle strength and oxidative capacity. *BMC musculoskeletal disorders*, 19(1), 173. <https://doi.org/10.1186/s12891-018-2095-6>
- Haas, G. J., Dunn, A. J., Marcinczyk, M., et al. (2019). Biomimetic sponges for regeneration of skeletal muscle following trauma. *J Biomed Mater Res A*, 107(1), 92-103. <https://doi.org/10.1002/jbm.a.36535>

- Hoffman, D. B., Raymond-Pope, C. J., Sorensen, J. R., et al. (2021). Temporal changes in the muscle extracellular matrix due to volumetric muscle loss injury. *Connect Tissue Res*, 1-14. <https://doi.org/10.1080/03008207.2021.1886285>
- Hood, D. A., Memme, J. M., Oliveira, A. N., & Triolo, M. (2019). Maintenance of skeletal muscle mitochondria in health, exercise, and aging. *Annual Review of Physiology*, 81, 19-41.
- Hyldahl, R. D., Nelson, B., Xin, L., et al. (2015). Extracellular matrix remodeling and its contribution to protective adaptation following lengthening contractions in human muscle. *Faseb j*, 29(7), 2894-2904. <https://doi.org/10.1096/fj.14-266668>
- Larouche, J., Greising, S. M., Corona, B. T., & Aguilar, C. A. (2018). Robust inflammatory and fibrotic signaling following volumetric muscle loss: a barrier to muscle regeneration. *Cell Death Dis*, 9(3), 409. <https://doi.org/10.1038/s41419-018-0455-7>
- Mase, V. J., Jr., Hsu, J. R., Wolf, S. E., et al. (2010). Clinical application of an acellular biologic scaffold for surgical repair of a large, traumatic quadriceps femoris muscle defect. *Orthopedics*, 33(7), 511. <https://doi.org/10.3928/01477447-20100526-24>
- Mendias, C. L., Schwartz, A. J., Grekin, J. A., et al. (2017). Changes in muscle fiber contractility and extracellular matrix production during skeletal muscle hypertrophy. *J Appl Physiol (1985)*, 122(3), 571-579. <https://doi.org/10.1152/jappphysiol.00719.2016>
- Mukund, K., & Subramaniam, S. (2020). Skeletal muscle: A review of molecular structure and function, in health and disease. *Wiley Interdiscip Rev Syst Biol Med*, 12(1), e1462. <https://doi.org/10.1002/wsbm.1462>
- Owens, B. D., Kragh, J. F., Jr., Macaitis, J., et al. (2007). Characterization of extremity wounds in Operation Iraqi Freedom and Operation Enduring Freedom. *J Orthop Trauma*, 21(4), 254-257. <https://doi.org/10.1097/BOT.0b013e31802f78fb>
- Owens, B. D., Kragh, J. F., Jr., Wenke, J. C., et al. (2008). Combat wounds in operation Iraqi Freedom and operation Enduring Freedom. *J Trauma*, 64(2), 295-299. <https://doi.org/10.1097/TA.0b013e318163b875>
- Pollot, B. E., & Corona, B. T. (2016). Volumetric Muscle Loss. *Methods Mol Biol*, 1460, 19-31. [https://doi.org/10.1007/978-1-4939-3810-0\\_2](https://doi.org/10.1007/978-1-4939-3810-0_2)
- Seifert, J. (2007). Incidence and economic burden of injuries in the United States. *Journal of Epidemiology and Community Health*, 61(10), 926-926. <https://doi.org/10.1136/jech.2007.059717>
- Shayan, M., & Huang, N. F. (2020). Pre-Clinical Cell Therapeutic Approaches for Repair of Volumetric Muscle Loss. *Bioengineering (Basel)*, 7(3). <https://doi.org/10.3390/bioengineering7030097>
- Sorensen, J. R., Skousen, C., Holland, A., et al. (2018). Acute extracellular matrix, inflammatory and MAPK response to lengthening contractions in elderly human skeletal muscle. *Exp Gerontol*, 106, 28-38. <https://doi.org/10.1016/j.exger.2018.02.013>
- Southern, W. M., Nichenko, A. S., Tehrani, K. F., et al. (2019). PGC-1alpha overexpression partially rescues impaired oxidative and contractile pathophysiology following volumetric muscle loss injury. *Sci Rep*, 9(1), 4079. <https://doi.org/10.1038/s41598-019-40606-6>
- Tanaka, A., Yoshimura, Y., Aoki, K., et al. (2017). Prediction of muscle strength and postoperative function after knee flexor muscle resection for soft tissue sarcoma of the lower limbs. *Orthop Traumatol Surg Res*, 103(7), 1081-1085. <https://doi.org/10.1016/j.otsr.2017.07.005>

Warren, G. L., Summan, M., Gao, X., et al. (2007). Mechanisms of skeletal muscle injury and repair revealed by gene expression studies in mouse models. *The Journal of physiology*, 582(2), 825-841.

CHAPTER 2  
CHARACTERIZATION OF EARLY METABOLIC PATHOPHYSIOLOGY AFTER  
VOLUMETRIC MUSCLE LOSS<sup>2</sup>

---

<sup>2</sup>McFaline-Figueroa, J., Hunda, E.T., Call, J.A. *Characterization of early metabolic pathophysiology after volumetric muscle loss*. To be submitted to *American Journal of Physiology* or similar.

## **Abstract**

Volumetric muscle loss (VML) injuries are characterized by non-recoverable loss of tissue due to trauma or surgery. These injuries result in severe deficits of contractile and metabolic function that continue deteriorating over time due to lack of mobility, muscle atrophy, problems recruiting existing muscle fibers, continuous inflammatory response, and damages to the mitochondrial network. While there exists a growing body of literature characterizing the effects of VML injury on muscle function, there is little to no research studying the progression of muscle decline in VML injury beginning shortly after injury. The purpose of this study was to evaluate the mitochondrial metabolic function of VML-injured tissue shortly after trauma onset and up to two weeks. Male C57BL/6 mice underwent a unilateral, 15% multi-muscle VML injury of the posterior hindlimb. Animals were then evaluated with metabolic functional outcomes at 1-, 3-, 5-, 7-, 10-, and 14-days post-injury, including metabolic flexibility by comparing carbohydrate and lipid-driven oxygen consumption of permeabilized muscle fibers. VML-injured tissue had decreased carbohydrate-driven metabolism compared to uninjured Control muscles that fluctuated over time ( $p < 0.0001$ ). Conversely, lipid metabolism was not affected over the course of the study ( $p = 0.1091$ ). Additionally, similar results were observed when evaluating enzymatic activity tied to carbohydrate (pyruvate dehydrogenase) and lipid (3-hydroxyacyl-CoA dehydrogenase) oxidation. A probe into possible mechanisms for metabolic inflexibility in VML injury revealed a possible tie with increased intracellular  $\text{Ca}^{2+}$  that resolves by 3-days post-injury.

## Introduction

Volumetric muscle loss injuries encompass a group of pathologies characterized by the frank loss of muscle tissue due to trauma or surgical removal (Grogan & Hsu, 2011). The result of these injuries is the marked, sustained decline of muscle contractile-metabolic function (Corona et al., 2015; Greising et al., 2017; Grogan & Hsu, 2011). Among these is the loss of strength, mobility, increase in fibrotic tissue, and whole-body and mitochondrial metabolic dysfunction (Chao et al., 2019; Corona et al., 2015; Dalske et al., 2021; Garg et al., 2015; William M Southern et al., 2019). Typically, these functional losses are permanent and increasing in severity over time, that can potentially lead to a cadre of secondary orthopedic diseases such as osteoarthritis and increased risk of metabolic diseases such as diabetes and cardiovascular disease.

Overall, research on the development of regenerative techniques to regrow tissue *de novo* after VML injury far outweighs the study of VML pathophysiology and there is not a focus on functional outcomes to measure recovery (Greising et al., 2019). The knowledge of the effects of long-term VML pathophysiology are modest and often in the context of comparisons to experimental treatments. What is more, despite the mounting characterization of the lasting contractile-metabolic insufficiencies caused by VML injury, there has been little to no effort to study the context in which this dysfunction develops.

VML pathophysiology progresses within an extracellular environment that is overwhelmed by cytokine, chemokine, and inflammatory responses (Garg et al., 2014; Larouche et al., 2018; Qualls et al., 2021). As such, it is difficult to choose one specific target to pursue during the development of regenerative therapies. However, the information that could be learned from systematically probing different aspects of the metabolism of VML-injured tissue can help direct focus for the creation of such treatments. Considering there is a robust change in mitochondrial

and whole-body metabolism following VML injury(Dalske et al., 2021; William M Southern et al., 2019), the purpose of this study is to characterize the changes in muscle metabolism in the early stages of VML injury in an effort to capture early indicators of metabolic dysfunction and inflexibility.

## **Materials and Methods**

### *Animals:*

Male C57BL/6 mice were housed at 20-23 °C on a 12:12-hr light-dark cycle, with food and water provided ad libitum. At the time of randomization to experimental groups, all mice were between 11-12 weeks of age (pre-surgical mass  $28.1 \pm 3.2$  g). All procedures were approved and performed in accordance with the guidelines and regulations of the Institutional Animal Care and Use Committee at the University of Georgia.

### *Experimental design:*

VML-injured mice underwent unilateral VML injury and were sacrificed at the following timepoints time points (n=3/group): 1, 3, 5, 7, 10, and 14-days. At the study endpoint, muscle mass, carbohydrate and fat-driven oxygen consumption, and mitochondrial membrane potential were assessed.

### *Surgical creation of VML injury:*

A dose of Buprenorphine (1.2 mg/kg) was given pre-operatively. A VML injury was performed unilaterally on the posterior compartment of anesthetized (isoflurane 1.5-2.0%) mice as previously described(Greising et al., 2018; William M. Southern et al., 2019). Briefly, left hindlimbs

were prepared by removing hair and the skin was aseptically prepared. An incision was made in the posterior of the limb to expose the muscle. Fascia and hamstrings were separated from the gastrocnemius muscle through blunt dissection. A small metal plate was inserted behind the gastrocnemius and soleus muscles and a 4-mm biopsy punch was used to remove a  $27.1 \pm 1.2$  mg portion. Skin was re-approximated using 5-0 vicryl sutures. Buprenorphine (1.2 mg/kg) was given at 12 and 24 hours and Meloxicam (2.0 mg/kg) was given at 24-, 48-, and 72-hours post-procedure.

#### *Mitochondrial Oxygen Consumption*

Mitochondrial metabolic function was measured using the phosphocreatine creatine kinase clamp technique as described by Fisher-Wellman et al. All experiments were carried out at 30°C in a 2 mL reaction volume. Buffer for all assays was Buffer Z supplemented with ATP (5 mM), creatine (5 mM), phosphocreatine (PCr, 1 mM) and creatine kinase (20U/mL). For each experiment, permeabilized skeletal muscle fiber bundles (2 mg) from the gastrocnemius muscles were energized with either glutamate (10mM), malate (2.5 mM) and succinate (10mM) or Palmytoyl-carnitine (10 mM) and malate (2.5 mM). Following substrate addition, titrations of PCr (1, 2, 4, 7, 16, and 31 mM) were performed to reduce oxygen consumption back to baseline.  $G'_{ATP}$  was calculated for each PCr titration and plotted against  $JO_2$  for each step. The resulting slope for each sample ( $\Delta G_{ATP}$  vs  $JO_2$ ) represents electron conductance through the electron transport chain.

#### *Mitochondrial Membrane Potential*

Fluorescent determination of mitochondrial membrane potential ( $\Delta\psi_m$ ) was performed at 30 °C in 0.2 mL of assay buffer using a Horiba Spectrofluorometer (FluoroMax Plus-C; Horiba Instruments Inc., Atlanta, GE, USA) as previously described. The  $\Delta\psi_m$  was determined via

tetramethylrhodamine, methyl ester (TMRM) by taking the fluorescence ratio of the excitation/emission parameters: excitation/emission (572/590 nm)/ (551/590 nm). Permeabilized muscle fiber were weighed (1~1.5 mg) and placed into cuvettes containing assay buffer supplemented with ATP (5mM), CK (200U/mL), and creatine (20mM). Following a 2-minute temperature equilibration, substrates were added to fuel the mitochondria (10mM glutamate, 1 mM Malate, 10 mM Succinate). Sequential PCr titrations were made to final concentrations of 1, 2, 4, 8, 16, 32, 64 mM that matched the mitochondrial respiration control approach. Following the PCr titrations, 1  $\mu$ M FCCP was used to assess maximum fluorescence.

#### *Citrate synthase activity*

Mitochondrial content was analyzed by citrate synthase enzyme (CS) activity as previously described(William M. Southern et al., 2019). Briefly, following muscle fiber collection for oxygen consumption experiments, the remainder of the gastrocnemius muscle was chopped into fine pieces and mixed. Approximately 40 mg of muscle was weighed and further homogenized in 33mM phosphate buffer (pH 7.4) at a muscle to buffer ratio of 1:40 using a glass tissue grinder. Homogenate was incubated with 5,5'-dithio-bis(2-nitrobenzoic acid (DTNB, 0.773mM), acetyl CoA (0.116mM), and oxaloacetate (0.441mM) in 100mM Tris buffer (pH 8.0). Activity of citrate synthase was monitored from the reduction of DTNB over time via measurement of absorbance at 412nm.

#### *Assessment of mitochondrial metabolic enzyme activity*

Activity for each mitochondrial respiratory complex was measured using a protocol modified from Thome, et al(Thome et al., 2019). Complex I activity was measured in 50mM potassium

phosphate buffer, 3mg/mL BSA, 240  $\mu$ M KCN, 0.4  $\mu$ M antimycin A, 50  $\mu$ M decyl-ubiquinone, and 80  $\mu$ M 2,6-dichlorophenolindophenol (DCPIP). NADH oxidation was measured through the reduction of DCPIP at 600 nm. Complex II activity was measured in buffer containing 10 mM  $\text{KH}_2\text{PO}_4$ , 2 mM EDTA, and 1 mg/mL BSA at pH 7.8 and supplemented with 0.2 mM ATP, 10 mM succinate, and 0.08 mM DCPIP. Following a 10-minute incubation, at 37°C, the assay was initiated by the addition of oxidized decyl-ubiquinone (0.08 mM) and reduction of DCPIP followed at 600 nm. b-hydroxyacyl CoA dehydrogenase (b-HAD) activity was measured by incubating muscle homogenate in a buffer containing 100 mM triethanolamine, 0.451 mM b-nicotinamide adenine dinucleotide (NADH) and 5 mM ethylenediaminetetraacetic acid (EDTA), as described previously(Call et al., 2008; Nichenko et al., 2016; Southern et al., 2017). Acetoacetyl CoA (0.1 mM) was used to start the reaction. Activity of b-hydroxy acyl CoA dehydrogenase was monitored from the oxidation of NADH over time as determined by its absorbance at 340 nm. Pyruvate dehydrogenase activity was measured from the reduction of  $\text{NAD}^+$  over time as determined by its fluorescence at Ex 340nm/Em450 nm.

#### *Intracellular calcium content*

Intracellular calcium content was determined via the complexation of calcium to 1,2-bis (o-aminophenoxy) ethane-N, N, N', N'-tetraacetic acid (BAPTA-AM). Briefly, whole gastrocnemius tissue was homogenized in a calcium-free buffer containing 120 mM KCl, 2 mM HEPES, 0.15 mM BAPTA-AM, and 0.5% w/v sodium dodecyl sulfate. Absorbance of tissue homogenate with and without 1 mM EGTA was used to calculate total intracellular calcium per mg of tissue.

### *In vitro model of calcium-induced dysfunction*

Uninjured muscle tissue was dissected into individual fibers and permeabilized as described above. Muscle fibers were incubated in a high calcium ion content for fifteen minutes before oxygen consumption was tested using the SUIT method. Mitochondrial leak respiration was accomplished by the addition of glutamate (10mM), malate (5mM), succinate (10mM). State III respiration was accomplished by adding ADP (5mM) after leak respiration had been recorded (Data not shown).

### *Statistical Analysis*

All data is represented as mean  $\pm$  standard deviation. A one-way ANOVA was used to determine differences between VML-injured limbs across timepoints. Control limbs from all timepoints were statistically insignificant (One-way ANOVA  $p=0.1078$ ) and were, therefore, pooled together for analysis. Statistically significant differences are indicated when the p-value was less than or equal to 0.05, and statistical trends are noted if a p-value was between 0.05 and 0.10. All statistical analyses were performed on Prism statistical software (GraphPad, San Diego, CA, Version 8).

## Results

Skeletal muscle with VML injuries become increasingly dysfunctional over time. Previous studies have described the disproportionate loss of contractile and metabolic function in the affected limb when considering the amount of tissue loss during injury (William M Southern et al., 2019) (William M. Southern et al., 2019). Here, we evaluated the gastrocnemius muscle mass of VML-injured mice across six early timepoints (Table 2.1). While body mass significantly increases, as expected, over time (Table 2.1, Tukey's  $p=0.0362$ ), gastrocnemius muscle mass does not follow this trend (Table 2.1). Apart from the 5-day timepoint, all VML-injured gastrocnemius muscles were significantly different from uninjured Control muscles (Table 2.1, Tukey's  $p=0.0018$ ). Interestingly, the 5-day timepoint had the largest gastrocnemius muscle masses across all injury groups. When normalizing muscle mass to body mass, VML-injured muscle at 3-, 10-, and 14-days post-injury are significantly smaller than uninjured Controls (Table 2.1, Tukey's  $p=0.0351$ ). VML-injured muscles at 5-days post-injury are proportionally significantly larger than those at 14-days (Table 2.1, Tukey's  $p=0.0347$ ).

Table 2.1: Mouse body mass and gastrocnemius muscle mass

	Experimental Group							OWA p-value
	1-day	3-day	5-day	7-day	10-day	14-day	Control	
Body Mass (g)	26.9 ± 1.4 <sup>ab</sup>	28.5 ± 1.0 <sup>b</sup>	28.5 ± 0.9 <sup>b</sup>	29.2 ± 0.1	31.0 ± 1.6	31.8 ± 0.34		<0.0001
Gastroc Mass (mg)	126.0 ± 8.5 <sup>cd</sup>	130.3 ± 9.6 <sup>#</sup>	157.5 ± 9.4	138.9 ± 7.3 <sup>#</sup>	133.7 ± 8.4 <sup>#</sup>	134.3 ± 4.7 <sup>#</sup>	174.3 ± 16.0	<0.0001
Gastroc: BM	4.7 ± 0.2	4.6 ± 0.5 <sup>#</sup>	5.4 ± 0.3 <sup>b</sup>	4.7 ± 0.2	4.3 ± 0.1 <sup>#</sup>	4.2 ± 0.2 <sup>#</sup>	5.5 ± 0.5	<0.0001

Values are means ± SD

<sup>a</sup>Different from 10-day

<sup>b</sup>Different from 14-day

<sup>c</sup>Different from 5-day

<sup>#</sup>Different from Control

## Oxygen consumption of acutely VML-injured muscle fibers

Considering the noticeable differences in total and proportional muscle mass in VML injuries, even at early timepoints, the next step was to determine how these changes were reflected in the mitochondrial metabolism. Previous studies have observed the change in whole-body metabolism in VML-injured mice despite having activity levels similar to healthy mice (Dalske et al., 2021). To capture these changes in early injury, mitochondrial metabolism was tested via oxygen consumption of permeabilized muscle fibers as a result of stimulation with either carbohydrate (pyruvate/malate/succinate) or fat (palmitoyl carnitine/malate) substrates using the metabolic stress test (creatine kinase clamp) (Fisher-Wellman et al., 2018).

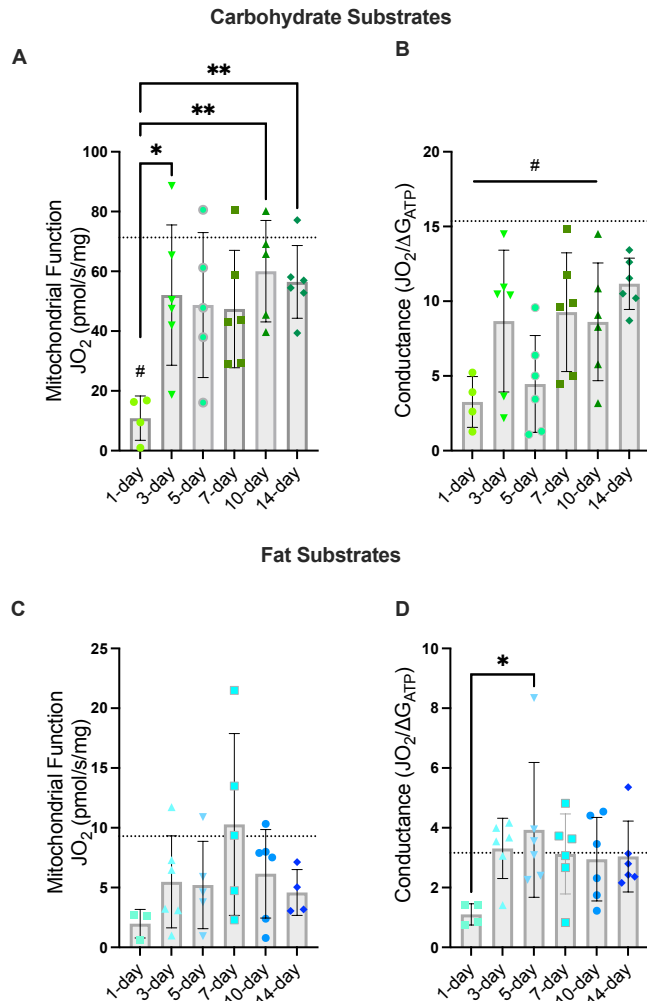


**Figure 2.1:** VML-injured tissue has suppressed carbohydrate but not lipid utilization. **A.** Carbohydrate utilization is decreased at 1-day compared to 3-, 10-, and 14-days post-injury and uninjured controls. **B.** Electron conductance is inhibited in carbohydrate-driven respiration at 1-, 3-, 5-, 7-, and 10-days post-injury. While there is no difference in maximal lipid-driven oxygen consumption (**C.**), there is a difference in conductance between 1-day and 5-days post-injury (**D.**). Data shown as means  $\pm$  SD. Analyzed via OWA. \* denotes difference between groups. # denotes difference to uninjured controls.

As expected, respiration was significantly repressed 1-day after injury compared to control tissue (black dashed line, Figure 2.1 A; Tukey's  $p=0.0496$ ) in the carbohydrate preparation. Carbohydrate-stimulated oxygen consumption was significantly reduced at 1-day compared to 3-, 10-, and 14-day VML injuries (Figure 2.1 A, Tukey's  $p=0.0231$ ). Gibbs free energy for ATP was calculated for each step of the metabolic stress test and plotted against the recorded oxygen consumption. The slope of the resulting line represents electron conductance, or the ease with which mitochondria can flow through the electron transport chain to create ATP. Electron conductance for VML-injured tissue was significantly lower compared to uninjured Control at 1-, 3-, 5-, 7-, and 10-days post-injury (Figure 2.1 B, Tukey's  $p=0.0483$ ).

There were no detectable differences in maximal coupled lipid-stimulated oxygen consumption across timepoints (Figure 2.1 C, Tukey's  $p=0.1392$ ). However, there was a significant difference in electron conductance between VML-injured tissue at 1-day and 5-days post-injury (Figure 2.1 D, Tukey's  $p=0.0475$ ). Interestingly, this increase in lipid-driven conductance coincides with an overall, non-significant decrease in carbohydrate-driven conductance.

### *Mitochondrial enzyme activity*

In the interest of delving deeper into the differences between carbohydrate- and lipid-driven metabolism, the activity of different mitochondrial enzymes was evaluated (Table 2.2). As expected, citrate synthase activity, a cognate of mitochondrial content inside the muscle fibers, was not significantly different across timepoints or compared to uninjured Controls (Table 2.2, Tukey's  $p=0.4232$ ). 3-hydroxyacyl-CoA dehydrogenase ( $\beta$ -HAD) is a key enzyme of beta-oxidation, a process in which lipid chain are broken down so that they may enter oxidative

phosphorylation.  $\beta$ -HAD activity was not different across groups or compared to uninjured Control samples (Table 2.2, Tukey's  $p=0.9476$ ).

Alternatively, enzyme activity for pyruvate dehydrogenase, a key enzyme of carbohydrate metabolism was significantly different from uninjured Controls at 3-days post-injury (Table 2.2, Tukey's  $p<0.0001$ ). Additionally, activity at this 3-day timepoint was significantly increased over every other experimental timepoint measured (Table 2.2, Tukey's  $p=0.0002$ ). Activity was similarly increased at 5-days compared to 14-days post-injury (Table 2.2, Tukey's  $p=0.0077$ ).

Activity at Complex I of the electron transport chain was unremarkable across timepoints and compared to uninjured Controls (Table 2.2, Tukey's  $p=7341$ ). Interestingly, there is a difference in Complex II activity between 10- and 14-days post-injury (Table 2.2, Tukey's  $p=0.0497$ ) and a trending difference between 3- and 10-days post-injury (Table 2.2, Tukey's  $p=0.0608$ ).

**Table 2.2.** Mitochondrial Enzyme Activity

Enzymatic Activity	Experimental Group							OWA p-value
	1-day	3-day	5-day	7-day	10-day	14-day	Control	
CS (mmol/min/g)	336 ± 43.1	283 ± 111	273 ± 65.8	281 ± 70.1	387 ± 9.17	419 ± 68.6	360 ± 42.5	0.2571
$\beta$ -HAD (mmol/min/g)	39.5 ± 2.0	46.3 ± 7.6	44.3 ± 3.5	44.6 ± 4.3	48.3 ± 6.9	48.6 ± 2.9	39.9 ± 5.3	0.9609
PDH (pmol/s/mg)	125.4 ± 8.8 <sup>b</sup>	334.4 ± 85.8 <sup>a#</sup>	192.0 ± 45.6 <sup>bc</sup>	156.9 ± 32.7 <sup>b</sup>	129.3 ± 65.5 <sup>b</sup>	95.4 ± 28.2 <sup>b</sup>	119.6 ± 17.4 <sup>b</sup>	<0.0001
Complex I (mmol/min/g)	17.9 ± 3.7	17.8 ± 2.1	20.7 ± 5.9	18.2 ± 2.3	17.1 ± 5.7	15.0 ± 3.6	17.9 ± 2.1	0.7301
Complex II (mmol/min/g)	24.6 ± 3.6	40.2 ± 9.2	28.5 ± 12.9	25.8 ± 6.8	19.5 ± 6.5 <sup>c</sup>	40.9 ± 8.7	27.6 ± 3.5	0.0209

CS – citrate synthase;  $\beta$ -HAD – 3-hydroxyacyl-CoA dehydrogenase; PDH – pyruvate dehydrogenase. Enzymatic activity normalized to citrate synthase activity as a measure of mitochondrial content. Enzymatic activity is represented as micromoles of product generated per minute per gram of protein. Values are means ± SD. OWA= One-Way ANOVA

<sup>a</sup>Different from all other groups

<sup>b</sup>Different from 3-day

<sup>c</sup>Different from 14-day

<sup>#</sup>Different from Control

Intracellular  $\text{Ca}^{2+}$  is known to activate the oxidative phosphorylation cascade in skeletal muscle (Glancy et al., 2013). However, this process is tightly regulated by intracellular  $\text{Ca}^{2+}$  stores

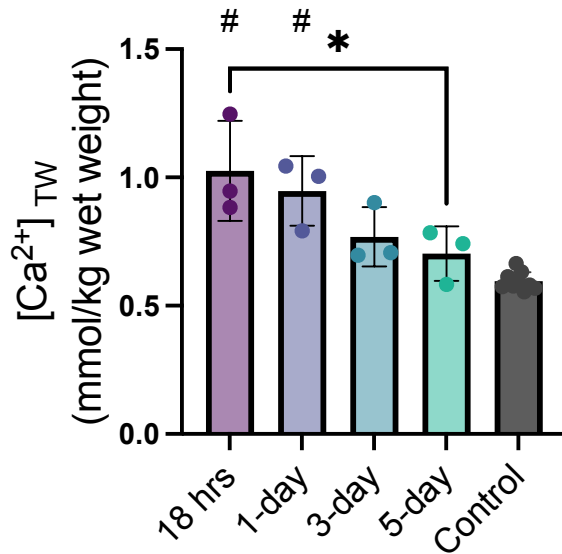


**Figure 2.2:** Total  $\text{Ca}^{2+}$  concentration in VML muscle. Intracellular  $\text{Ca}^{2+}$  concentration of VML-injured tissue is increased through 1-day post-injury. Data represented as means  $\pm$  SD. Analyzed via OWA. \* denotes significant differences between groups. # denotes significant differences compared to uninjured Control.

and the mitochondrial permeability transition pore (mPTP). During VML injury, cut muscle fibers are exposed to extracellular environment, where calcium ion concentrations are greater than those within the muscle cell, until the fiber is able to seal but is unclear whether this disruption on  $\text{Ca}^{2+}$  homeostasis affects the muscle fiber, long term. To determine whether VML-injured tissue contained elevated intracellular  $\text{Ca}^{2+}$  concentration, VML-injured tissue was homogenized in  $\text{Ca}^{2+}$ -free medium with 1,2-bis (o-aminophenoxy) ethane-N, N, N', N'-tetraacetic acid (BAPTA-AM).

Shortly after VML injury, intracellular  $\text{Ca}^{2+}$  is significantly increased compared to uninjured tissue (Figure 2.2, Tukey's  $p=0.0001$ ) and to VML tissue 5-days post-injury (Figure 2.2, Tukey's  $p=0.0114$ ). Intracellular  $\text{Ca}^{2+}$  concentration remains elevated 1-day post-injury (Figure 2.2, Tukey's  $p=0.0009$ ).

To further study the involvement of  $\text{Ca}^{2+}$  in VML injury, we designed an *in vitro* system where uninjured, permeabilized muscle fibers were incubated in extracellular concentrations of  $\text{Ca}^{2+}$ . Mitochondrial metabolic function was then tested via an oxygen consumption test using the SUIT method. Complex I and II were individually stimulated with the titration of

glutamate/malate, and succinate, respectively. Rotenone was used to suppress Complex I function. Both  $\text{Ca}^{2+}$ -incubated, and 1-day VML-injured tissue showed decrease function of Complex I and

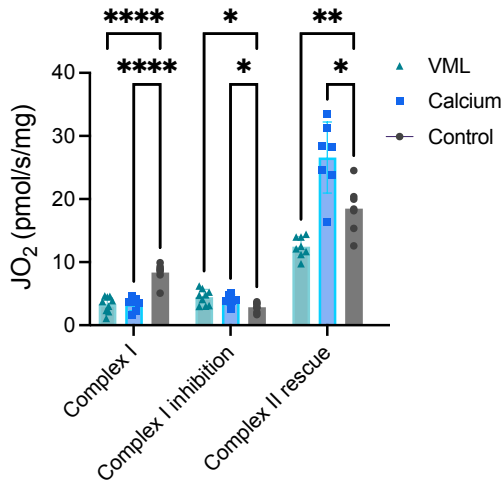


Figure 2.3: *In vitro* modeling of  $\text{Ca}^{2+}$  involvement in VML injury. Uninjured permeabilized muscle fibers incubated in  $\text{Ca}^{2+}$  respond similarly to substrate titration as VML-injured tissue, suggesting  $\text{Ca}^{2+}$  involvement in VML. Data is shown as means  $\pm$  SD. Analyzed via Two-way ANOVA. \* denotes differences between groups.

failed to decrease oxygen consumption when given Rotenone compared to Control (Figure 2.3, Dunnett's  $p=0.0493$ ). All groups rescued oxygen consumption following the titration of succinate into the reaction bath, though VML-injured muscle remained lower than control (Figure 2.3, Dunnett's  $p=0.0086$ ).

## Discussion

Volumetric muscle loss injuries are known to have severe permanent contractile and metabolic deficiencies. While there is a wealth of studies surrounding VML injuries, the majority have been devoted to developing treatment strategies to either regenerate lost tissue volume or improve muscle quality after the initial trauma. There are only a few studies elucidating the effects of injury on normal muscle function. Fewer still are the studies where a systematic approach of cataloguing changes within the muscle in early instances after injury. The logic behind this decision is assumed to be the lack of treatment options immediately after injury, especially as the main concern is

patient and limb stabilization. However, the lack of knowledge in this area is a blind spot for the development of effective pharmacological or regenerative therapies. To help address this knowledge gap, we endeavored to describe the changes in metabolic flexibility during early VML injury as these early changes could contribute to the long-term dysfunction that is characteristic of the disease.

Consistent with previous studies, VML-injured muscle fails to gain mass over time disproportionately to the volume of tissue lost during trauma(William M Southern et al., 2019). In our study, there was only one timepoint that showed mass comparable to uninjured Controls, which was 5-days post-injury. However, it is possible that this timepoint coincided with peak inflammatory response post-injury, and the additional mass is due to increased fluid retention in the affected limb(Panci & Chazaud, 2021; Smith et al., 2008). Considering that VML injuries are known for maintaining a pattern of sustained inflammation (Aguilar et al., 2018; Greising et al., 2016; Greising et al., 2017) , even 28 days after injury, it is possible the deterioration of true muscle mass is more severe than what can observed under normal circumstances.

While it is unsurprising that mitochondrial oxygen consumption was affected by injury, it was expected that overall oxygen consumption would be suppressed, regardless of what substrate was used to stimulate respiration. Previous research found that whole-body metabolism was affected after VML injury, independent of physical activity(Dalske et al., 2021). Overall, VML-injured mice had lower respiratory exchange rate (RER) compared to uninjured controls, despite the fact their activity levels were not different. Additionally, this study saw a difference in whole-body oxidation of carbohydrates and lipids at 6 weeks post-injury, where carbohydrate oxidation decreased while lipid oxidation increased. Early VML injury follows a similar pattern at a local level—carbohydrate-driven respiration is affected while lipid-driven respiration remains

undisturbed. This finding, combined with the enzymatic activity tied to carbohydrate and lipid-driven respiration (changes in PDH while  $\beta$ -HAD remains stable), suggest that 1) these changes in metabolism begin on a local level soon after initial injury and worsen over time, and 2) carbohydrate metabolism is more susceptible to the myriad of changes occurring in the muscle after VML.

Admittedly, the extracellular environment immediately following VML is a combination of dysregulated cytokine, chemokine, and inflammatory cell signaling, all working in conjunction to address the injury and involves more muscle-cytokine crosstalk than other injury models(Larouche et al., 2022; Qualls et al., 2021). Therefore, injured muscle fibers are responding to a plethora of external stimuli that may affect their metabolic function. Nevertheless, the decision to look at  $\text{Ca}^{2+}$  homeostasis within the injured muscle was made based on the ubiquity of  $\text{Ca}^{2+}$  in cellular signaling and its known ties to oxidative phosphorylation(Glaney et al., 2013) and the enzyme pyruvate dehydrogenase(Gherardi et al., 2019; Lander et al., 2018; Scrima et al., 2020; Zhang et al., 2021). At normal levels,  $\text{Ca}^{2+}$  is a regulator of oxidative phosphorylation in skeletal muscle but when muscle cells are overloaded with the ion it results in endoplasmic reticulum stress, the activation of mitochondrial calpain and the subsequent degradation of the enzymes that drive the electron transport chain(Mohsin et al., 2020). The recapitulation of metabolic dysfunction seen in VML using an *in vitro* system in this study, suggests that  $\text{Ca}^{2+}$ -involvement is part of the puzzle of VML pathophysiology.

There are still unknowns to be uncovered in acute VML injury. We do not yet know how this traumatic injury affects mitochondrial membrane potential in early injury pathophysiological development and whether that is reflected in the observed metabolic dysfunction. The involvement of  $\text{Ca}^{2+}$  overload has also not been sufficiently vetted as a main cause for metabolic dysfunction.

Further studies delving into the various mechanisms of  $\text{Ca}^{2+}$  handling within the cell, including internal reserves and action of the mPTP should be done to confirm. In conclusion, this work contributes a detailed mitochondrial metabolic profile of early VML injury that could help clarify the needs of injured tissue for the development of regenerative therapies.

## References

- Aguilar, C. A., Greising, S. M., Watts, A., et al. (2018). Multiscale analysis of a regenerative therapy for treatment of volumetric muscle loss injury. *Cell death discovery*, 4(1), 1-11.
- Call, J. A., Voelker, K. A., Wolff, A. V., et al. (2008). Endurance capacity in maturing mdx mice is markedly enhanced by combined voluntary wheel running and green tea extract. *Journal of Applied Physiology*, 105(3), 923-932. <https://doi.org/10.1152/jappphysiol.00028.2008>
- Chao, T., Burmeister, D. M., Corona, B. T., & Greising, S. M. (2019). Oxidative pathophysiology following volumetric muscle loss injury in a porcine model. *J Appl Physiol (1985)*, 126(6), 1541-1549. <https://doi.org/10.1152/jappphysiol.00026.2019>
- Corona, B. T., Rivera, J. C., Owens, J. G., et al. (2015). Volumetric muscle loss leads to permanent disability following extremity trauma. *Journal of Rehabilitation Research & Development*, 52(7).
- Dalske, K. A., Raymond-Pope, C. J., McFaline-Figueroa, J., et al. (2021). Independent of physical activity, volumetric muscle loss injury in a murine model impairs whole-body metabolism. *PloS one*, 16(6), e0253629. <https://doi.org/10.1371/journal.pone.0253629>
- Fisher-Wellman, K. H., Davidson, M. T., Narowski, T. M., et al. (2018). Mitochondrial diagnostics: a multiplexed assay platform for comprehensive assessment of mitochondrial energy fluxes. *Cell reports*, 24(13), 3593-3606. e3510.
- Garg, K., Ward, C. L., & Corona, B. T. (2014). Asynchronous inflammation and myogenic cell migration limit muscle tissue regeneration mediated by a cellular scaffolds. *Inflamm Cell Signal*, 1(4). <https://doi.org/10.14800/ics.530>
- Garg, K., Ward, C. L., Hurtgen, B. J., et al. (2015). Volumetric muscle loss: persistent functional deficits beyond frank loss of tissue. *Journal of Orthopaedic Research*, 33(1), 40-46.
- Gherardi, G., Nogara, L., Ciciliot, S., et al. (2019). Loss of mitochondrial calcium uniporter rewires skeletal muscle metabolism and substrate preference. *Cell Death Differ*, 26(2), 362-381. <https://doi.org/10.1038/s41418-018-0191-7>
- Glancy, B., Willis, W. T., Chess, D. J., & Balaban, R. S. (2013). Effect of calcium on the oxidative phosphorylation cascade in skeletal muscle mitochondria. *Biochemistry*, 52(16), 2793-2809. <https://doi.org/10.1021/bi3015983>
- Greising, S. M., Corona, B. T., McGann, C., et al. (2019). Therapeutic Approaches for Volumetric Muscle Loss Injury: A Systematic Review and Meta-Analysis. *Tissue Engineering Part B: Reviews*, 25(6), 510-525. <https://doi.org/10.1089/ten.teb.2019.0207>
- Greising, S. M., Dearth, C. L., & Corona, B. T. (2016). Regenerative and rehabilitative medicine: a necessary synergy for functional recovery from volumetric muscle loss injury. *Cells Tissues Organs*, 202(3-4), 237-249.
- Greising, S. M., Rivera, J. C., Goldman, S. M., et al. (2017). Unwavering pathobiology of volumetric muscle loss injury. *Scientific reports*, 7(1), 1-14.
- Greising, S. M., Warren, G. L., Southern, W. M., et al. (2018). Early rehabilitation for volumetric muscle loss injury augments endogenous regenerative aspects of muscle strength and oxidative capacity. *BMC musculoskeletal disorders*, 19(1), 173-173. <https://doi.org/10.1186/s12891-018-2095-6>
- Grogan, B. F., & Hsu, J. R. (2011). Volumetric muscle loss. *J Am Acad Orthop Surg*, 19 Suppl 1, S35-37. <https://doi.org/10.5435/00124635-201102001-00007>
- Lander, N., Chiurillo, M. A., Bertolini, M. S., et al. (2018). Calcium-sensitive pyruvate dehydrogenase phosphatase is required for energy metabolism, growth, differentiation, and

- infectivity of *Trypanosoma cruzi*. *J Biol Chem*, 293(45), 17402-17417. <https://doi.org/10.1074/jbc.RA118.004498>
- Larouche, J., Greising, S. M., Corona, B. T., & Aguilar, C. A. (2018). Robust inflammatory and fibrotic signaling following volumetric muscle loss: a barrier to muscle regeneration. *Cell Death Dis*, 9(3), 409. <https://doi.org/10.1038/s41419-018-0455-7>
- Larouche, J. A., Fraczek, P. M., Kurpiers, S. J., et al. (2022). Neutrophil and natural killer cell imbalances prevent muscle stem cell-mediated regeneration following murine volumetric muscle loss. *Proc Natl Acad Sci U S A*, 119(15), e2111445119. <https://doi.org/10.1073/pnas.2111445119>
- Mohsin, A. A., Thompson, J., Hu, Y., et al. (2020). Endoplasmic reticulum stress-induced complex I defect: Central role of calcium overload. *Arch Biochem Biophys*, 683, 108299. <https://doi.org/10.1016/j.abb.2020.108299>
- Nichenko, A. S., Southern, W. M., Atuan, M., et al. (2016). Mitochondrial maintenance via autophagy contributes to functional skeletal muscle regeneration and remodeling. *American Journal of Physiology-Cell Physiology*, 311(2), C190-C200. <https://doi.org/10.1152/ajpcell.00066.2016>
- Panci, G., & Chazaud, B. (2021). Inflammation during post-injury skeletal muscle regeneration. *Seminars in Cell & Developmental Biology*, 119, 32-38. <https://doi.org/https://doi.org/10.1016/j.semcdb.2021.05.031>
- Qualls, A. E., Southern, W. M., & Call, J. A. (2021). Mitochondria-cytokine crosstalk following skeletal muscle injury and disuse: a mini-review. *Am J Physiol Cell Physiol*, 320(5), C681-c688. <https://doi.org/10.1152/ajpcell.00462.2020>
- Scrima, R., Cela, O., Agriesti, F., et al. (2020). Mitochondrial calcium drives clock gene-dependent activation of pyruvate dehydrogenase and of oxidative phosphorylation. *Biochim Biophys Acta Mol Cell Res*, 1867(11), 118815. <https://doi.org/10.1016/j.bbamcr.2020.118815>
- Smith, C., Kruger, M. J., Smith, R. M., & Myburgh, K. H. (2008). The Inflammatory Response to Skeletal Muscle Injury. *Sports Medicine*, 38(11), 947-969. <https://doi.org/10.2165/00007256-200838110-00005>
- Southern, W. M., Nichenko, A. S., Shill, D. D., et al. (2017). Skeletal muscle metabolic adaptations to endurance exercise training are attainable in mice with simvastatin treatment. *PLoS one*, 12(2), e0172551. <https://doi.org/10.1371/journal.pone.0172551>
- Southern, W. M., Nichenko, A. S., Tehrani, K. F., et al. (2019). PGC-1 $\alpha$  overexpression partially rescues impaired oxidative and contractile pathophysiology following volumetric muscle loss injury. *Scientific reports*, 9(1), 1-17.
- Southern, W. M., Nichenko, A. S., Tehrani, K. F., et al. (2019). PGC-1 $\alpha$  overexpression partially rescues impaired oxidative and contractile pathophysiology following volumetric muscle loss injury. *Scientific reports*, 9(1), 4079-4079. <https://doi.org/10.1038/s41598-019-40606-6>
- Thome, T., Salyers, Z. R., Kumar, R. A., et al. (2019). Uremic metabolites impair skeletal muscle mitochondrial energetics through disruption of the electron transport system and matrix dehydrogenase activity. *Am J Physiol Cell Physiol*, 317(4), C701-C713. <https://doi.org/10.1152/ajpcell.00098.2019>
- Zhang, J., Zhang, L., Nie, J., et al. (2021). Calcineurin inactivation inhibits pyruvate dehydrogenase complex activity and induces the Warburg effect. *Oncogene*, 40(49), 6692-6702. <https://doi.org/10.1038/s41388-021-02065-0>

CHAPTER 3  
PHARMACEUTICAL AGENTS FOR CONTRACTILE-METABOLIC DYSFUNCTION  
AFTER VML INJURY<sup>3</sup>

---

<sup>3</sup>McFaline-Figueroa, J., Schifino, A. G., Nichenko, A. S., Lord, M. N., Hunda, E. T., Winders, E. A., ... & Call, J. A. (2022). Pharmaceutical agents for contractile-metabolic dysfunction after volumetric muscle loss. *Tissue Engineering Part A*, 28(17-18), 795-806.

## **Abstract**

Volumetric muscle loss (VML) injuries represent a majority of military servicemember casualties and are common in civilian populations following blunt and/or penetrating traumas. Characterized as a skeletal muscle injury with permanent functional impairments, there are currently no standards for rehabilitation, leading to life-long disability. Toward developing rehabilitative strategies, previous research demonstrates that the remaining muscle after a VML injury lacks similar levels of plasticity or adaptability as healthy, uninjured skeletal muscle. This may be due in part to impaired innervation and vascularization of the remaining muscle as well as disrupted molecular signaling cascades commonly associated with muscle adaptation. The primary objective of this study was to assess the ability of four pharmacological agents with a strong record of modulating muscle contractile and metabolic function to improve functional deficits in a murine model of VML injury. Male C57BL/6 mice underwent a 15% multi-muscle VML injury of the posterior hindlimb and were randomized into drug treatment groups (formoterol, AICAR, pioglitazone, or sildenafil) or untreated VML group. At the end of 60 days, the injury model was first validated by comparison to age-matched injury naïve mice. Untreated VML mice had 22% less gastrocnemius muscle mass, 36% less peak-isometric torque, and 27% less maximal mitochondrial oxygen consumption rate compared to uninjured mice ( $p < 0.01$ ). Experimental drug groups were, then, compared to VML untreated, and there was minimal evidence of efficacy for AICAR, pioglitazone, or sildenafil in improving contractile and metabolic functional outcomes. However, formoterol-treated VML mice had 18% greater peak-isometric torque ( $p < 0.01$ ) and permeabilized muscle fibers had 36% greater State III mitochondrial oxygen consumption rate ( $p < 0.01$ ) compared to VML untreated, suggesting an overall improvement in muscle condition. There was minimal evidence that these benefits came from greater mitochondrial biogenesis and/or

mitochondrial complex protein content but could be due to greater enzyme activities levels for complex I and complex II. These findings suggest that formoterol treatment is candidate to pair with a rehabilitative approach to maximize functional improvements in VML-injured muscle.

Keywords: muscle strength, traumatic injury, regenerative rehabilitation, mitochondria respiration

### **Impact Statement**

Volumetric muscle loss (VML) injuries result in deficiencies in strength and mobility that have a severe impact on patient quality of life. Despite breakthroughs in tissue engineering, there are currently no treatments available that can restore function to the affected limb. Our data show that treatment of VML injuries with clinically available and FDA-approved formoterol, a beta-agonist, significantly improves strength and metabolism of VML-injured muscle. Formoterol is therefore a promising candidate for combined therapeutic approaches (i.e., regenerative rehabilitation) such as pairing formoterol with structured rehabilitation or cell-seeded biomaterials as it may provide greater functional improvements than either strategy alone.

### **Introduction**

Volumetric muscle loss (VML) injuries are characterized by the large-scale loss of tissue due to traumatic event or necessary surgical removal(Corona et al., 2016; Garg et al., 2015; Greising et al., 2016; Grogan et al., 2011). The extent of this loss overwhelms the remaining muscle's ability to repair and regenerate, leading to a skeletal muscle dysfunction, limitations in mobility, and overall decline of patient quality of life(Corona et al., 2015). As it stands, there exists no long-term support for skeletal muscle tissues after VML injuries due to a lack of clinical standards of care to

address the damage or to systematically address the functional decline after trauma(Frenkel & Aronow, 2020; Grogan et al., 2011). Several studies in the regenerative medicine field have responded with the development of approaches that replace and/or stimulate the *de novo* growth of skeletal muscle tissue within the VML injury defect. However, these approaches have not been rigorously demonstrated to rescue function(Das et al., 2020; Greising et al., 2019; Lalegül-Ülker et al., 2019; Mori et al., 2015; Nakayama et al., 2019).

An alternative approach to replacing or regenerating the lost muscle is to focus efforts on maximizing the quality and/or quantity of the remaining muscle after a VML injury. The remaining muscle typically represents a larger mass than that which could possibly be regenerated and, while limited, portions of the remaining muscle maintain partial innervation and vascularity(Anderson et al., 2019; Sorensen et al., 2021). A significant hurdle to treatment is that the contractile properties and metabolic function (i.e., oxygen consumption and mitochondrial enzyme activities) of the remaining muscle are significantly impaired following VML injury(Chao et al., 2019; Dalske et al., 2021; Dienes et al., 2021; Greising et al., 2018; Southern et al., 2019; Ziemkiewicz et al., 2022). This decline in contractile and metabolic function is due to a combination of factors, including, the loss of contractile units and replacement with fibrotic tissue, severe inflammatory response, and structural damage to the mitochondrial network(Aguilar et al., 2018; Corona et al., 2013; Corona et al., 2016; Greising et al., 2016; Greising et al., 2017; Hoffman et al., 2021; Hyldahl et al., 2015; Larouche et al., 2018; Shayan & Huang, 2020; Southern et al., 2019). Therapeutic modalities to enhance muscle function after VML will need to address these underlying pathophysiology in order to advance toward a clinical standard.

Metabolic function is a component of skeletal muscle physiology that is often overlooked in regenerative medicine therapy; but importantly, metabolism plays a critical role in meeting the

energy demands associated with muscle repair and regeneration(Duguez et al., 2002; Nichenko et al., 2016; Wagatsuma et al., 2011; Wang et al., 2013) and single hindlimb VML injury influences whole-body metabolism in mice, highlighting the significance of muscle metabolism on whole-body homeostasis(Dalske et al., 2021). Previously, a forced over-expression of the transcription factor PGC-1 $\alpha$  (peroxisome proliferator-activated receptor gamma, cofactor 1 alpha) partially rescued contractile and metabolic function of muscle tissue after a VML injury(Southern et al., 2019). PGC-1 $\alpha$  drives metabolic gene expression and this approach was a proof-of-concept demonstrating that addressing metabolic deficits in VML-injured muscle is worth further investigation as a therapeutic strategy. However, virogenetic manipulation is not currently a feasible approach for a clinical setting. Thus, our goal was to evaluate alternative approaches to produce a similar functional rescue in remaining muscle metabolic function with clinical feasibility in mind. To this end, four pharmacological adjuvants (AICAR, pioglitazone, sildenafil, and formoterol), with previous history of improving muscle function, were tested herein.

We chose these four agents based on the likelihood they would address the sustained deficiencies in strength and mitochondrial metabolic function that is characteristic of VML(Chao et al., 2019; Dalske et al., 2021; Dienes et al., 2021; Greising et al., 2018; Southern et al., 2019; Ziemkiewicz et al., 2022). AICAR (5-aminoimidazole-4-carboxamide riboside) is an adenosine monophosphate (AMP) analog capable of acting on the AMP-dependent protein kinase (AMPK). Use of AICAR has been shown to prevent cachectic muscle wasting(Hall et al., 2018), decrease inflammatory signaling in skeletal muscle models of diabetes(Lihn et al., 2008), and improve contractile properties in fukutin-deficient mice(Southern et al., 2020). Pioglitazone (PIO) is a PPAR agonist that modulates insulin sensitivity(Fiorentino et al., 2021; Skov et al., 2008; Yokota et al., 2017) and can ameliorate mitochondrial dysfunction caused by diseases like diabetes,

metabolic syndrome, and polycystic ovary syndrome(Fiorentino et al., 2021; Rabøl et al., 2010; Skov et al., 2008; Takada et al., 2014; Wessels et al., 2015; Yokota et al., 2017). Sildenafil (SIL) is a competitive phosphodiesterase-5 inhibitor that prevents the breakdown of cGMP by modulating nitric oxide, a known regulator of skeletal muscle function. Use of SIL has been reported to improve mitochondrial metabolism(Nyberg et al., 2015), improve Ca<sup>2+</sup> storage and use in muscle fibers(Huang et al., 2016), and reduces exercise-induced skeletal muscle damage in models of muscular dystrophy(Batra et al., 2019; Nelson et al., 2014). Formoterol (FOR) is a bronchodilator present in long-lasting inhalers that binds to  $\beta_2$ -adrenergic receptors ( $\beta_2$ AR), a type of G-protein coupled receptor (GPCR) that is abundant in skeletal muscle. It has been successfully used to improve the oxidative capacity of skeletal muscle(Sullo et al., 2013), muscle force production(Natalie E. Scholpa et al., 2019) increase mitochondrial biogenesis and function(Gómez-SanMiguel et al., 2016; Kenley et al., 2008; Penna et al., 2019; Salazar-Degracia et al., 2018), prevent muscle wasting(Conte et al., 2011; Ryall et al., 2006), and promote muscle regeneration and hypertrophy(Conte et al., 2011; Ryall et al., 2006). Taken together, there was sufficient evidence to believe these four treatments offered the most promising outcomes to be tested on VML injury.

Considering this breadth of evidence in improving skeletal muscle strength and metabolism in other disease models, we hypothesized that the administration of these drugs would lead to functional improvement in VML-injured muscle. In lieu of advancing the molecular signaling events associated with these pharmaceuticals, the primary objective here was to test the efficacy of these agents to improve contractile and metabolic function in the remaining muscle after VML injury.

## **Materials and Methods**

### *Animals:*

Male C57BL/6 mice were housed at 20-23 °C on a 12:12-hr light-dark cycle, with food and water provided ad libitum. At the time of randomization to experimental groups, all mice were between 10-11 weeks of age (pre-surgical mass  $26.76 \pm 1.75$  g). All procedures were approved and performed in accordance with the guidelines and regulations of the Institutional Animal Care and Use Committee at the University of Georgia.

### *Experimental design:*

VML-injured mice underwent unilateral VML injury and then were randomized into one of the following experimental groups: AICAR (n=9), PIO (n=15), FOR (n=15), SIL (n=10), or no treatment (VML, n=15). A cohort of injury naïve mice (n=9) were included as uninjured controls and did not receive any pharmaceutical intervention. Uninjured mice were statistically compared to VML untreated to validate the injury model compared to previous studies in terms of muscle mass, strength, and metabolic function. Administration of pharmacological adjuvants for the experimental VML groups started 24-hours post-injury and continued to two months. This duration of treatment was selected in the hopes of surpassing the point of sustained inflammation, which has been observed up to 28 days following VML injury (Aguilar et al., 2018). Drugs were incorporated directly into normal mouse chow (TestDiet, Richmond, IA) in the FOR (0.3 mg/kg/day), SIL (1 mg/kg/day), and PIO (20 mg/kg/day) groups, and animals were allowed to feed ad libitum. The AICAR group received daily subcutaneous injections (250 mg/kg aqueous solution) for the duration of the experiment. Doses were chosen after review of previous work on the effect of each of the drugs on muscle and key references (Adamo et al., 2010; Busquets et al., 2011; Frias et al., 2016; Goto et al., 2013; Halseth et al., 2002; Kobilo et al., 2014; Moon et al.,

2017; Narkar et al., 2008; Pagel-Langenickel et al., 2008; Penna et al., 2019; Percival et al., 2012; Sanchis-Gomar et al., 2014; Sasaki et al., 2014; Natalie E. Scholpa et al., 2019; Toledo et al., 2016; Valatsou et al., 2017). At the study endpoint, muscle mass, muscle strength, and metabolic function were assessed.

*Surgical creation of VML injury:*

A dose of Buprenorphine (1.2 mg/kg) was given pre-operatively. A VML injury was performed unilaterally on the posterior compartment of anesthetized (isoflurane 1.5-2.0%) mice as previously described (Greising et al., 2018; Southern et al., 2019). Briefly, left hindlimbs were prepared by removing hair and the skin was aseptically prepared. An incision was made in the posterior of the limb to expose the muscle. Fascia and hamstrings were separated from the gastrocnemius muscle through blunt dissection. A small metal plate was inserted behind the gastrocnemius and soleus muscles and a 4-mm biopsy punch was used to remove a  $23.9 \pm 3.7$  mg portion. Skin was re-approximated using 5-0 vicryl sutures. Buprenorphine (1.2 mg/kg) was given at 12 and 24 hours and Meloxicam (2.0 mg/kg) was given at 24-, 48-, and 72-hours post-procedure.

*In vivo muscle strength:*

Peak-isometric torque of the left hindlimb plantarflexor muscles (soleus/gastrocnemius/plantaris muscles) was assessed *in vivo* as previously described (Baltgalvis et al., 2012; Call & Lowe, 2016). Briefly, mice were anaesthetized using 1.5-3.0% isoflurane at an oxygen flowrate of 0.4L/min. The left hindlimb was depilated and aseptically prepared before the peroneal nerve was severed. The foot was placed in a custom footplate attached to a servomotor (Model 300C-LR; Aurora Scientific, Aurora, Ontario, Canada), and platinum-iridium needle electrodes (Model E2-12; Grass Technologies, West Warwick, RI) were placed percutaneously on either side of the sciatic nerve

to elicit isolated contraction of the hindlimb plantarflexors. Peak-isometric torque was measured at stable body temperature (37°C) with the ankle joint maintained at 90° by a magnetic stabilizer clamp on the knee. Peak-isometric torque was defined as the greatest torque measured during a 250-ms stimulation using 1-ms square-wave pulses at a frequency ranging from 150 to 200 Hz. Stimulation parameters were optimized between 0.6 and 3.0 mA (Model 701C; Aurora Scientific) and were determined by 0.1 mA step increases until an increase in amperage resulted in no further increase in torque produced. Fatigability of the plantarflexors was assessed with 90 submaximal contractions performed over 3 minutes using 250-ms stimulations at 60 Hz stimulation frequency. Following functional measurements, mice were euthanized via CO<sub>2</sub> inhalation and cervical dislocation, and hindlimb muscles were processed for additional analyses.

#### *Oxygen consumption of permeabilized muscles*

High resolution respirometry (Oroboros O2k) of permeabilized muscle fibers was used to assess mitochondrial oxygen consumption rates as previously described (Nichenko et al., 2021; Southern et al., 2019). Briefly, the medial portion of the gastrocnemius muscle, adjacent to the injury site, was dissected into fiber bundles and permeabilized with saponin as previously described. Mitochondrial leak respiration was accomplished by the addition of glutamate (10mM), malate (5mM), succinate (10mM). State III respiration was accomplished by adding ADP (5mM) after leak respiration had been recorded. After state III respiration was reached, Cytochrome C (10µM) was added to assess mitochondrial membrane quality to ensure no damage was obtained during the muscle fiber bundle dissection and permeabilization steps. Any test where a cytochrome C rate exceeded a 10% increase over the state III respiration rate was deemed damaged and excluded from further analysis. Finally, FCCP (1µM) was added to obtain an uncoupled respiration rate. Baseline rates (i.e., the rate before any substrates are added) were subtracted out from all

other rates and rates were normalized to wet weight of muscle fiber bundles added to chamber and citrate synthase values to account for differences in mitochondrial content(Southern et al., 2019).

#### *Citrate synthase activity*

Mitochondrial content was analyzed by citrate synthase enzyme (CS) activity as previously described(Southern et al., 2019). Briefly, following muscle fiber collection for oxygen consumption experiments, the remainder of the gastrocnemius muscle was chopped into fine pieces and mixed. Approximately 40 mg of muscle was weighed and further homogenized in 33mM phosphate buffer (pH 7.4) at a muscle to buffer ratio of 1:40 using a glass tissue grinder. Homogenate was incubated with 5,5'-dithio-bis(2-nitrobenzoic acid (DTNB, 0.773mM), acetyl CoA (0.116mM), and oxaloacetate (0.441mM) in 100mM Tris buffer (pH 8.0). Activity of citrate synthase was monitored from the reduction of DTNB over time via measurement of absorbance at 412nm.

#### *Assessment of mitochondrial respiratory complex activity*

Activity for each mitochondrial respiratory complex was measured using a protocol modified from Thome, et al(Thome et al., 2019). Complex I activity was measured in 50mM potassium phosphate buffer, 3mg/mL BSA, 240  $\mu$ M KCN, 0.4  $\mu$ M antimycin A, 50  $\mu$ M decyl-ubiquinone, and 80  $\mu$ M 2,6-dichlorophenolindophenol (DCPIP). NADH oxidation was measured through the reduction of DCPIP at 600 nm. Complex II activity was measured in buffer containing 10 mM  $\text{KH}_2\text{PO}_4$ , 2 mM EDTA, and 1 mg/mL BSA at pH 7.8 and supplemented with 0.2 mM ATP, 10 mM succinate, and 0.08 mM DCPIP. Following a 10-minute incubation, at 37°C, the assay was initiated by the addition of oxidized decyl-ubiquinone (0.08 mM) and reduction of DCPIP followed at 600 nm. Succinate dehydrogenase (SDH) activity was measured as described previously(Dalske et al.,

2021; Foltz et al., 2016; Nichenko et al., 2021). Muscle homogenate was sequentially incubated with 16.2 mM sodium succinate and 0.32 mM sodium cyanide before adding assay buffer containing 0.327 mM AlCl<sub>3</sub>, 0.327 mM CaCl<sub>2</sub> and 0.021 mM cytochrome c. SDH activity was monitored via the reduction of cytochrome c at 550 nm.  $\beta$ -hydroxyacyl CoA dehydrogenase ( $\beta$ -HAD) activity was measured by incubating muscle homogenate in a buffer containing 100 mM triethanolamine, 0.451 mM  $\beta$ -nicotinamide adenine dinucleotide (NADH) and 5 mM ethylenediaminetetraacetic acid (EDTA), as described previously(Call et al., 2008; Nichenko et al., 2016; Southern et al., 2017). Acetoacetyl CoA (0.1 mM) was used to start the reaction. Activity of  $\beta$ -hydroxy acyl CoA dehydrogenase was monitored from the oxidation of NADH over time as determined by its absorbance at 340 nm.

#### *Quantitative Real Time PCR (RT-qPCR)*

RNA was isolated from frozen tibialis anterior muscles from FOR-treated and untreated VML-injured muscles using a RNeasy kit (QIAGEN). cDNA was generated using a High-Capacity cDNA Reverse Transcription Kit (Applied Biosystems). Universal SYBR Green Supermix (Bio-Rad) and the following sequence-specific primer was used to assess mRNA levels for the following: *PGC-1 $\alpha$*  and *PGC-1 $\beta$*  were evaluated to assess mitochondrial biogenesis; *COXIV*, *ND-1*, *ND6*, and *NDUFB6* were probed to assess the electron transport chain; *Fos* was probed due to previous studies showing FOR treatment modulating its expression(Kellenberger et al., 1998) (Supplemental Table 2). Expression was normalized to the expression of the *18S* gene. Relative gene expression was calculated using the  $2^{-\Delta\Delta CT}$  method.

## Statistical Analysis

All data is represented as mean  $\pm$  standard deviation. A two-tailed, unpaired t-test was used to validate the injury model (i.e., VML untreated) against uninjured. A one-way ANOVA was used to determine differences between VML untreated and VML-injured mice receiving a pharmacological agent with Dunnett's test for post-hoc analyses. Statistically significant differences are indicated when the p-value was less than or equal to 0.05, and statistical trends are noted if a p-value was between 0.05 and 0.10. All statistical analyses were performed on Prism statistical software (GraphPad, San Diego, CA, Version 8).

## Results

### *Drug treatment effect on body mass and muscle quantity*

Table 3.1: Mouse body mass and gastrocnemius muscle mass

	Experimental Group					OWA p-value
	VML	AIC	PIO	FOR	SIL	
Body Mass (g)	31.81 $\pm$ 1.54	29.60 $\pm$ 0.92 <sup>#</sup>	31.24 $\pm$ 2.28	32.00 $\pm$ 1.55	30.85 $\pm$ 2.00	0.0274
Gastrocnemius Mass (mg)	139.6 $\pm$ 33.3	146.2 $\pm$ 28.1	145.9 $\pm$ 24.1	174.8 $\pm$ 16.7 <sup>#</sup>	158.2 $\pm$ 20.8	0.0037
Gastroc: BM	4.19 $\pm$ 0.98	4.95 $\pm$ 0.90	4.65 $\pm$ 0.76	5.43 $\pm$ 0.50 <sup>#</sup>	5.12 $\pm$ 0.55 <sup>#</sup>	0.0037

Values are means  $\pm$  SD

<sup>#</sup>Different from VML

VML-injured muscle suffers from a permanent deficit in muscle mass as well as impaired contractile and metabolic function compared to uninjured muscle (Greising et al., 2018; Southern et al., 2019). Herein, untreated VML mice had 22% less gastrocnemius muscle mass, 36% less peak-isometric torque, and 27% less maximal oxygen consumption rate compared to uninjured mice (Figure 3.1). We first evaluated the effectiveness of our chosen treatments at increasing muscle mass 60 days following VML injury in comparison to a VML injury left untreated. FOR-treated mice had both 20% larger VML-injured gastrocnemius muscles (Dunnett's  $p=0.0015$ ) and

a 23% higher gastrocnemius muscle to body mass ratio (Dunnett's  $p=0.0012$ ; Table 3.1) compared to untreated VML. SIL-treated mice had an 18% higher gastrocnemius muscle to body mass ratio (Dunnett's  $p=0.0471$ ). These data show that several candidate pharmacological agents resulted in muscle-specific mass changes. We next sought to determine the extent to which these changes affected VML-injured muscle function.

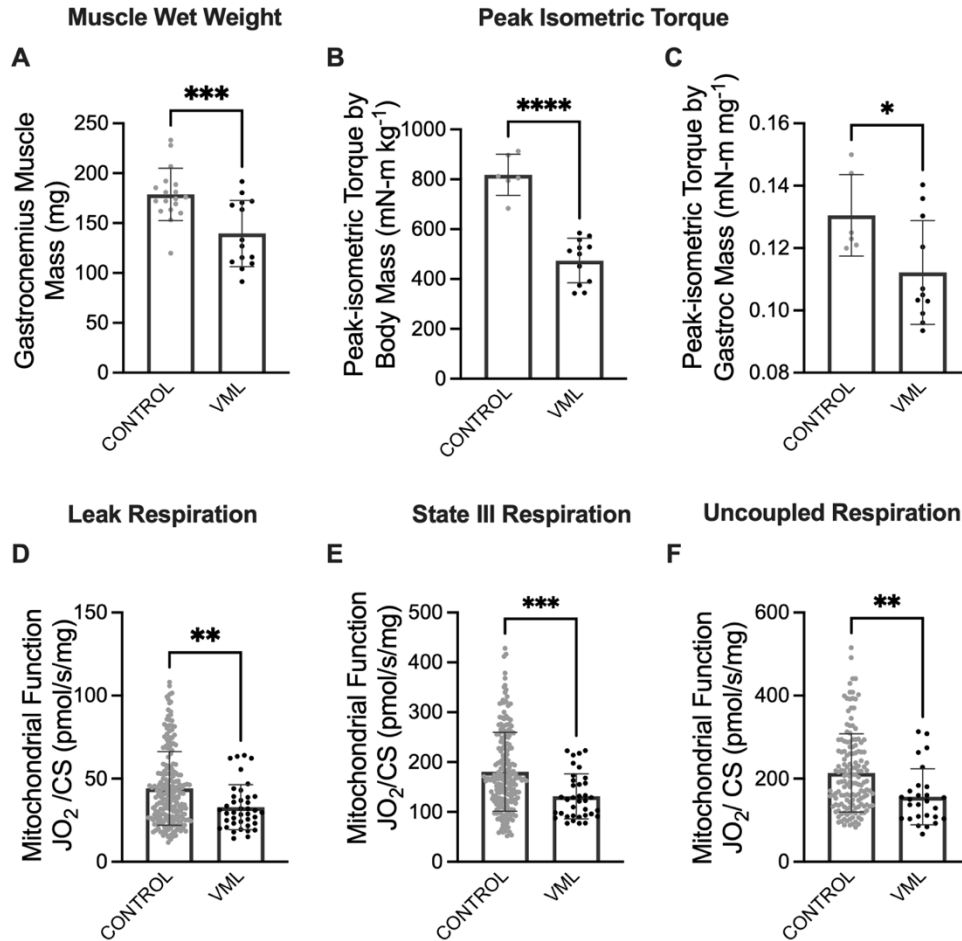


**Figure 3.1:** VML-injured tissue has a contractile and metabolic deficit compared to uninjured control limbs. **A.** Gastrocnemius muscle mass is significantly reduced following VML injury. Peak isometric torque normalized by kilograms of body mass ( $\text{kg}^{-1}$ , **B**) and milligrams of gastrocnemius muscle mass ( $\text{mg}^{-1}$ , **C**) is significantly reduced in VML-injured limbs compared to uninjured controls. Similarly, oxygen consumption driven by Leak (**D**), State III (**E**), and Uncoupled (**F**) respiration is significantly reduced in VML injured tissue compared to healthy, uninjured Controls. In panels **D-F** pmol/s/mg is the rate of oxygen flux per milligram of tissue. Data analyzed by Student's t-test, \* denotes differences compared to uninjured Controls of  $p \leq 0.05$ . Data are means  $\pm$  SD.

*Strength, fatigue, and contractile properties following treatment*

Contractile function was assessed by measuring peak isometric torque of the plantarflexors. Normalized to body mass ( $\text{mN}\cdot\text{m kg}^{-1}$ ), FOR-treated mice produced  $\sim 18\%$  greater peak-isometric torque than of untreated VML mice (Dunnett's  $p=0.0024$ , Figure 3.2A). When normalized to gastrocnemius muscle mass ( $\text{mN}\cdot\text{m mg}^{-1}$ ), however, there were no significant differences across treated and untreated VML-injured mice (Dunnett's  $p=0.0526$ , Figure 3.2B). Peak-isometric torque tracings were also evaluated for changes in contractile properties with injury and treatment (Figure 3.2C). Rate of contraction development was  $\sim 29\%$  greater in FOR-treated mice compared to that of untreated VML mice (Dunnett's  $p=0.0157$ , Table 3.2). There were no differences across treated and untreated groups for all other contractile properties, including time-to-peak contraction, half-relaxation time, and submaximal torques at 40 and 60 Hz relative to peak (Table 3.2). These data suggest strength gains in FOR-treated mice is driven by greater muscle mass.

Table 3.2. Contractile Properties

	Experimental Group					OWA p-value
	VML	AIC	PIO	FOR	SIL	
Avg +dP/dt (mN-m/s)	280.6 $\pm$ 64.4	289.1 $\pm$ 57.7	327.1 $\pm$ 56.3	364.0 $\pm$ 93.0 <sup>#</sup>	308.8 $\pm$ 77.8	0.0385
Avg -dP/dt (mN-m/s)	336.6 $\pm$ 61.6	332.6 $\pm$ 84.5	377.6 $\pm$ 91.1	416.7 $\pm$ 100.6	360.3 $\pm$ 85.5	0.0037
Time to Peak (s)	0.077 $\pm$ 0.011	0.079 $\pm$ 0.013	0.078 $\pm$ 0.013	0.073 $\pm$ 0.015	0.078 $\pm$ 0.012	0.8184
½ RT (s)	0.053 $\pm$ 0.005	0.052 $\pm$ 0.009	0.053 $\pm$ 0.009	0.052 $\pm$ 0.009	0.051 $\pm$ 0.004	0.9711
40 Hz/Peak	0.43 $\pm$ 0.14	0.49 $\pm$ 0.16	0.48 $\pm$ 0.17	0.48 $\pm$ 0.18	0.45 $\pm$ 0.17	0.8870
60 Hz/Peak	0.75 $\pm$ 0.11	0.78 $\pm$ 0.09	0.76 $\pm$ 0.10	0.77 $\pm$ 0.11	0.77 $\pm$ 0.06	0.9261

Values are means  $\pm$  SD. OWA= One-Way ANOVA

<sup>#</sup>Different from VML

A contractile fatigue protocol was used to assess muscle fatigue. Percentage of torque loss was calculated by comparing the torque generated at the first contraction vs the final contraction

(90<sup>th</sup>; Figure 3.2D). Only AICAR-treated mice had less torque loss compared to untreated VML mice, suggesting less fatigability (-48% vs -61%, Dunnett's  $p=0.0004$ ; Figure 3.2E).

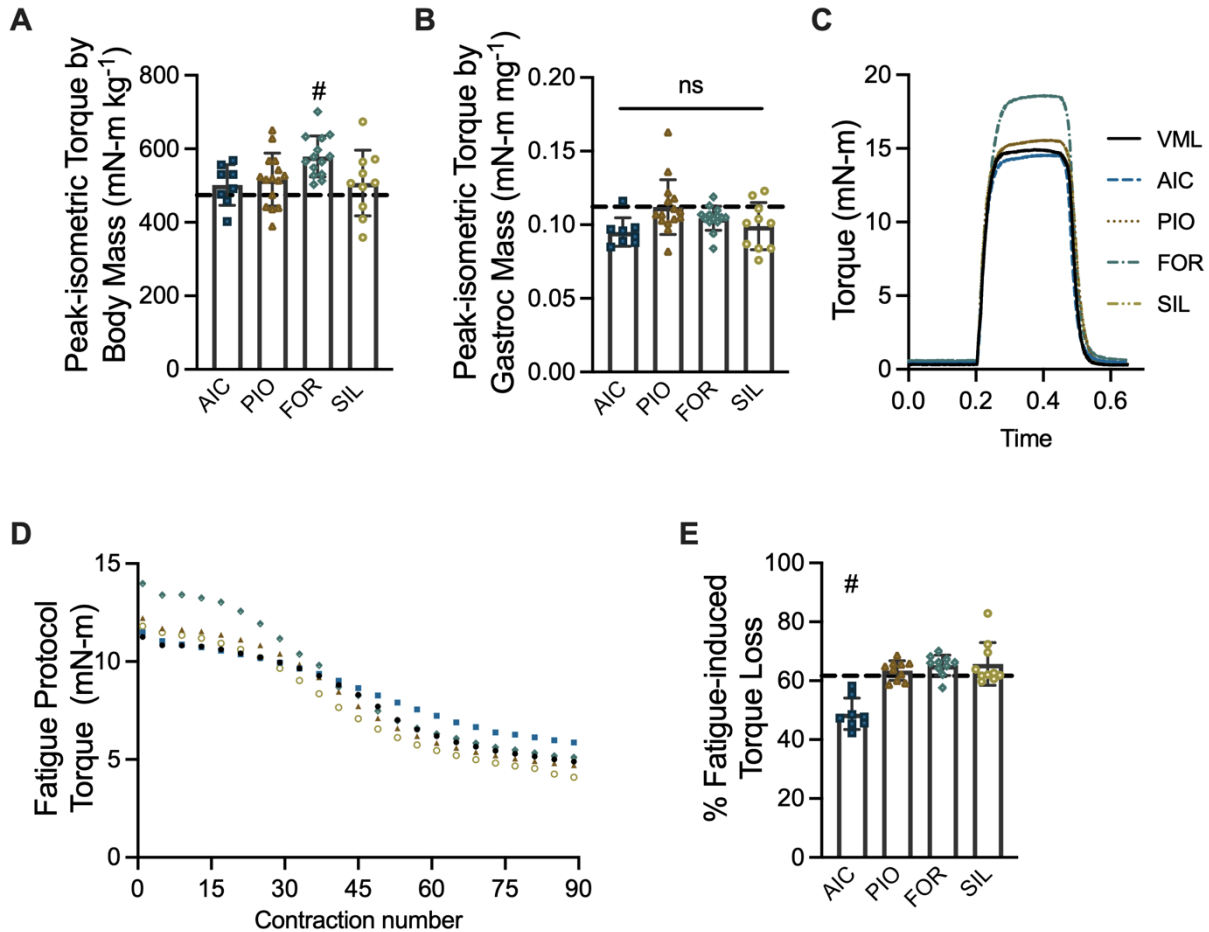
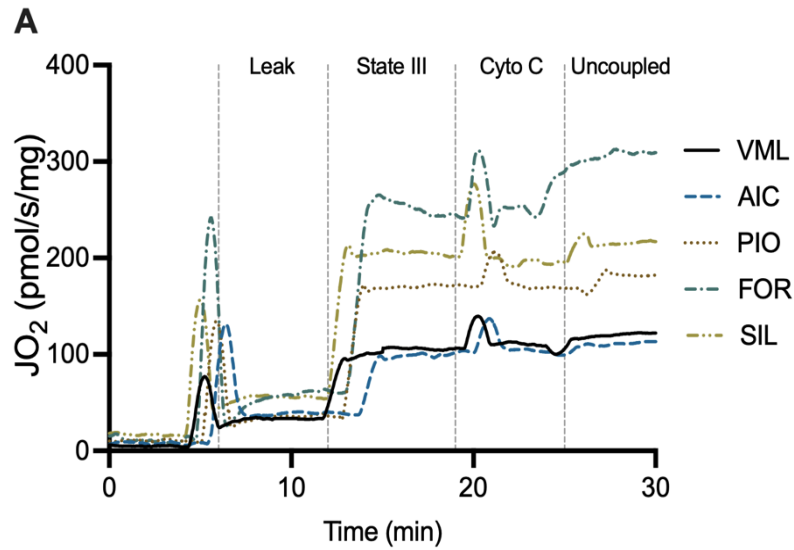


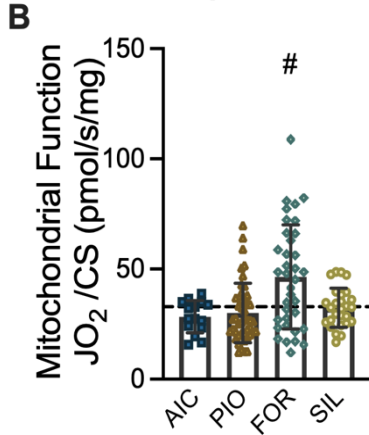
**Figure 3.2:** Effect of pharmacological adjuvant administration on the contractile function of VML-injured limbs. **A.** Peak-isometric torque normalized to kilograms of body mass was significantly higher in formoterol-treated mice compared to untreated VML mice (dashed line). **B.** However, when peak isometric force is normalized to milligrams of gastrocnemius muscle mass, there is no significant difference between treated and untreated VML mice (dashed line). **C.** Torque tracings of tetanic contractions were analyzed to determine contractile properties for experimental and control group. **D.** Torque tracings throughout the fatigue protocol were used to analyze contractile force loss. **E.** Post-fatigue torque loss did not improve with treatment and was significantly less in AICAR-treated animals compared to untreated VML mice (dashed line). Data analyzed by one-way ANOVA, # denotes differences compared to untreated VML of  $p \leq 0.05$ . Data are means  $\pm$  SD.

### *Oxygen Consumption of treated muscle fibers*

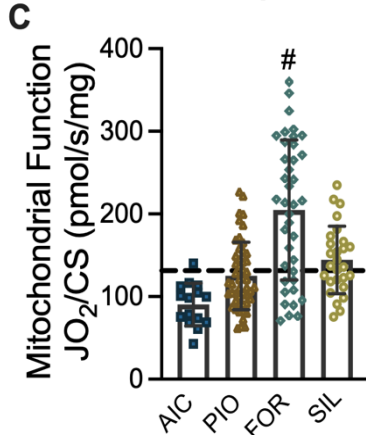
Metabolic function was assessed via oxygen consumption rate of permeabilized gastrocnemius muscle fibers at leak, State III, and uncoupled respiratory states (Figure 3A). Oxygen consumption rates are shown normalized to CS activity to account for mitochondrial content (Dunnett's  $p=0.0347$ , Table 3)(Larsen et al., 2012). The oxygen consumption rate during Leak state respiration was ~41% greater in FOR-treated mice than it was in untreated VML controls (Dunnett's  $p=0.0007$ , Figure 3B). Oxygen consumption rates during State III respiration were 36% greater in FOR-treated mice compared to untreated VML controls (Dunnett's  $p<0.0001$ , Figure 3C). Oxygen consumption rates during uncoupled respiration was 53% higher in FOR-treated mice compared to untreated VML controls (Dunnett's  $p=0.0001$ , Figure 3D). The addition of cytochrome C had no significant effect on oxygen consumption rates supporting that permeabilized muscle fiber bundles were without significant damage (Figure 3E).



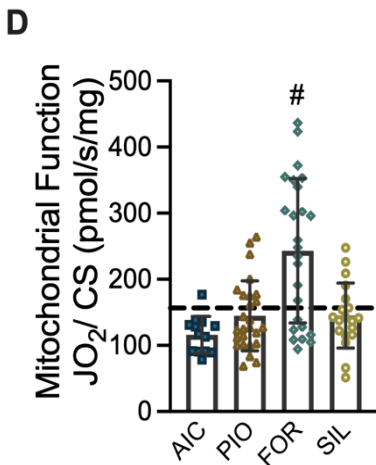
**B Leak Respiration**



**C State III Respiration**



**D Uncoupled Respiration**



**E Cytochrome C test**

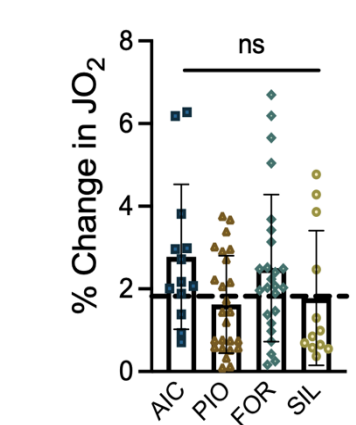


**Figure 3.3:** Drug treatments improved oxidative capacity following VML injury. **A.** Pharmacological adjuvants had no adverse effects on normal oxygen consumption, nor did it affect the integrity of the mitochondria. In all oxygen consumption experiments, oxygen flux rates were normalized to mass of permeabilized muscle fiber and mitochondrial content. FOR treatment significantly improved oxygen consumption during Leak (**B**), State III (**C**), and Uncoupled (**D**) respiration when compared to untreated VML mice. **E.** Titration of cytochrome C had no significant effect on oxygen consumption rates, corroborating that permeabilized muscle fibers evaluating had not undergone significant damage. Data analyzed by one-way ANOVA, # denotes differences compared to untreated VML of  $p \leq 0.05$ . Data are means  $\pm$  SD.

### Mitochondrial Enzyme Analysis

Further analysis of metabolic function and muscle oxidative capacity was assessed by mitochondrial enzyme activity of the two primary electron transport chain complexes for electron carrier oxidation. Complex I activity for both AICAR- and FOR-treated mice was significantly greater than VML untreated (~31.7% greater, Dunnett's  $p=0.0193$ , Table 3). Complex II activity was 45% greater in FOR-treated mice compared to untreated VML (Dunnett's  $p=0.0188$ , Table 3). To supplement these findings, mitochondrial capacity to oxidize specific substrates, namely carbohydrates and fats, was evaluated by enzyme activity of succinate dehydrogenase (SDH) and  $\beta$ -hydroxyacyl CoA dehydrogenase ( $\beta$ -HAD), respectively. SDH activity was 48.7% higher in SIL-treated mice than VML untreated (Dunnett's  $p=0.0029$ , Table 3).  $\beta$ -HAD activity was significantly greater in FOR-treated mice than in untreated VML mice (29.0% greater, Dunnett's  $p=0.0187$ , Table 3). Overall, oxygen consumption rates and mitochondrial enzyme assays suggest a modest effect of FOR treatment on skeletal muscle metabolic function.

Table 3.3: Mitochondrial Enzyme Activity

Enzymatic Activity ( $\mu\text{mol}/\text{min}/\text{g}$ )	Experimental Group					OWA p-value
	VML	AIC	PIO	FOR	SIL	
Citrate Synthase	429.0 $\pm$ 141.9	494.7 $\pm$ 92.9	356.1 $\pm$ 104.6	323.6 $\pm$ 135.0 <sup>#</sup>	353.2 $\pm$ 78.8	0.0070
Succinate Dehydrogenase	6.96 $\pm$ 2.98	8.14 $\pm$ 4.07	7.71 $\pm$ 3.98	8.64 $\pm$ 4.44	12.21 $\pm$ 3.96 <sup>#</sup>	0.0163
$\beta$ -Hydroxyacyl CoA Dehydrogenase	32.07 $\pm$ 13.02	30.94 $\pm$ 8.19	39.32 $\pm$ 10.99	45.17 $\pm$ 14.12 <sup>#</sup>	0.078 $\pm$ 0.012	0.0294
Complex I	17.88 $\pm$ 2.87	23.51 $\pm$ 3.03	19.72 $\pm$ 4.13	23.57 $\pm$ 6.47 <sup>#</sup>	17.09 $\pm$ 3.51	0.0010
Complex II	57.49 $\pm$ 26.70	42.11 $\pm$ 6.33	60.93 $\pm$ 17.61	83.47 $\pm$ 28.93 <sup>#</sup>	62.29 $\pm$ 18.94	0.0032

Enzymatic activity normalized to citrate synthase activity as a measure of mitochondrial content. Enzymatic activity is represented as micromoles of product generated per minute per gram of protein. Values are means  $\pm$  SD. OWA= One-Way ANOVA

<sup>#</sup>Different from VML

### Mitochondrial Gene and Protein Expression

Based on the data collected throughout this study, it is apparent that the treatment of VML-injured muscle with FOR helped improve contractile and metabolic function. To determine whether these improvements are attributable to changes in the expression of mitochondrial metabolism-specific genes and/or proteins, tibialis anterior (TA) muscles were analyzed from the VML-injured untreated and FOR-treated mice. The TA muscle was used due to lack of leftover biological material from the injured gastrocnemius muscle. However, we chose the TA muscle from the injured limb for its proximity to the injury site and because it is subject to the inflammatory process as the gastrocnemius muscle heals. FOR treatment did not change *PGC-1 $\alpha$*  or *c-Fos* expression compared to VML untreated controls, and furthermore, *PGC-1 $\beta$*  and *COX-IV* expression was significantly lower (~24 and 26% reduction, respectively). In contrast, mRNA content for *ND-6* and *NDUFB6*, subunits of complex I (NADH:Ubiquinone Oxireductase chain protein 6 and Subunit B6) were 45% greater with FOR treatment compared to VML untreated. No change was observed in the expression of NADH dehydrogenase subunit 1 (*ND-1*). Lastly, OXPHOS protein immunoblot data yielded no significant differences between FOR-treated and untreated VML mice at any individual respiratory complex (complexes I – V; data not shown).

Table 3.4. Relative gene expression (mRNA/18S)

Gene	Experimental Group		Student's t-test p-value
	VML	FOR	
<i>Pgc1a</i>	1.01 ± 0.21	0.98 ± 0.34	0.7300
<i>Pgc1b</i>	0.96 ± 0.22	0.73 ± 0.25 <sup>#</sup>	0.0060
<i>Cox4</i>	0.97 ± 0.12	0.72 ± 0.18 <sup>#</sup>	<0.0001
<i>Nd1</i>	0.98 ± 0.17	1.02 ± 0.32	0.6317
<i>Nd6</i>	1.13 ± 0.37	2.07 ± 0.83 <sup>#</sup>	0.0001
<i>Ndufb6</i>	0.82 ± 0.24	1.51 ± 0.79 <sup>#</sup>	0.0012
<i>Fos</i>	1.23 ± 0.78	1.08 ± 0.64	0.5440

Values are means ± SD.

<sup>#</sup>Different from VML

## Discussion

There currently exists a therapeutic desert to address long-lasting skeletal muscle functional deficits after a VML injury. This is due in part to a vast majority of VML-related research focusing on regeneration of the lost tissue as opposed to functional restoration of the remaining muscle, and to a low percentage of published VML studies that include clinically-relevant outcome measurements of muscle function (Greising et al., 2019). To address this clinical-need gap, we used functional outcomes of muscle strength and metabolic function to evaluate four FDA-approved pharmacological adjuvants' effects on the remaining muscle after a VML injury. This study represents the first step toward identifying regenerative rehabilitation approaches (Perez-Terzic & Childers, 2014), those that combine a regenerative medicine approach that can modulate cellular physiology, such as those described herein, with physical rehabilitation to enhance skeletal muscle function after a VML. Our primary finding was that FOR had the most evidence for a beneficial effect, and there was minimal evidence for efficacy of AICAR, PIO, and SIL in a mouse model of VML.

The treatments evaluated throughout this study (i.e., AICAR, PIO, FOR and SIL) all have a track record of augmenting skeletal muscle strength in animal models of disease and injury (Busquets et al., 2011; Conte et al., 2011; Hall et al., 2018; Penna et al., 2019; Percival et al., 2012; Salazar-Degracia et al., 2018; Southern et al., 2020; Takada et al., 2014). VML injury results in a permanent loss of muscle strength even when normalizing for changes in body mass and muscle mass, as shown here and previously reported (Dienes et al., 2021; Greising et al., 2018; Southern et al., 2019; Ziemkiewicz et al., 2022). FOR's effect on VML-injured muscle strength was largely diminished when strength was normalized to gastrocnemius muscle mass, the primary plantarflexion muscle. Combined with the fact that FOR treatment was associated with larger

remaining gastrocnemius muscle masses, this indicates FOR's benefit for VML-injured muscle strength in maintaining and/or enhancing the quantity of muscle (i.e., mass) as opposed to influencing its quality.

FOR may exert its effects on muscle quantity by increasing protein synthesis, decreasing protein degradation, and/or improving viability of the remaining muscle fibers by enhancing neuromuscular junction stability(Conte et al., 2011; Harcourt et al., 2007; Lynch & Ryall, 2008). For example, skeletal muscles from young and old rats treated with FOR following a traumatic freeze injury had greater incorporation of [U-<sup>14</sup>C] phenylalanine (a marker of protein synthesis), and this was associated with greater muscle force production(Conte et al., 2011). Also, FOR treatment in dystrophic mice that are characterized by progressive rounds of fiber damage and repair, was associated with fewer ubiquitinated proteins suggesting a decline in protein degradation(Harcourt et al., 2007). VML is also characterized by an accumulation of collagen proteins (i.e., fibrosis)(Corona et al., 2018), and formoterol in its vaporized form can influence the collagen protein turnover(Autio et al., 1996; Heuck et al., 2000). A functional measurement associated with collagen protein within VML-injured muscle, passive stiffness about the ankle joint(Greising et al., 2018), was not different between VML untreated and FOR-treated mice, (Supplemental Figure 3); however, we cannot rule out the possibility that fibrotic tissue changes within the VML-injured muscle (e.g., type of collagen and orientation) influenced the transmission of contractile force(Dolan et al., 2022).

Another option, most intriguing in the context of VML, is FOR's potential signaling effects on cyclic AMP(Anderson et al., 2014; Donnelly et al., 2010; Patel et al., 2017), which plays an important role in maintaining acetylcholine receptors at the neuromuscular junction(Barradeau et al., 2001; Rudolf et al., 2014). The remaining muscle fibers after a VML injury are characterized

by greater denervation and poly-innervation indicative of neuromuscular junction instability(Quarta et al., 2017; Sorensen et al., 2021). Furthermore, within the remaining muscle there is a greater proportion of smaller, slow muscle fibers (i.e., less contractile force) that may implicate a preferential loss of larger, faster muscle fibers after injury(Chao et al., 2019; Dalske et al., 2021). Further investigation into FOR's effects on remaining muscle innervation and fiber-type distribution will likely yield insight into the benefit of FOR treatment on muscle mass observed in this study.

Similar to contractile function, each evaluated drug–AICAR(Hall et al., 2018), PIO(Pagel-Langenickel et al., 2008; Rabøl et al., 2010; Takada et al., 2014), FOR(Penna et al., 2019; Sullo et al., 2013), and SIL(Tetsi et al., 2019)– has previous evidence of improving mitochondrial respiration in skeletal muscle in a variety of disease models. As reported here and previously, VML injury results in a significant and lasting deficit in mitochondrial oxygen consumption rate(Dalske et al., 2021; Greising et al., 2018; Southern et al., 2019). Lower oxygen consumption rates do not explicitly implicate a dysfunction, as bioenergetic factors related to ATP supply and demand as well as the proportion of muscle fiber-types comprising the muscle can influence respiration(Schmidt et al., 2021). However, previous research into the structure of the mitochondrial network following a VML injury shows disorganization near the injury site that stretches into the remaining muscle(Forouhesh Tehrani et al., 2021; Southern et al., 2019), and this lends support to an interpretation of mitochondrial dysfunction following VML.

The effectiveness of FOR to modulate mitochondrial function, content, and structure has been shown widely across tissues and disease/injury models such as diabetic renal failure, traumatic brain injury, and skeletal muscle after a spinal cord injury, ischemia-reperfusion, and cancer-induced cachexia(Cleveland et al., 2020; Jesinkey et al., 2014; Salazar-Degracia et al.,

2018; Natalie E. Scholpa et al., 2019; N. E. Scholpa et al., 2019; Vekaria et al., 2020). Herein, FOR treatment led to significant improvement in State III and maximal (uncoupled) respiration of permeabilized muscle fibers from the remaining muscle after a VML injury. We believed that FOR would activate signaling cascades that directly activated the transcription factor PGC-1 $\alpha$  and maintained high transcription of this gene for the duration of treatment as this was supported by at least one study that utilized FOR after a spinal cord injury(Natalie E. Scholpa et al., 2019). However, our data did not support this hypothesis. After further literature review, we saw that data concerning PGC-1 $\alpha$  activation with FOR treatment was ambiguous(Penna et al., 2019; Salazar-Degracia et al., 2018; Natalie E. Scholpa et al., 2019; Sullo et al., 2013). Importantly, literature has reported an increase in PGC-1 $\alpha$  transcription in acute stages of treatment (~8-24 hours) that then wanes to basal levels(Duplanty et al., 2018; Koopman et al., 2010; Pearen et al., 2008; Pearen et al., 2009). Therefore, FOR-induced mitochondrial biogenesis via PGC1 $\alpha$  is either not supported as a mechanism of improvement in our VML model or its levels have stabilized at two months of treatment.

Another potential mechanism of FOR-induced improvements in mitochondrial respiration is related to electron transfer efficiency and mitochondrial complex protein content. Our results were mixed in this regard as we did detect greater gene expression for complex 1 subunits *Nd6* (mtDNA) and *Ndufb6* (nDNA) as well as greater complex I enzyme activity but immunoblots for total Complex I protein content showed no changes. It remains a possibility that improvements in mitochondrial function with FOR are independent of biogenesis and protein content and may reflect a greater capacity to deal with cellular stress. For example, in a model of traumatic brain injury, FOR treatment was associated with better mitochondrial-Ca<sup>2+</sup> buffering that may reflect an enhanced ability of the mitochondrial network to adapt to acute cellular stresses such as changes

in calcium homeostasis(Vekaria et al., 2020). Currently, the benefit of FOR treatment on mitochondrial respiration in VML remains unclear; however, toward the goal of validating pharmacological agents to combine with rehabilitation in future studies to address VML, FOR does have promising functional outcomes.

The improvements in functional capacity following FOR administration hold promise that VML-injured muscle is capable of metabolic adaptations despite the adverse cellular environment following injury. Our data suggests that FOR treatment leads to the improvement of contractile and mitochondrial function via the maintenance of remaining muscle mass and improvement of overall oxidative capacity, possibly at Complex I. Administration of physical rehabilitation following VML injury has been shown to improve contractile function(Greising et al., 2018; Southern et al., 2019). Therefore, further studies should investigate the integration of rehabilitative approaches with FOR treatment in the hopes of magnifying the improvements conferred by drug administration or rehabilitation alone. In conclusion, this work provides a thorough evaluation of FDA-approved adjuvants to improve muscle function after VML and names a therapeutic candidate that can be easily translated for in-clinic use.

### **Authorship Confirmation**

J.M-F, S.M.G. and J.A.C. designed the experiments. J.M-F., A.G.S., A.S.N., M.N.L., E. H., E.W., E.E.N., S.M.G. and J.A.C. performed the experiments, collected, and analyzed the data. All authors have read and approved of the manuscript.

### **Author Disclosure**

No competing financial interests exist.

**Funding Statement**

Funding support from the Department of Defense, through the Clinical & Rehabilitative Medicine Research Program, FY18 Neuromusculoskeletal Injuries Rehabilitation Research Award (W81XWH-18-1-0710 to SMG (UMN) and JAC (UGA)).

**Acknowledgements**

None.

## References

- Adamo, C. M., Dai, D.-F., Percival, J. M., et al. (2010). Sildenafil reverses cardiac dysfunction in the mdx mouse model of Duchenne muscular dystrophy. *Proceedings of the National Academy of Sciences of the United States of America*, 107(44), 19079-19083. <https://doi.org/10.1073/pnas.1013077107>
- Aguilar, C. A., Greising, S. M., Watts, A., et al. (2018). Multiscale analysis of a regenerative therapy for treatment of volumetric muscle loss injury. *Cell death discovery*, 4(1), 1-11.
- Anderson, R., Theron, A. J., Steel, H. C., et al. (2014). The beta-2-adrenoreceptor agonists, formoterol and indacaterol, but not salbutamol, effectively suppress the reactivity of human neutrophils in vitro. *Mediators Inflamm*, 2014, 105420. <https://doi.org/10.1155/2014/105420>
- Anderson, S. E., Han, W. M., Srinivasa, V., et al. (2019). Determination of a Critical Size Threshold for Volumetric Muscle Loss in the Mouse Quadriceps. *Tissue Engineering Part C: Methods*, 25(2), 59-70. <https://doi.org/10.1089/ten.tec.2018.0324>
- Autio, P., Karjalainen, J., Risteli, L., et al. (1996). Effects of an inhaled steroid (budesonide) on skin collagen synthesis of asthma patients in vivo. *Am J Respir Crit Care Med*, 153(3), 1172-1175. <https://doi.org/10.1164/ajrccm.153.3.8630563>
- Baltgalvis, K. A., Call, J. A., Cochrane, G. D., et al. (2012). Exercise training improves plantar flexor muscle function in mdx mice. *Med Sci Sports Exerc*, 44(9), 1671-1679. <https://doi.org/10.1249/MSS.0b013e31825703f0>
- Barradeau, S., Imaizumi-Scherrer, T., Weiss, M. C., & Faust, D. M. (2001). Muscle-regulated expression and determinants for neuromuscular junctional localization of the mouse R1alpha regulatory subunit of cAMP-dependent protein kinase. *Proc Natl Acad Sci U S A*, 98(9), 5037-5042. <https://doi.org/10.1073/pnas.081393598>
- Batra, A., Vohra, R. S., Chrzanowski, S. M., et al. (2019). Effects of PDE5 inhibition on dystrophic muscle following an acute bout of downhill running and endurance training. *Journal of applied physiology (Bethesda, Md. : 1985)*, 126(6), 1737-1745. <https://doi.org/10.1152/jappphysiol.00664.2018>
- Busquets, S., Toledo, M., Sirisi, S., et al. (2011). Formoterol and cancer muscle wasting in rats: Effects on muscle force and total physical activity. *Exp Ther Med*, 2(4), 731-735. <https://doi.org/10.3892/etm.2011.260>
- Call, J. A., & Lowe, D. A. (2016). Eccentric Contraction-Induced Muscle Injury: Reproducible, Quantitative, Physiological Models to Impair Skeletal Muscle's Capacity to Generate Force. *Methods Mol Biol*, 1460, 3-18. [https://doi.org/10.1007/978-1-4939-3810-0\\_1](https://doi.org/10.1007/978-1-4939-3810-0_1)
- Call, J. A., Voelker, K. A., Wolff, A. V., et al. (2008). Endurance capacity in maturing mdx mice is markedly enhanced by combined voluntary wheel running and green tea extract. *Journal of Applied Physiology*, 105(3), 923-932. <https://doi.org/10.1152/jappphysiol.00028.2008>
- Chao, T., Burmeister, D. M., Corona, B. T., & Greising, S. M. (2019). Oxidative pathophysiology following volumetric muscle loss injury in a porcine model. *J Appl Physiol (1985)*, 126(6), 1541-1549. <https://doi.org/10.1152/jappphysiol.00026.2019>
- Cleveland, K. H., Brosius, F. C., 3rd, & Schnellmann, R. G. (2020). Regulation of mitochondrial dynamics and energetics in the diabetic renal proximal tubule by the  $\beta(2)$ -adrenergic receptor agonist formoterol. *Am J Physiol Renal Physiol*, 319(5), F773-f779. <https://doi.org/10.1152/ajprenal.00427.2020>

- Conte, T. C., Silva, L. H., Silva, M. T., et al. (2011). The  $\beta$ 2-Adrenoceptor Agonist Formoterol Improves Structural and Functional Regenerative Capacity of Skeletal Muscles From Aged Rat at the Early Stages of Postinjury. *The Journals of Gerontology: Series A*, 67A(5), 443-455. <https://doi.org/10.1093/gerona/qlr195>
- Corona, B. T., Garg, K., Ward, C. L., et al. (2013). Autologous minced muscle grafts: a tissue engineering therapy for the volumetric loss of skeletal muscle. *American Journal of Physiology-Cell Physiology*, 305(7), C761-C775.
- Corona, B. T., Rivera, J. C., & Greising, S. M. (2018). Inflammatory and Physiological Consequences of Debridement of Fibrous Tissue after Volumetric Muscle Loss Injury. *Clin Transl Sci*, 11(2), 208-217. <https://doi.org/10.1111/cts.12519>
- Corona, B. T., Rivera, J. C., Owens, J. G., et al. (2015). Volumetric muscle loss leads to permanent disability following extremity trauma. *Journal of Rehabilitation Research & Development*, 52(7).
- Corona, B. T., Wenke, J. C., & Ward, C. L. (2016). Pathophysiology of volumetric muscle loss injury. *Cells Tissues Organs*, 202(3-4), 180-188.
- Dalske, K. A., Raymond-Pope, C. J., McFaline-Figueroa, J., et al. (2021). Independent of physical activity, volumetric muscle loss injury in a murine model impairs whole-body metabolism. *PLoS one*, 16(6), e0253629. <https://doi.org/10.1371/journal.pone.0253629>
- Das, S., Browne, K. D., Laimo, F. A., et al. (2020). Pre-innervated tissue-engineered muscle promotes a pro-regenerative microenvironment following volumetric muscle loss. *Communications Biology*, 3(1), 330. <https://doi.org/10.1038/s42003-020-1056-4>
- Dienes, J., Browne, S., Farjun, B., et al. (2021). Semisynthetic Hyaluronic Acid-Based Hydrogel Promotes Recovery of the Injured Tibialis Anterior Skeletal Muscle Form and Function. *ACS Biomater Sci Eng*, 7(4), 1587-1599. <https://doi.org/10.1021/acsbiomaterials.0c01751>
- Dolan, C. P., Motherwell, J. M., Franco, S. R., et al. (2022). Evaluating the potential use of functional fibrosis to facilitate improved outcomes following volumetric muscle loss injury. *Acta Biomater*, 140, 379-388. <https://doi.org/10.1016/j.actbio.2021.11.032>
- Donnelly, L. E., Tudhope, S. J., Fenwick, P. S., & Barnes, P. J. (2010). Effects of formoterol and salmeterol on cytokine release from monocyte-derived macrophages. *Eur Respir J*, 36(1), 178-186. <https://doi.org/10.1183/09031936.00158008>
- Duguez, S., Féasson, L., Denis, C., & Freyssenet, D. (2002). Mitochondrial biogenesis during skeletal muscle regeneration. *Am J Physiol Endocrinol Metab*, 282(4), E802-809. <https://doi.org/10.1152/ajpendo.00343.2001>
- Duplanty, A. A., Siggins, R. W., Allerton, T., et al. (2018). Myoblast mitochondrial respiration is decreased in chronic binge alcohol administered simian immunodeficiency virus-infected antiretroviral-treated rhesus macaques. *Physiol Rep*, 6(5). <https://doi.org/10.14814/phy2.13625>
- Fiorentino, T. V., Monroy, A., Kamath, S., et al. (2021). Pioglitazone corrects dysregulation of skeletal muscle mitochondrial proteins involved in ATP synthesis in type 2 diabetes. *Metabolism - Clinical and Experimental*, 114. <https://doi.org/10.1016/j.metabol.2020.154416>
- Foltz, S. J., Luan, J., Call, J. A., et al. (2016). Four-week rapamycin treatment improves muscular dystrophy in a fukutin-deficient mouse model of dystroglycanopathy. *Skeletal muscle*, 6, 20-20. <https://doi.org/10.1186/s13395-016-0091-9>

- Forouhesh Tehrani, K., Pendleton, E. G., Southern, W. M., et al. (2021). Spatial frequency metrics for analysis of microscopic images of musculoskeletal tissues. *Connect Tissue Res*, 62(1), 4-14. <https://doi.org/10.1080/03008207.2020.1828381>
- Frenkel, D., & Aronow, W. S. (2020). Role for risk factor treatment in the management of atrial fibrillation. *Hosp Pract* (1995), 48(4), 180-187. <https://doi.org/10.1080/21548331.2020.1784663>
- Frias, F. d. T., de Mendonça, M., Martins, A. R., et al. (2016). MyomiRs as Markers of Insulin Resistance and Decreased Myogenesis in Skeletal Muscle of Diet-Induced Obese Mice. *Frontiers in endocrinology*, 7, 76-76. <https://doi.org/10.3389/fendo.2016.00076>
- Garg, K., Ward, C. L., Hurtgen, B. J., et al. (2015). Volumetric muscle loss: persistent functional deficits beyond frank loss of tissue. *Journal of Orthopaedic Research*, 33(1), 40-46.
- Gómez-SanMiguel, A. B., Gomez-Moreira, C., Nieto-Bona, M. P., et al. (2016). Formoterol decreases muscle wasting as well as inflammation in the rat model of rheumatoid arthritis. *American Journal of Physiology-Endocrinology and Metabolism*, 310(11), E925-E937. <https://doi.org/10.1152/ajpendo.00503.2015>
- Goto, K., Iso, T., Hanaoka, H., et al. (2013). Peroxisome proliferator-activated receptor- $\gamma$  in capillary endothelia promotes fatty acid uptake by heart during long-term fasting. *Journal of the American Heart Association*, 2(1), e004861-e004861. <https://doi.org/10.1161/JAHA.112.004861>
- Greising, S. M., Corona, B. T., McGann, C., et al. (2019). Therapeutic Approaches for Volumetric Muscle Loss Injury: A Systematic Review and Meta-Analysis. *Tissue Engineering Part B: Reviews*, 25(6), 510-525. <https://doi.org/10.1089/ten.teb.2019.0207>
- Greising, S. M., Dearth, C. L., & Corona, B. T. (2016). Regenerative and rehabilitative medicine: a necessary synergy for functional recovery from volumetric muscle loss injury. *Cells Tissues Organs*, 202(3-4), 237-249.
- Greising, S. M., Rivera, J. C., Goldman, S. M., et al. (2017). Unwavering pathobiology of volumetric muscle loss injury. *Scientific reports*, 7(1), 1-14.
- Greising, S. M., Warren, G. L., Southern, W. M., et al. (2018). Early rehabilitation for volumetric muscle loss injury augments endogenous regenerative aspects of muscle strength and oxidative capacity. *BMC musculoskeletal disorders*, 19(1), 173-173. <https://doi.org/10.1186/s12891-018-2095-6>
- Grogan, B. F., Hsu, J. R., & Consortium, S. T. R. (2011). Volumetric muscle loss. *JAAOS-Journal of the American Academy of Orthopaedic Surgeons*, 19, S35-S37.
- Hall, D. T., Griss, T., Ma, J. F., et al. (2018). The AMPK agonist 5-aminoimidazole-4-carboxamide ribonucleotide (AICAR), but not metformin, prevents inflammation-associated cachectic muscle wasting. *EMBO molecular medicine*, 10(7), e8307. <https://doi.org/10.15252/emmm.201708307>
- Halseth, A. E., Ensor, N. J., White, T. A., et al. (2002). Acute and chronic treatment of ob/ob and db/db mice with AICAR decreases blood glucose concentrations. *Biochemical and Biophysical Research Communications*, 294(4), 798-805. [https://doi.org/https://doi.org/10.1016/S0006-291X\(02\)00557-0](https://doi.org/https://doi.org/10.1016/S0006-291X(02)00557-0)
- Harcourt, L. J., Schertzer, J. D., Ryall, J. G., & Lynch, G. S. (2007). Low dose formoterol administration improves muscle function in dystrophic mdx mice without increasing fatigue. *Neuromuscul Disord*, 17(1), 47-55. <https://doi.org/10.1016/j.nmd.2006.08.012>

- Heuck, C., Heickendorff, L., & Wolthers, O. D. (2000). A randomised controlled trial of short term growth and collagen turnover in asthmatics treated with inhaled formoterol and budesonide. *Arch Dis Child*, 83(4), 334-339. <https://doi.org/10.1136/adc.83.4.334>
- Hoffman, D. B., Raymond-Pope, C. J., Sorensen, J. R., et al. (2021). Temporal changes in the muscle extracellular matrix due to volumetric muscle loss injury. *Connective Tissue Research*, 1-14.
- Huang, M., Lee, K. J., Kim, K.-J., et al. (2016). The maintenance ability and Ca(2+) availability of skeletal muscle are enhanced by sildenafil. *Experimental & molecular medicine*, 48(12), e278-e278. <https://doi.org/10.1038/emm.2016.134>
- Hyldahl, R. D., Nelson, B., Xin, L., et al. (2015). Extracellular matrix remodeling and its contribution to protective adaptation following lengthening contractions in human muscle. *The FASEB Journal*, 29(7), 2894-2904.
- Jesinkey, S. R., Funk, J. A., Stallons, L. J., et al. (2014). Formoterol restores mitochondrial and renal function after ischemia-reperfusion injury. *J Am Soc Nephrol*, 25(6), 1157-1162. <https://doi.org/10.1681/asn.2013090952>
- Kellenberger, S., Muller, K., Richener, H., & Bilbe, G. (1998). Formoterol and isoproterenol induce c-fos gene expression in osteoblast-like cells by activating beta2-adrenergic receptors. *Bone*, 22(5), 471-478. [https://doi.org/10.1016/s8756-3282\(98\)00026-x](https://doi.org/10.1016/s8756-3282(98)00026-x)
- Kenley, R. A., Denissenko, M. F., Mullin, R. J., et al. (2008). Formoterol fumarate and roxithromycin effects on muscle mass in an animal model of cancer cachexia. *Oncol Rep*, 19(5), 1113-1121. <https://doi.org/10.3892/or.19.5.1113>
- Kobilo, T., Guerrieri, D., Zhang, Y., et al. (2014). AMPK agonist AICAR improves cognition and motor coordination in young and aged mice. *Learning & memory (Cold Spring Harbor, N.Y.)*, 21(2), 119-126. <https://doi.org/10.1101/lm.033332.113>
- Koopman, R., Gehrig, S. M., Leger, B., et al. (2010). Cellular mechanisms underlying temporal changes in skeletal muscle protein synthesis and breakdown during chronic {beta}-adrenoceptor stimulation in mice. *J Physiol*, 588(Pt 23), 4811-4823. <https://doi.org/10.1113/jphysiol.2010.196725>
- Lalegül-Ülker, Ö., Şeker, Ş., Elçin, A. E., & Elçin, Y. M. (2019). Encapsulation of bone marrow-MSCs in PRP-derived fibrin microbeads and preliminary evaluation in a volumetric muscle loss injury rat model: modular muscle tissue engineering. *Artificial Cells, Nanomedicine, and Biotechnology*, 47(1), 10-21. <https://doi.org/10.1080/21691401.2018.1540426>
- Larouche, J., Greising, S. M., Corona, B. T., & Aguilar, C. A. (2018). Robust inflammatory and fibrotic signaling following volumetric muscle loss: a barrier to muscle regeneration. *Cell death & disease*, 9(3), 1-3.
- Larsen, S., Nielsen, J., Hansen, C. N., et al. (2012). Biomarkers of mitochondrial content in skeletal muscle of healthy young human subjects. *J Physiol*, 590(14), 3349-3360. <https://doi.org/10.1113/jphysiol.2012.230185>
- Lihn, A. S., Pedersen, S. B., Lund, S., & Richelsen, B. (2008). The anti-diabetic AMPK activator AICAR reduces IL-6 and IL-8 in human adipose tissue and skeletal muscle cells. *Molecular and Cellular Endocrinology*, 292(1), 36-41. <https://doi.org/https://doi.org/10.1016/j.mce.2008.06.004>
- Lynch, G. S., & Ryall, J. G. (2008). Role of beta-adrenoceptor signaling in skeletal muscle: implications for muscle wasting and disease. *Physiol Rev*, 88(2), 729-767. <https://doi.org/10.1152/physrev.00028.2007>

- Moon, Y., Balke, J. E., Madorma, D., et al. (2017). Nitric Oxide Regulates Skeletal Muscle Fatigue, Fiber Type, Microtubule Organization, and Mitochondrial ATP Synthesis Efficiency Through cGMP-Dependent Mechanisms. *Antioxidants & redox signaling*, 26(17), 966-985. <https://doi.org/10.1089/ars.2016.6630>
- Mori, R., Kamei, N., Okawa, S., et al. (2015). Promotion of skeletal muscle repair in a rat skeletal muscle injury model by local injection of human adipose tissue-derived regenerative cells [<https://doi.org/10.1002/term.1659>]. *Journal of Tissue Engineering and Regenerative Medicine*, 9(10), 1150-1160. <https://doi.org/https://doi.org/10.1002/term.1659>
- Nakayama, K. H., Quarta, M., Paine, P., et al. (2019). Treatment of volumetric muscle loss in mice using nanofibrillar scaffolds enhances vascular organization and integration. *Communications Biology*, 2(1), 170. <https://doi.org/10.1038/s42003-019-0416-4>
- Narkar, V. A., Downes, M., Yu, R. T., et al. (2008). AMPK and PPARdelta agonists are exercise mimetics. *Cell*, 134(3), 405-415. <https://doi.org/10.1016/j.cell.2008.06.051>
- Nelson, M. D., Rader, F., Tang, X., et al. (2014). PDE5 inhibition alleviates functional muscle ischemia in boys with Duchenne muscular dystrophy. *Neurology*, 82(23), 2085-2091. <https://doi.org/10.1212/WNL.0000000000000498>
- Nichenko, A. S., Sorensen, J. R., Southern, W. M., et al. (2021). Lifelong Ulk1-Mediated Autophagy Deficiency in Muscle Induces Mitochondrial Dysfunction and Contractile Weakness. *Int J Mol Sci*, 22(4). <https://doi.org/10.3390/ijms22041937>
- Nichenko, A. S., Southern, W. M., Atuan, M., et al. (2016). Mitochondrial maintenance via autophagy contributes to functional skeletal muscle regeneration and remodeling. *American Journal of Physiology-Cell Physiology*, 311(2), C190-C200. <https://doi.org/10.1152/ajpcell.00066.2016>
- Nyberg, M., Piil, P., Egelund, J., et al. (2015). Potentiation of cGMP signaling increases oxygen delivery and oxidative metabolism in contracting skeletal muscle of older but not young humans. *Physiological reports*, 3(8), e12508. <https://doi.org/10.14814/phy2.12508>
- Pagel-Langenickel, I., Bao, J., Joseph, J. J., et al. (2008). PGC-1alpha integrates insulin signaling, mitochondrial regulation, and bioenergetic function in skeletal muscle. *The Journal of biological chemistry*, 283(33), 22464-22472. <https://doi.org/10.1074/jbc.M800842200>
- Patel, B. S., Kugel, M. J., Baehring, G., & Ammit, A. J. (2017). Doxofylline does not increase formoterol-induced cAMP nor MKP-1 expression in ASM cells resulting in lack of anti-inflammatory effect. *Pulm Pharmacol Ther*, 45, 34-39. <https://doi.org/10.1016/j.pupt.2017.04.006>
- Pearen, M. A., Myers, S. A., Raichur, S., et al. (2008). The orphan nuclear receptor, NOR-1, a target of beta-adrenergic signaling, regulates gene expression that controls oxidative metabolism in skeletal muscle. *Endocrinology*, 149(6), 2853-2865. <https://doi.org/10.1210/en.2007-1202>
- Pearen, M. A., Ryall, J. G., Lynch, G. S., & Muscat, G. E. (2009). Expression profiling of skeletal muscle following acute and chronic beta2-adrenergic stimulation: implications for hypertrophy, metabolism and circadian rhythm. *BMC Genomics*, 10, 448. <https://doi.org/10.1186/1471-2164-10-448>
- Penna, F., Ballarò, R., Martínez-Cristobal, P., et al. (2019). Autophagy Exacerbates Muscle Wasting in Cancer Cachexia and Impairs Mitochondrial Function. *Journal of Molecular Biology*, 431(15), 2674-2686. <https://doi.org/https://doi.org/10.1016/j.jmb.2019.05.032>

- Percival, J. M., Whitehead, N. P., Adams, M. E., et al. (2012). Sildenafil reduces respiratory muscle weakness and fibrosis in the mdx mouse model of Duchenne muscular dystrophy. *The Journal of pathology*, 228(1), 77-87. <https://doi.org/10.1002/path.4054>
- Perez-Terzic, C., & Childers, M. K. (2014). Regenerative rehabilitation: a new future? *Am J Phys Med Rehabil*, 93(11 Suppl 3), S73-78. <https://doi.org/10.1097/phm.0000000000000211>
- Quarta, M., Cromie, M., Chacon, R., et al. (2017). Bioengineered constructs combined with exercise enhance stem cell-mediated treatment of volumetric muscle loss. *Nature Communications*, 8(1), 15613. <https://doi.org/10.1038/ncomms15613>
- Rabøl, R., Boushel, R., Almdal, T., et al. (2010). Opposite effects of pioglitazone and rosiglitazone on mitochondrial respiration in skeletal muscle of patients with type 2 diabetes. *Diabetes, Obesity and Metabolism*, 12(9), 806-814. <https://doi.org/https://doi.org/10.1111/j.1463-1326.2010.01237.x>
- Rudolf, R., Khan, M. M., Labeit, S., & Deschenes, M. R. (2014). Degeneration of neuromuscular junction in age and dystrophy. *Front Aging Neurosci*, 6, 99. <https://doi.org/10.3389/fnagi.2014.00099>
- Ryall, J. G., Sillence, M. N., & Lynch, G. S. (2006). Systemic administration of beta2-adrenoceptor agonists, formoterol and salmeterol, elicit skeletal muscle hypertrophy in rats at micromolar doses. *British journal of pharmacology*, 147(6), 587-595. <https://doi.org/10.1038/sj.bjp.0706669>
- Salazar-Degracia, A., Busquets, S., Argilés, J. M., et al. (2018). Effects of the beta2 agonist formoterol on atrophy signaling, autophagy, and muscle phenotype in respiratory and limb muscles of rats with cancer-induced cachexia. *Biochimie*, 149, 79-91. <https://doi.org/https://doi.org/10.1016/j.biochi.2018.04.009>
- Sanchis-Gomar, F., Pareja-Galeano, H., & Martinez-Bello, V. E. (2014). PPARgamma agonist pioglitazone does not enhance performance in mice [<https://doi.org/10.1002/dta.1587>]. *Drug Testing and Analysis*, 6(9), 922-929. <https://doi.org/https://doi.org/10.1002/dta.1587>
- Sasaki, T., Nakata, R., Inoue, H., et al. (2014). Role of AMPK and PPAR $\gamma$ 1 in exercise-induced lipoprotein lipase in skeletal muscle. *American Journal of Physiology-Endocrinology and Metabolism*, 306(9), E1085-E1092. <https://doi.org/10.1152/ajpendo.00691.2013>
- Schmidt, C. A., Fisher-Wellman, K. H., & Neuffer, P. D. (2021). From OCR and ECAR to energy: Perspectives on the design and interpretation of bioenergetics studies. *J Biol Chem*, 297(4), 101140. <https://doi.org/10.1016/j.jbc.2021.101140>
- Scholpa, N. E., Simmons, E. C., Tilley, D. G., & Schnellmann, R. G. (2019).  $\beta$ (2)-adrenergic receptor-mediated mitochondrial biogenesis improves skeletal muscle recovery following spinal cord injury. *Experimental neurology*, 322, 113064-113064. <https://doi.org/10.1016/j.expneurol.2019.113064>
- Scholpa, N. E., Williams, H., Wang, W., et al. (2019). Pharmacological Stimulation of Mitochondrial Biogenesis Using the Food and Drug Administration-Approved  $\beta$ (2)-Adrenoreceptor Agonist Formoterol for the Treatment of Spinal Cord Injury. *J Neurotrauma*, 36(6), 962-972. <https://doi.org/10.1089/neu.2018.5669>
- Shayan, M., & Huang, N. F. (2020). Pre-clinical cell therapeutic approaches for repair of volumetric muscle loss. *Bioengineering*, 7(3), 97.
- Skov, V., Glintborg, D., Knudsen, S., et al. (2008). Pioglitazone enhances mitochondrial biogenesis and ribosomal protein biosynthesis in skeletal muscle in polycystic ovary syndrome. *PloS one*, 3(6), e2466-e2466. <https://doi.org/10.1371/journal.pone.0002466>

- Sorensen, J. R., Hoffman, D. B., Corona, B. T., & Greising, S. M. (2021). Secondary denervation is a chronic pathophysiologic sequela of volumetric muscle loss. *J Appl Physiol (1985)*, *130*(5), 1614-1625. <https://doi.org/10.1152/jappphysiol.00049.2021>
- Southern, W. M., Nichenko, A. S., Qualls, A. E., et al. (2020). Mitochondrial dysfunction in skeletal muscle of fukutin-deficient mice is resistant to exercise- and 5-aminoimidazole-4-carboxamide ribonucleotide-induced rescue. *Experimental Physiology*, *105*(10), 1767-1777. <https://doi.org/https://doi.org/10.1113/EP088812>
- Southern, W. M., Nichenko, A. S., Shill, D. D., et al. (2017). Skeletal muscle metabolic adaptations to endurance exercise training are attainable in mice with simvastatin treatment. *PloS one*, *12*(2), e0172551. <https://doi.org/10.1371/journal.pone.0172551>
- Southern, W. M., Nichenko, A. S., Tehrani, K. F., et al. (2019). PGC-1 $\alpha$  overexpression partially rescues impaired oxidative and contractile pathophysiology following volumetric muscle loss injury. *Scientific reports*, *9*(1), 4079-4079. <https://doi.org/10.1038/s41598-019-40606-6>
- Sullo, N., Roviezzo, F., Matteis, M., et al. (2013). Skeletal Muscle Oxidative Metabolism in an Animal Model of Pulmonary Emphysema. *American Journal of Respiratory Cell and Molecular Biology*, *48*(2), 198-203. <https://doi.org/10.1165/rcmb.2012-0167OC>
- Takada, S., Hirabayashi, K., Kinugawa, S., et al. (2014). Pioglitazone ameliorates the lowered exercise capacity and impaired mitochondrial function of the skeletal muscle in type 2 diabetic mice. *European Journal of Pharmacology*, *740*, 690-696. <https://doi.org/https://doi.org/10.1016/j.ejphar.2014.06.008>
- Tetsi, L., Charles, A.-L., Georg, I., et al. (2019). Effect of the Phosphodiesterase 5 Inhibitor Sildenafil on Ischemia-Reperfusion-Induced Muscle Mitochondrial Dysfunction and Oxidative Stress. *Antioxidants (Basel, Switzerland)*, *8*(4), 93. <https://doi.org/10.3390/antiox8040093>
- Thome, T., Salyers, Z. R., Kumar, R. A., et al. (2019). Uremic metabolites impair skeletal muscle mitochondrial energetics through disruption of the electron transport system and matrix dehydrogenase activity. *Am J Physiol Cell Physiol*, *317*(4), C701-C713. <https://doi.org/10.1152/ajpcell.00098.2019>
- Toledo, M., Busquets, S., Penna, F., et al. (2016). Complete reversal of muscle wasting in experimental cancer cachexia: Additive effects of activin type II receptor inhibition and  $\beta$ -2 agonist [<https://doi.org/10.1002/ijc.29930>]. *International Journal of Cancer*, *138*(8), 2021-2029. <https://doi.org/https://doi.org/10.1002/ijc.29930>
- Valatsou, A., Briasoulis, A., Vogiatzi, G., et al. (2017). Beneficial Effects of Sildenafil on Tissue Perfusion and Inflammation in a Murine Model of Limb Ischemia and Atherosclerosis. *Curr Vasc Pharmacol*, *15*(3), 282-287. <https://doi.org/10.2174/1570161115666170126123258>
- Vekaria, H. J., Hubbard, W. B., Scholpa, N. E., et al. (2020). Formoterol, a  $\beta$ (2)-adrenoreceptor agonist, induces mitochondrial biogenesis and promotes cognitive recovery after traumatic brain injury. *Neurobiol Dis*, *140*, 104866. <https://doi.org/10.1016/j.nbd.2020.104866>
- Wagatsuma, A., Kotake, N., & Yamada, S. (2011). Muscle regeneration occurs to coincide with mitochondrial biogenesis. *Mol Cell Biochem*, *349*(1-2), 139-147. <https://doi.org/10.1007/s11010-010-0668-2>
- Wang, X., Pickrell, A. M., Rossi, S. G., et al. (2013). Transient systemic mtDNA damage leads to muscle wasting by reducing the satellite cell pool. *Hum Mol Genet*, *22*(19), 3976-3986. <https://doi.org/10.1093/hmg/ddt251>

- Wessels, B., Ciapaite, J., van den Broek, N. M. A., et al. (2015). Pioglitazone treatment restores in vivo muscle oxidative capacity in a rat model of diabetes. *Diabetes, Obesity and Metabolism*, 17(1), 52-60. <https://doi.org/https://doi.org/10.1111/dom.12388>
- Yokota, T., Kinugawa, S., Hirabayashi, K., et al. (2017). Pioglitazone improves whole-body aerobic capacity and skeletal muscle energy metabolism in patients with metabolic syndrome. *Journal of diabetes investigation*, 8(4), 535-541. <https://doi.org/10.1111/jdi.12606>
- Ziemkiewicz, N., Hilliard, G. M., Dunn, A. J., et al. (2022). Laminin-111-Enriched Fibrin Hydrogels Enhance Functional Muscle Regeneration Following Trauma. *Tissue Eng Part A*. <https://doi.org/10.1089/ten.TEA.2021.0096>

## CHAPTER 4

### FORMOTEROL TREATMENT IMPROVES CONTRACTILE-METABOLIC FUNCTION AFTER VOLUMETRIC MUSCLE LOSS INDEPENDENT OF REHABILITATION<sup>4</sup>

---

<sup>4</sup>McFaline-Figueroa, J., Schifino, A. G., Heo, JW., Raymond-Pope, C., Winders, E. A., Greising, S.M. & Call, J. A. (2022). Formoterol treatment improves contractile-metabolic function after volumetric muscle loss independent of rehabilitation.  
To be submitted to *Biomaterials*

## **Abstract**

Volumetric muscle loss is a type of traumatic muscle injury characterized by the irrecoverable loss of tissue. They typically result in the persistent decline of both contractile and metabolic function. Many studies have aimed at improving muscle function following VML injury with varying degrees of success. One of the major drawbacks is the lack of functional testing to validate the effectiveness of the treatment, resulting in therapies that do not translate to clinical improvements. Previously, formoterol (FOR) was shown to rescue both oxidative and contractile function after injury compared to untreated VML controls. This placed FOR as an ideal candidate for further therapeutic development. The purpose of this study was to determine if the combination of FOR with a rehabilitative or regenerative approach could possibly amplify the drug's effects and offer a more robust functional improvement. VML-injured mice were maintained on a FOR diet for 2 months and prescribed early (EWR+FOR) or late (LWR+FOR) rehabilitation intervention in the form of voluntary wheel running. Another cohort of animals received FOR (BIO+FOR) or blank (BIO) as a direct injection using a biomaterial scaffold, directly to the site of injury. We hypothesized that the combination of FOR with early rehab intervention would result in the best functional rescue amongst the experimental groups. At the end of the study, contractile and metabolic function was tested and compared to untreated controls. LWR+FOR had the best improvement in both oxidative capacity (~21% increase) and contractile function (~20% increase). LWR+FOR also had increased mitochondrial content and gastrocnemius muscle mass compared to untreated VML controls. Taken together, these results suggest that consistent FOR administration followed by a rehabilitation regimen may offer the best combination for the improvement of muscle function after VML.

## **Introduction**

Volumetric muscle loss (VML) injuries encompass a series of pathologies where a significant, non-recoverable portion of tissue is lost due to trauma or surgery (Grogan & Hsu, 2011). These injuries result in the loss of contractile and metabolic function of the affected limb, leading to the development of secondary orthopedic diseases, decrease in mobility, and overall decline of patient quality of life (Corona et al., 2015; Corona et al., 2016; Garg et al., 2015). As such, VML injuries and their resulting co-morbidities put a burden on the public healthcare system, especially considering the compounding effect of age on a population with already decreased mobility (Rivera & Corona, 2016). One of the main concerns with VML injuries is the lack of treatment options or standard protocols to address the injury to the soft tissue until the wound is healed, at which point, long-term damage to the muscle may have already occurred.

Previous studies have determined that VML-injured tissue suffers from decreased contractile and metabolic function (Chao et al., 2019; Corona et al., 2012; Greising et al., 2017; Greising et al., 2018; William M Southern et al., 2019). Overall, strength produced by these muscles is significantly less than normal, healthy tissue and this decrease is disproportionate to the expected deficit when considering the lost tissue volume. Additionally, mitochondrial metabolic metabolism, as measured via oxygen consumption of the muscle, is significantly decreased compared to uninjured controls (Chao et al., 2019; McFaline-Figueroa et al., 2022; William M Southern et al., 2019). To add to this dysfunction, other studies have shown that VML injury produces metabolic deficits at a whole-body level. Respiratory exchange rates (RER) in VML-injured mice are significantly lower than uninjured mice despite having similar levels of activity (Dalske et al., 2021). Moreover, the rate of oxidation of carbohydrates and lipids is affected in VML-injured mice compared to uninjured age-matched controls.

There is a wealth of research devoted to developing regenerative therapies to ameliorate these functional deficits. However, few of these approaches include robust functional testing as a measure of treatment effectiveness (Greising et al., 2019). The therapies that have been put through functional testing have yielded modest results in improving contractile-metabolic function after VML injury. Virogenetic overexpression of PGC-1 $\alpha$  has been shown to partially rescue metabolic function in a model of VML (William M Southern et al., 2019). While promising, the technique used for this approach is not feasible for use in a clinical setting. A screen of pharmaceutical agents with evidence of stimulating PGC-1 $\alpha$  expression in other muscle pathologies yielded formoterol fumarate (FOR), a  $\beta$ -2-adrenergic receptor agonist, as a viable candidate for further development due to its ability to modestly rescue both metabolic and contractile function after VML (McFaline-Figueroa et al., 2022).

Regenerative rehabilitation is the practice of combining regenerative therapies (eg. pharmaceuticals, growth factors, scaffolds, stem cells, etc.) with means of rehabilitation. Previous studies have identified that early rehabilitation intervention offered improvement to functional outcomes of VML-injured limbs (Greising et al., 2018). Similarly, various studies have seen improvement of muscle quality following the delivery of a biologically active payload directly to the site of injury following VML injury (Chen & Walters, 2013; Corona et al., 2014; Goldman et al., 2018). Therefore, the purpose of this study was twofold to determine: 1) whether the combination of FOR with rehabilitation improved contractile and metabolic function, and 2) whether the length and time of rehab intervention affected the final functional outcomes. As an additional query, we investigated whether the use of a polymer scaffold to deliver FOR directly to the site of injury significantly improve contractile and metabolic function while allowing for a

more targeted treatment approach. We hypothesize that the combination of FOR with early rehabilitation will offer the best overall improvement of muscle function over no treatment.

## **Materials and Methods**

### *Animals:*

Male C57BL/6 mice were housed at 20-23 °C on a 12:12-hr light-dark cycle, with food and water provided ad libitum. At the time of randomization to experimental groups, all mice were between 10-11 weeks of age (pre-surgical mass  $28.16 \pm 1.56$  g). All procedures were approved and performed in accordance with the guidelines and regulations of the Institutional Animal Care and Use Committee at the University of Georgia.

### *Experimental design:*

#### *Rehabilitation Intervention*

VML-injured mice underwent unilateral VML injury and then were randomized into one of the following experimental groups: HR+FOR (n=8), LR+FOR (n=8), or no treatment (VML, n=14). A cohort of injury naïve mice (n=15) were included as uninjured controls and did not receive any pharmaceutical intervention. Uninjured mice were statistically compared to VML untreated to validate the injury model compared to previous studies in terms of muscle mass, strength, and metabolic function. Administration of pharmacological adjuvants for the experimental VML groups started 24-hours post-injury and continued to two months. FOR was incorporated directly into normal mouse chow (TestDiet, Richmond, IA; 0.3 mg/kg/day) and animals were allowed to feed ad libitum. FOR-treated mice were individually housed and allowed access to a running wheel for 2 months (HR+FOR) or given 1 month of rest and one month of wheel access (LR+FOR). At the study endpoint, muscle mass, muscle strength, and metabolic function were assessed.

### Biomaterial Intervention

VML-injured mice underwent unilateral VML injury and then were randomized into one of the following experimental groups: Blank biomaterial (n=8) or FOR-loaded biomaterial (n=9). Administration of biomaterial carrier consisted of a single dose injection of Blank (PEG-DA) or FOR-loaded (0.54 mg FOR + PEG-DA) gel particulate started one month following VML injury and monitored for an additional month. At the study endpoint (two months), muscle mass, muscle strength, and metabolic function were assessed.

### *Surgical creation of VML injury:*

A dose of Buprenorphine (1.2 mg/kg) was given pre-operatively. A VML injury was performed unilaterally on the posterior compartment of anesthetized (isoflurane 1.5-2.0%) mice as previously described (Greising et al., 2018; William M. Southern et al., 2019). Briefly, left hindlimbs were prepared by removing hair and the skin was aseptically prepared. An incision was made in the posterior of the limb to expose the muscle. Fascia and hamstrings were separated from the gastrocnemius muscle through blunt dissection. A small metal plate was inserted behind the gastrocnemius and soleus muscles and a 4-mm biopsy punch was used to remove a  $28.4 \pm 1.6$  mg portion. Skin was re-approximated using 5-0 vicryl sutures. Buprenorphine (1.2 mg/kg) was given at 12 and 24 hours and Meloxicam (2.0 mg/kg) was given at 24-, 48-, and 72-hours post-procedure.

### *Voluntary wheel running:*

FOR-treated mice were housed individually and given free access to a running wheel (Columbus Instruments, Columbus, Ohio) for either 2 months or 1 month after 1 month of rest. Sedentary VML mice were housed in a standard mouse cage without access to a running wheel. Daily running

totals were calculated from wheel revolutions collected at 5 min intervals and are presented as a daily average of distance ran.

*PEG-DA synthesis:*

3.4 kDa poly(ethylene glycol) (PEG) was functionalized, as previously described. Briefly, 3.4 kDa PEG was dissolved in distilled methylene chloride (DCM) in a three-neck round-bottom flask and stirred under nitrogen flow. Triethylamine in DCM was added to the PEG at a 1:1 ratio. Subsequently, a 100% molar excess of acryloyl chloride (AcCl) in 15-20 mL of DCM was added dropwise and then closed and kept under nitrogen overnight. Potassium carbonate ( $K_2CO_3$ ) was added to the solution to remove trimethylamine hydrochloride by-product and allowed to separate into organic and aqueous phases. After separation of the organic phase, the PEG-DA was precipitated using cold diethyl ether and dried overnight at RT. A sample of dried PEG-DA was diluted in deuterated water ( $D_2O$ ) and analyzed using proton nuclear magnetic resonance for the presence of acrylate peaks around 5.8-6.4 ppm. The finished product was stored at -20 °C until use.

*Biomaterial fabrication:*

PEG-DA was combined at a 10 wt% total solution ratio with sterile phosphate buffered saline (PBS), thermal initiators ammonium persulfate (APS, 0.018M) and N,N,N',N'-tetramethylethane-1,2-diamine (TEMED, 0.018M) and bovine serum albumin (BSA) equivalent to 20 wt% of the solution. The solution was pulled up into a 1 mL syringe and allowed to gel at 37 °C. Following crosslinking, the mixture was pushed through a 40  $\mu$ m filter into a microcentrifuge with sterile PBS. This process was repeated three more times before being passively filtered to remove gel

pieces smaller than 40  $\mu\text{m}$ . Particulate was imaged at 20x magnification and sized using FIJI software.

*FOR-loading and in vitro release:*

Approximately 500  $\mu\text{L}$  of filtered and sized gel particulate were centrifuged, and all excess PBS was aspirated. FOR (5.7 mg/mL) was dissolved in sterile PBS containing 5% dimethyl sulfoxide (DMSO), to aid dissolution. Lost volume was replaced with 5% DMSO PBS with or without FOR and vortexed to ensure thorough mixing. Particulate was allowed to load overnight at 4  $^{\circ}\text{C}$ . After loading, each tube was filled with 500  $\mu\text{L}$  of PBS and incubated at 37  $^{\circ}\text{C}$  for the release study. PBS was exchanged at appropriate timepoints and stored at -20  $^{\circ}\text{C}$  for subsequent analysis.

*In vitro* release of FOR was analyzed using methyl orange, as described previously. Briefly, release samples were adjusted to pH4 and mixed with equal parts methanol and methyl orange dye. FOR was extracted with chloroform, vortexed for 1 min, and 3000 rpm for 2 min. The absorbance of the organic layer was measured at 428 nm against a reagent blank.

*Biomaterial delivery:*

VML-injured mice were allowed to recover naturally for 30 days before being randomly divided into the blank or FOR-loaded biomaterials group. Animals were anesthetized under isoflurane (1.5-2%), hair was removed, and skin was aseptically prepared for biomaterial injection. 100  $\mu\text{L}$  of biomaterial was injected into the muscle fascia of the affected limb with a 25G needle.

### *In vivo muscle strength:*

Peak-isometric torque of the left hindlimb plantarflexor muscles (soleus/gastrocnemius/plantaris muscles) was assessed *in vivo* as previously described (Baltgalvis et al., 2012; Call & Lowe, 2016). Briefly, mice were anaesthetized using 1.5-3.0% isoflurane at an oxygen flowrate of 0.4L/min. The left hindlimb was depilated and aseptically prepared before the peroneal nerve was severed. The foot was placed in a custom footplate attached to a servomotor (Model 300C-LR; Aurora Scientific, Aurora, Ontario, Canada), and platinum-iridium needle electrodes (Model E2-12; Grass Technologies, West Warwick, RI) were placed percutaneously on either side of the sciatic nerve to elicit isolated contraction of the hindlimb plantarflexors. Peak-isometric torque was measured at stable body temperature (37°C) with the ankle joint maintained at 90° by a magnetic stabilizer clamp on the knee. Peak-isometric torque was defined as the greatest torque measured during a 250-ms stimulation using 1-ms square-wave pulses at a frequency ranging from 150 to 200 Hz. Stimulation parameters were optimized between 0.6 and 3.0 mA (Model 701C; Aurora Scientific) and were determined by 0.1 mA step increases until an increase in amperage resulted in no further increase in torque produced. Fatigability of the plantarflexors was assessed with 90 submaximal contractions performed over 3 minutes using 250-ms stimulations at 60 Hz stimulation frequency. Following functional measurements, mice were euthanized via CO<sub>2</sub> inhalation and cervical dislocation, and hindlimb muscles were processed for additional analyses.

### *Mitochondrial Oxygen Consumption*

Mitochondrial metabolic function was measured using the phosphocreatine creatine kinase clamp technique as described by Fisher-Wellman et al. All experiments were carried out at 30°C in a 2 mL reaction volume. Buffer for all assays was Buffer Z supplemented with ATP (5 mM), creatine

(5 mM), phosphocreatine (PCr, 1 mM) and creatine kinase (20U/mL). For each experiment, permeabilized skeletal muscle fiber bundles (2 mg) from the gastrocnemius muscles were energized with glutamate (10mM), malate (2.5 mM) and succinate (10mM). Following substrate addition, titrations of PCr (1, 2, 4, 7, 16, and 31 mM) were performed to reduce oxygen consumption back to baseline.  $G'_{ATP}$  was calculated for each PCr titration and plotted against  $JO_2$  for each step. The resulting slope for each sample ( $\Delta G_{ATP}$  vs  $JO_2$ ) represents electron conductance through the electron transport chain.

#### *Mitochondrial Membrane Potential*

Fluorescent determination of mitochondrial membrane potential ( $\Delta\psi_m$ ) was performed at 30 °C in 0.2 mL of assay buffer using a Horiba Spectrofluorometer (FluoroMax Plus-C; Horiba Instruments Inc., Atlanta, GE, USA) as previously described. The  $\Delta\psi_m$  was determined via tetramethylrhodamine, methyl ester (TMRM) by taking the fluorescence ratio of the excitation/emission parameters: excitation/emission (572/590 nm)/(551/590 nm). Permeabilized muscle fiber were weighed (1~1.5 mg) and placed into cuvettes containing assay buffer supplemented with ATP (5mM), CK (200U/mL), and creatine (20mM). Following a 2-minute temperature equilibration, substrates were added to fuel the mitochondria (10mM glutamate, 1 mM Malate, 10 mM Succinate). Sequential PCr titrations were made to final concentrations of 1, 2, 4, 8, 16, 32, 64 mM that matched the mitochondrial respiration control approach. Following the PCr titrations, 1  $\mu$ M FCCP was used to assess maximum fluorescence.

### *Citrate synthase activity*

Mitochondrial content was analyzed by citrate synthase enzyme (CS) activity as previously described (William M. Southern et al., 2019). Briefly, following muscle fiber collection for oxygen consumption experiments, the remainder of the gastrocnemius muscle was chopped into fine pieces and mixed. Approximately 40 mg of muscle was weighed and further homogenized in 33mM phosphate buffer (pH 7.4) at a muscle to buffer ratio of 1:40 using a glass tissue grinder. Homogenate was incubated with 5,5'-dithio-bis(2-nitrobenzoic acid (DTNB, 0.773mM), acetyl CoA (0.116mM), and oxaloacetate (0.441mM) in 100mM Tris buffer (pH 8.0). Activity of citrate synthase was monitored from the reduction of DTNB over time via measurement of absorbance at 412nm.

### *Assessment of mitochondrial respiratory complex activity*

Activity for each mitochondrial respiratory complex was measured using a protocol modified from Thome, et al (Thome et al., 2019). Complex I activity was measured in 50mM potassium phosphate buffer, 3mg/mL BSA, 240  $\mu$ M KCN, 0.4  $\mu$ M antimycin A, 50  $\mu$ M decyl-ubiquinone, and 80  $\mu$ M 2,6-dichlorophenolindophenol (DCPIP). NADH oxidation was measured through the reduction of DCPIP at 600 nm. Complex II activity was measured in buffer containing 10 mM  $\text{KH}_2\text{PO}_4$ , 2 mM EDTA, and 1 mg/mL BSA at pH 7.8 and supplemented with 0.2 mM ATP, 10 mM succinate, and 0.08 mM DCPIP. Following a 10-minute incubation, at 37°C, the assay was initiated by the addition of oxidized decyl-ubiquinone (0.08 mM) and reduction of DCPIP followed at 600 nm.

### *Histological Analysis*

Whole gastrocnemius muscles were collected from VML, FOR, and FOR+LWR experimental groups and cryopreserved in OCT. Muscle was cut in 5  $\mu\text{m}$  sections across the entirety of the muscle in sequential slices and mounted on slides. Sequential sections were stained using hematoxylin and eosin as a morphological stain, and for succinate dehydrogenase and nicotinamide adenine dinucleotide oxidation activity.

## **Results**

### *In vitro analysis of biomaterial scaffold*

Following creation of the poly(ethylene glycol) diacrylate (PEG-DA) and bovine serum gel particulate, the batches were imaged and measured using ImageJ to account for batch-to-batch variability (Supplemental Figure 4.1). Gel batches were centrifuged, and the supernatant removed to allow for partial drying on the material inside the clean hood. Sterile PBS-DMSO was used to dissolve FOR in a minimal volume which was used to load the biomaterial overnight. Gels were resuspended in sterile 1% BSA-PBS for an *in vitro* release. Medium was collected every other day for one month and stored in  $-20\text{ }^{\circ}\text{C}$  until analysis. The non-degradable gels released  $\sim 30\%$  of the total FOR load across 30 days (Supplemental Figure 4.2).

### *Effects of treatment on gross anatomy of VML-injured muscles*

Treatment of VML-injured mice with FOR, rehabilitation or biomaterial carrier did not significantly affect animal body mass, though body mass for LWR and BIO+FOR was trending compared to untreated VML controls (Table 4.1, Dunnett's  $p=0.0683$ ). Then, we determined the effect of our treatment strategies on the mass of the gastrocnemius muscle. Gastrocnemius muscle

mass in LWR+FOR, BIO, and BIO+FOR groups was significantly larger compared to uninjured VML mice (Table 4.1, Dunnett's  $p=0.0014$ ). When normalizing that muscle mass to total body mass, all experimental groups had larger muscle to body mass ratios compared to untreated VML (Table 4.1, Dunnett's  $p=0.0033$ ).

**Table 4.1:** Mouse body mass and gastrocnemius muscle mass

	<b>Experimental Group</b>					<b>OWA p-value</b>
	VML	EWR+FOR	LWR+FOR	BIO	BIO+FOR	
Body Mass (g)	29.7±2.1	30.5±0.5	31.5±2.1	31.2±1.6	31.4±1.1	0.0721
Gastrocnemius Mass (mg)	120.5±15.4	145.2±10.6	165.3±23.5 <sup>#</sup>	210.0±48.9 <sup>#</sup>	198.9±30.1 <sup>#</sup>	<0.0001
Gastroc: BM	4.1±0.4	4.8±0.4 <sup>#</sup>	5.2±0.5 <sup>#</sup>	6.7±1.2 <sup>#</sup>	6.3±0.9 <sup>#</sup>	<0.0001

Values are means ± SD

<sup>#</sup>Different from VML

### *Strength and contractile properties following intervention*

Increase in gastrocnemius muscle mass did not correlate in improvement of peak isometric torque production across all treatments. LWR+FOR was trending towards improved torque normalized by body mass compared to untreated VML (Figure 4.1A, Dunnett's  $p=0.0547$ ). When normalized to gastrocnemius muscle mass, no group showed improvement over untreated VML mice. Both experimental biomaterial groups had lower peak isometric torque normalized to body mass compared to untreated VML (Figure 4.1B, Dunnett's  $p=0.0095$ ).

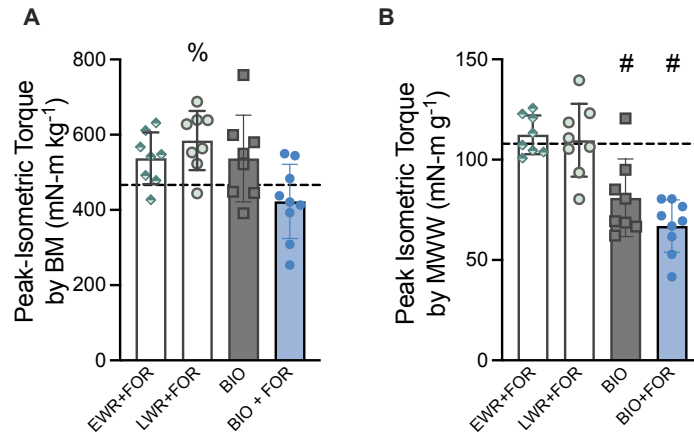


**Figure 4.1:** Effect of regenerative rehabilitation strategies on the contractile function of VML-injured limbs. **A.** Peak-isometric torque normalized to kilograms of body mass was trending higher in late intervention rehab mice compared to untreated VML mice (dashed line). **B.** However, when peak isometric force is normalized to milligrams of gastrocnemius muscle mass, there is no significant difference between treated and untreated VML mice (dashed line). Data analyzed by one-way ANOVA, # denotes differences compared to untreated VML. % denotes trend compared to untreated VML. Data are means  $\pm$  SD.

When evaluating the contractile properties of the experimental groups, there were no differences in rate of contraction between treatment groups and untreated controls, but rate of relaxation was significantly higher (~23%) in LWR+FOR treatment mice compared to untreated controls in the rate of relaxation (Table 4.2, Dunnett's  $p=0.0321$ ). Submaximal peak contractions at 60 Hz were significantly higher in both biomaterial interventions compared to untreated controls (Table 4.2, Dunnett's  $p=0.0182$ ).

**Table 4.2.** Contractile Properties

	Experimental Group					OWA p-value
	VML	HR+FOR	LR+FOR	BIO	BIO+FOR	
Avg +dP/dt (mN-m/s)	594.5 $\pm$ 114.7	600.3 $\pm$ 95.23	660.9 $\pm$ 97.2	586.6 $\pm$ 101.4	555.9 $\pm$ 111.1	0.3770
Avg -dP/dt (mN-m/s)	530.7 $\pm$ 65.5	568.2 $\pm$ 68.2	690.2 $\pm$ 120.4 <sup>#</sup>	513.2 $\pm$ 240.2	546.0 $\pm$ 148.5	0.0690
½ RT (s)	0.042 $\pm$ 0.004	0.047 $\pm$ 0.007	0.044 $\pm$ 0.006	0.0460 $\pm$ 0.005	0.046 $\pm$ 0.008	0.5447
40 Hz/Peak	0.28 $\pm$ 0.13	0.34 $\pm$ 0.08	0.31 $\pm$ 0.11	0.38 $\pm$ 0.14	0.27 $\pm$ 0.12	0.3300
60 Hz/Peak	0.40 $\pm$ 0.19	0.47 $\pm$ 0.13	0.41 $\pm$ 0.23	0.67 $\pm$ 0.14 <sup>#</sup>	0.61 $\pm$ 0.14 <sup>#</sup>	0.0028

Values are means  $\pm$  SD. OWA= One-Way ANOVA

<sup>#</sup>Different from VML

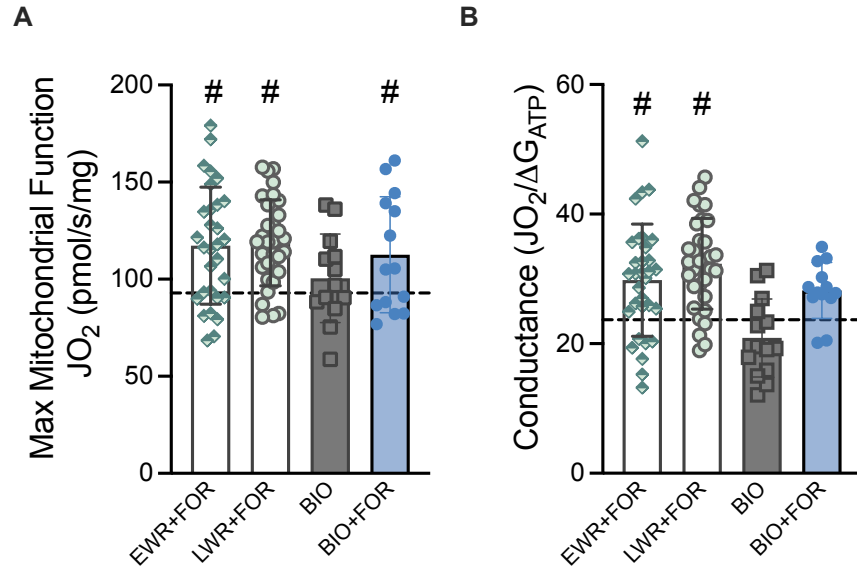


**Figure 4.2:** Effect of regenerative rehabilitation approaches on mitochondrial metabolism. **A.** The combination of formoterol with rehabilitation resulted in the improvement of maximal coupled oxygen consumption independent of rehabilitation intervention. Direct delivery of formoterol with a biomaterial scaffold also improved oxygen consumption compared to untreated VML control. **B.** However, this increase of maximal oxygen consumption only resulted in the subsequent increase in electron conductance in rehabilitation intervention groups. Data shown as means  $\pm$  SD. Analyzed via one-way ANOVA. # denotes difference compared to untreated VML (dashed lines) where  $p < 0.05$ .

#### *Effect of treatment on mitochondrial metabolism*

The combination of FOR and rehab resulted in the significant increase in maximal coupled oxygen consumption (State III), regardless of time of intervention ( $\sim 21\%$ , Figure 4.2A, Dunnett's  $p = 0.0003$ ). The delivery of FOR directly to the site of injury using a biomaterial scaffold similarly increased maximal respiration compared to untreated VML ( $\sim 20\%$ , Figure 4.2A, Dunnett's  $p = 0.0495$ ). Next, we calculated electron conductance across the electron transport chain for each treatment group. Both combinatorial FOR and rehab groups had improved conductance compared to untreated VML ( $\sim 22\%$ , Figure 4.2, Dunnett's  $p = 0.0009$ ). However, the increase in maximal coupled oxygen consumption observed in the BIO+FOR group was not accompanied by a similar increase in electron conductance (Figure 4.2B, Dunnett's  $p = 0.1669$ ).

### *Mitochondrial enzyme activity at Complex I & II*

Mitochondrial content was estimated via citrate synthase activity. Interestingly, late rehab intervention (LWR+FOR) and BIO+FOR prescriptions resulted in significantly decreased mitochondrial content compared to untreated VML (Table 4.3, Dunnett's  $p=0.0418$ ). However, Complex I activity was only increased in EWR+FOR intervention animals (Table 4.3, Dunnett's  $p=0.0236$ ). There was no change in Complex II activity across any of the experimental groups compared to untreated VML controls.

Table 4.3: Mitochondrial Enzyme Activity

Enzymatic Activity ( $\mu\text{mol}/\text{min}/\text{g}$ )	Experimental Group					OWA p-value
	VML	EWR+FOR	LWR+FOR	BIO	BIO+FOR	
Citrate Synthase	429.0 $\pm$ 141.9	494.7 $\pm$ 92.9	356.1 $\pm$ 104.6 <sup>#</sup>	270 $\pm$ 88.4	220.6 $\pm$ 51.76 <sup>#</sup>	0.0004
Complex I	18.3 $\pm$ 5.0	26.3 $\pm$ 3.5 <sup>#</sup>	15.7 $\pm$ 5.2	19.3 $\pm$ 7	21.7 $\pm$ 1.9	0.0215
Complex II	16.7 $\pm$ 10.4	21.5 $\pm$ 10.0	13.69 $\pm$ 9.0	24.1 $\pm$ 6.3	23.8 $\pm$ 7.0	0.1129

Enzymatic activity normalized to citrate synthase activity as a measure of mitochondrial content. Enzymatic activity is represented as micromoles of product generated per minute per gram of protein. Values are means  $\pm$  SD. OWA= One-Way ANOVA

<sup>#</sup>Different from VML

### *Histological analysis of VML-injured muscle after treatment*

To determine whether the changes observed in the LWR+FOR group was due to an increase in fiber number or oxidative activity, whole gastrocnemius muscles were cryoembedded in optimum cutting temperature (OCT) medium and serially sectioned in five distinct regions and stained with hematoxylin and eosin, succinate dehydrogenase and NADH affinity dyes (Figure 4.3A). Overall, there were no discernable differences in fiber number, SDH positive or NADH positive fibers between experimental and untreated control groups (Figure 4.3B-D).

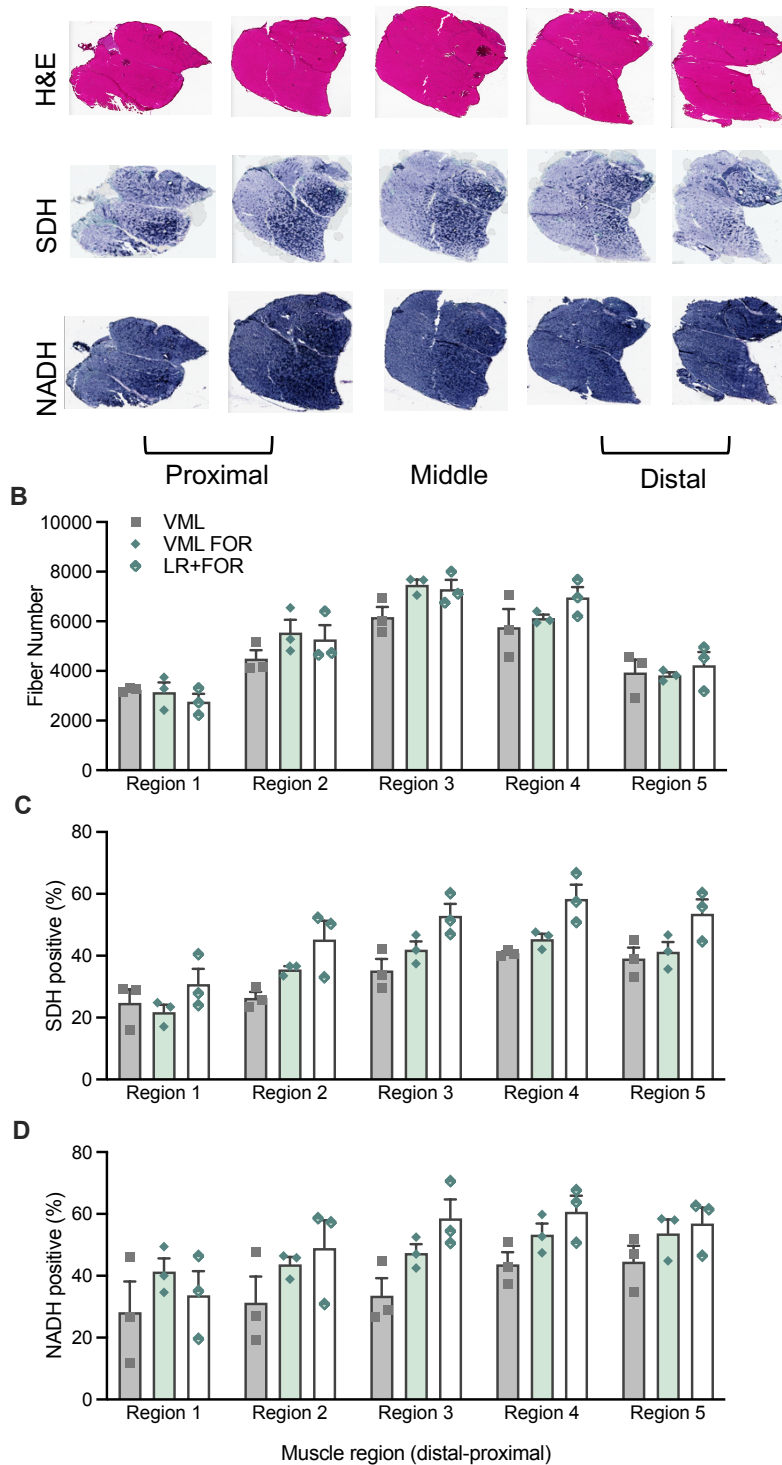


**Figure 4.3:** Histological analysis of best-faring regenerative rehabilitation treatment. A. Representative sections of H&E, SDH and NADH activity staining of VML injured muscle. B. Fiber number analysis was conducted on each region of the muscle for each selected treatment group. There were no detectable differences in fiber number between groups. Similarly, there was no significant difference in B. SDH activity or C. NADH concentration across treatment groups. Data represented as means  $\pm$  SD. Analyzed via one-way ANOVA.

## Discussion

The biggest problem facing VML injury patients is the lack of treatment options that address the soft tissue damage. This lack of options guarantees a loss of contractile and metabolic function that cannot be rescued when the patient is ready to undergo traditional physical therapy. This treatment desert is due in part to the emphasis of *de novo* tissue regeneration rather than the optimization of the remaining tissue. There exists a need for therapeutics that can be administered early after injury and could potentially prime the affected tissue and improve plasticity so that it may be able to receive the benefits of rehabilitation, be it in the form of voluntary exercise, stretching, or electrostimulation. Moreover, there needs to be an effort to improve the performance of therapeutics that have already shown moderate success in the treatment of VML injuries. To address this gap, we used a combination of rehabilitation and regenerative medicine approaches in conjunction with the drug formoterol, which had previously been shown to partially rescue contractile and metabolic function after VML(McFaline-Figueroa et al., 2022).

Voluntary wheel running was chosen as a rehabilitation technique because previous studies have found that improves mitochondrial metabolic function and recruitment of muscle satellite cells compared to sedentary animals after VML (William M Southern et al., 2019; Washington et al., 2021). This rehabilitation method has also been successfully used in other muscle pathologies to improve the outcomes of regenerative therapies, such as in murine models of muscular dystrophy(Call et al., 2008; Hamm et al., 2021). Importantly, voluntary wheel running also speaks directly to patient willingness to engage in exercise after injury. Mice in the study had unlimited access to their running wheels either 3 days (EWR+FOR) or 1 month (LWR+FOR) post-injury while receiving a constant dose of FOR in their food and we able to increase or decrease their exercise load depending on their comfort.

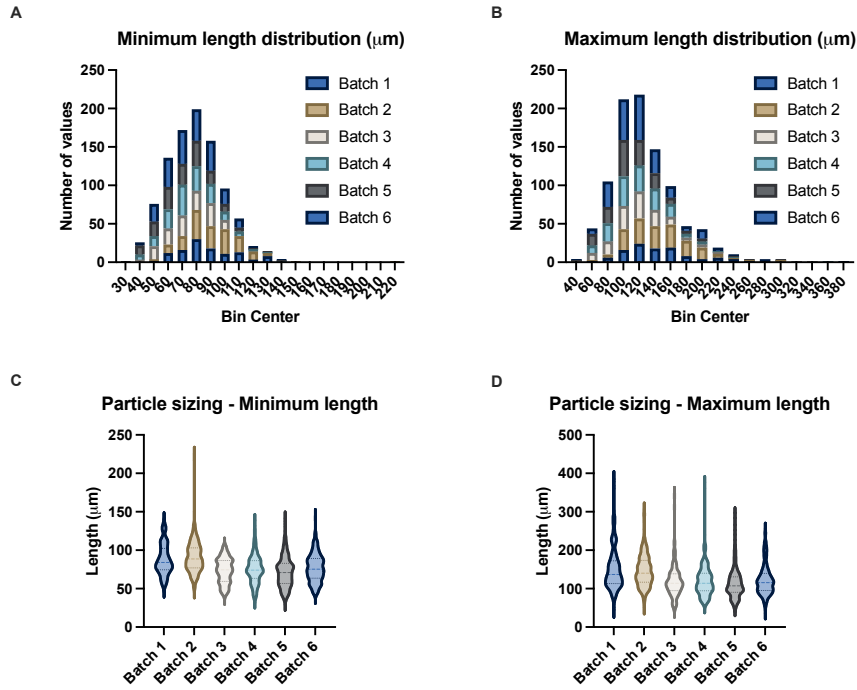
Exercise is a known activator of the PGC-1 $\alpha$  pathway and induces mitochondrial biogenesis, which can, in turn, improve muscle function (Petrie et al., 2020; William M Southern et al., 2019). We hoped that the combination of exercise with a drug with proven potential to improve contractile and metabolic function after VML injury would provide the best possible environment for muscle recover. Interestingly, contrary to our hypothesis, our results suggest that a period of rest prior to exposure to exercise rather than continued exercise immediately after injury onset offers best possible combination of contractile and metabolic function rescue. It is possible that FOR treatment requires rest to provide the benefits of muscle hypertrophy and increased mitochondrial metabolism while the muscle heals before the muscle can be strengthened.

Alternatively, we wanted to determine whether the presentation of FOR would significantly alter the drug's effects. To answer this question, we created a synthetic polymer scaffold capable of sequestering FOR to the internal meshwork and releasing the drug by diffusion over the course of a month. One caveat to consider with this formulation is that the polymer was created using a non-degradable formulation, therefore the bulk of the material would remain in the injury defect after injection. While the inclusion of a non-tissue construct within the injury defect might pose a problem in other circumstances, the size of the gel particulate was small enough that they were able to shift as they were injected into the muscle fascia rather than being a solid mass. However, we have demonstrated that the injection of biomaterial into the injury defect, whether it be blank or loaded with FOR, did not significantly increase limb stiffness (Supplementary Figure 4.4, Dunnett's  $p=0.2090$ ). Further studies should be done to elucidate the reason behind the improvement of maximal coupled respiration (Figure 4.2A) but not in electron conductance (Figure 4.2B) compared to untreated VML controls. Nonetheless, as a preliminary foray into the use of biomaterial scaffolds combined with functional assessments, we can conclude that the direct

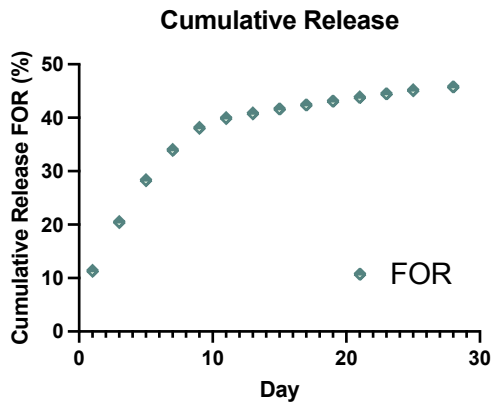
delivery of FOR into the void after VML injury could be a promising strategy when used as an early intervention with the caveat that a degradable formulation should be used to accomplish full delivery of the payload.

The improvements in functional capacity following FOR administration combined with different regenerative and rehabilitative techniques hold promise that the muscle remaining after VML injury can be stimulated to yield improvement over nontreatment. Our data suggests that FOR treatment coupled with a period of rest and voluntary exercise leads to the improvement of contractile and mitochondrial function, possibly due to muscle hypertrophy, as demonstrated by an increase in muscle mass, and increased mitochondrial content. Further studies should be focused on the development of degradable biomaterial formulations that could allow for the immediate administration of FOR, post-injury with no risk of adverse immune effects. In conclusion, this work provides a solid basis for the creation of a multi-approach therapy for VML injuries with FOR at the center of the treatment program.

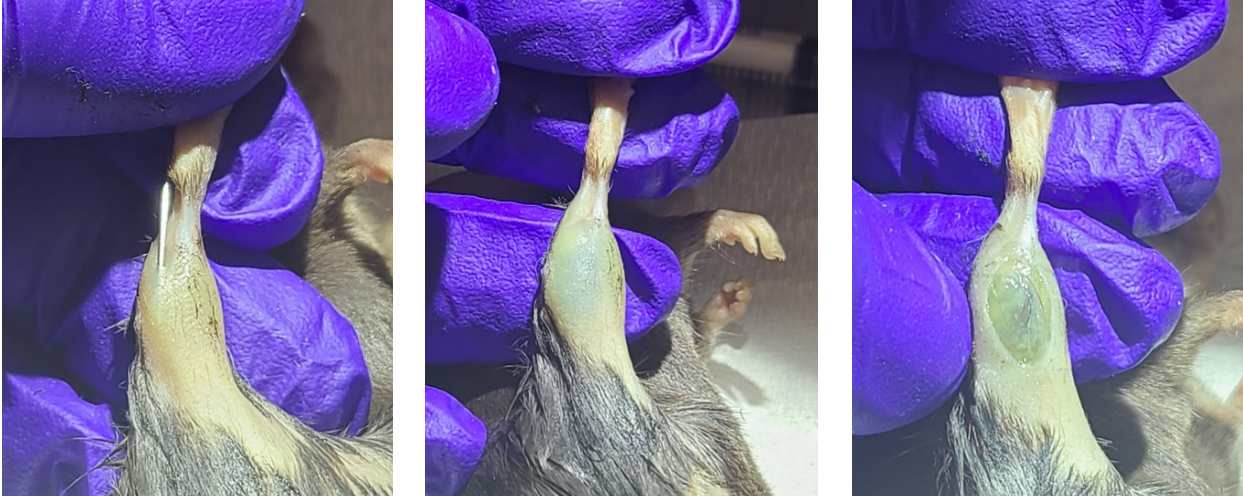
## Supplemental Materials



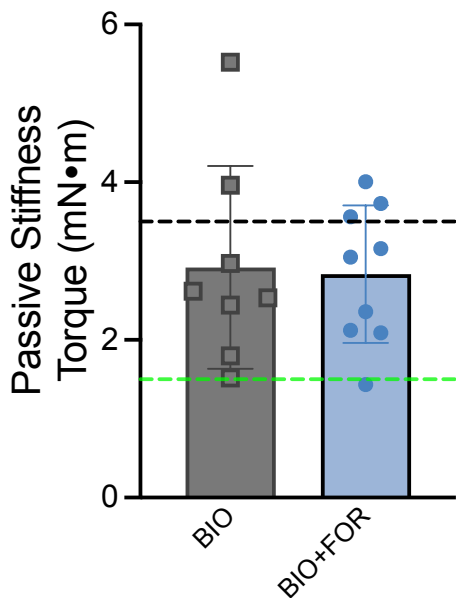
**Supplemental Figure 4.1:** Sizing distribution for gel particulates. The protocol used to create gel particulates yielded similar minimum and maximum lengths, indicating there was high batch-to-batch reproducibility.



**Supplemental Figure 4.2:** Cumulative release of FOR from non-degradable PEG-DA-BSA over 30 days. Non-degradable gels allowed for the detectable release of  $\sim 45\%$  of FOR *in vitro*.



**Supplemental Figure 4.3:** Injection protocol for biomaterial. To maintain reproducibility, all injections were done in the same area on each animal. Briefly, the needle was aligned with the Achilles tendon and inserted under the skin. Then, the needle was overdirected toward the skin and pressed toward the muscle mid-belly. Blank and FOR-loaded biomaterials were injected into the affected limb in 100  $\mu\text{L}$  doses under general anesthesia. Upon needle removal, the animal was maintained under anesthesia for two minutes to allow the material to settle.



**Supplemental Figure 4.4:** Passive stiffness of limbs injected with biomaterial. Injection of PEG-DA-BSA gel particulate (40-120  $\mu\text{m}$  size) into the lower hindlimb fascia, adjacent to the gastrocnemius muscle after VML injury does not cause significant increase in passive limb stiffness compared to untreated VML (black dashed line) or uninjured limbs (green dashed line). Data shown as means  $\pm$  SD. Analyzed via one-way ANOVA.

## References

- Baltgalvis, K. A., Call, J. A., Cochrane, G. D., et al. (2012). Exercise training improves plantar flexor muscle function in mdx mice. *Med Sci Sports Exerc*, 44(9), 1671-1679. <https://doi.org/10.1249/MSS.0b013e31825703f0>
- Call, J. A., & Lowe, D. A. (2016). Eccentric Contraction-Induced Muscle Injury: Reproducible, Quantitative, Physiological Models to Impair Skeletal Muscle's Capacity to Generate Force. *Methods Mol Biol*, 1460, 3-18. [https://doi.org/10.1007/978-1-4939-3810-0\\_1](https://doi.org/10.1007/978-1-4939-3810-0_1)
- Call, J. A., Voelker, K. A., Wolff, A. V., et al. (2008). Endurance capacity in maturing mdx mice is markedly enhanced by combined voluntary wheel running and green tea extract. *Journal of Applied Physiology*, 105(3), 923-932. <https://doi.org/10.1152/jappphysiol.00028.2008>
- Chao, T., Burmeister, D. M., Corona, B. T., & Greising, S. M. (2019). Oxidative pathophysiology following volumetric muscle loss injury in a porcine model. *J Appl Physiol (1985)*, 126(6), 1541-1549. <https://doi.org/10.1152/jappphysiol.00026.2019>
- Chen, X. K., & Walters, T. J. (2013). Muscle-derived decellularised extracellular matrix improves functional recovery in a rat latissimus dorsi muscle defect model. *J Plast Reconstr Aesthet Surg*, 66(12), 1750-1758. <https://doi.org/10.1016/j.bjps.2013.07.037>
- Corona, B. T., Machingal, M. A., Criswell, T., et al. (2012). Further development of a tissue engineered muscle repair construct in vitro for enhanced functional recovery following implantation in vivo in a murine model of volumetric muscle loss injury. *Tissue Eng Part A*, 18(11-12), 1213-1228. <https://doi.org/10.1089/ten.TEA.2011.0614>
- Corona, B. T., Rivera, J. C., Owens, J. G., et al. (2015). Volumetric muscle loss leads to permanent disability following extremity trauma. *Journal of Rehabilitation Research & Development*, 52(7).
- Corona, B. T., Ward, C. L., Baker, H. B., et al. (2014). Implantation of in vitro tissue engineered muscle repair constructs and bladder acellular matrices partially restore in vivo skeletal muscle function in a rat model of volumetric muscle loss injury. *Tissue Eng Part A*, 20(3-4), 705-715. <https://doi.org/10.1089/ten.TEA.2012.0761>
- Corona, B. T., Wenke, J. C., & Ward, C. L. (2016). Pathophysiology of volumetric muscle loss injury. *Cells Tissues Organs*, 202(3-4), 180-188.
- Dalske, K. A., Raymond-Pope, C. J., McFaline-Figueroa, J., et al. (2021). Independent of physical activity, volumetric muscle loss injury in a murine model impairs whole-body metabolism. *PloS one*, 16(6), e0253629. <https://doi.org/10.1371/journal.pone.0253629>
- Garg, K., Ward, C. L., Hurtgen, B. J., et al. (2015). Volumetric muscle loss: persistent functional deficits beyond frank loss of tissue. *Journal of Orthopaedic Research*, 33(1), 40-46.
- Goldman, S. M., Henderson, B. E. P., Walters, T. J., & Corona, B. T. (2018). Co-delivery of a laminin-111 supplemented hyaluronic acid based hydrogel with minced muscle graft in the treatment of volumetric muscle loss injury. *PloS one*, 13(1), e0191245. <https://doi.org/10.1371/journal.pone.0191245>
- Greising, S. M., Corona, B. T., McGann, C., et al. (2019). Therapeutic Approaches for Volumetric Muscle Loss Injury: A Systematic Review and Meta-Analysis. *Tissue Engineering Part B: Reviews*, 25(6), 510-525. <https://doi.org/10.1089/ten.teb.2019.0207>
- Greising, S. M., Rivera, J. C., Goldman, S. M., et al. (2017). Unwavering pathobiology of volumetric muscle loss injury. *Scientific reports*, 7(1), 1-14.

- Greising, S. M., Warren, G. L., Southern, W. M., et al. (2018). Early rehabilitation for volumetric muscle loss injury augments endogenous regenerative aspects of muscle strength and oxidative capacity. *BMC musculoskeletal disorders*, 19(1), 173-173. <https://doi.org/10.1186/s12891-018-2095-6>
- Grogan, B. F., & Hsu, J. R. (2011). Volumetric muscle loss. *J Am Acad Orthop Surg*, 19 Suppl 1, S35-37. <https://doi.org/10.5435/00124635-201102001-00007>
- Hamm, S. E., Fathalikhani, D. D., Bukovec, K. E., et al. (2021). Voluntary wheel running complements microdystrophin gene therapy to improve muscle function in mdx mice. *Mol Ther Methods Clin Dev*, 21, 144-160. <https://doi.org/10.1016/j.omtm.2021.02.024>
- McFaline-Figueroa, J., Schifino, A. G., Nichenko, A. S., et al. (2022). Pharmaceutical agents for contractile-metabolic dysfunction after volumetric muscle loss. *Tissue Engineering Part A*, 28(17-18), 795-806.
- Petrie, M. A., Sharma, A., Taylor, E. B., et al. (2020). Impact of short- and long-term electrically induced muscle exercise on gene signaling pathways, gene expression, and PGC1 $\alpha$  methylation in men with spinal cord injury. *Physiol Genomics*, 52(2), 71-80. <https://doi.org/10.1152/physiolgenomics.00064.2019>
- Rivera, J. C., & Corona, B. T. (2016). Muscle-related Disability Following Combat Injury Increases With Time. *US Army Med Dep J*, 30-34.
- Southern, W. M., Nichenko, A. S., Tehrani, K. F., et al. (2019). PGC-1 $\alpha$  overexpression partially rescues impaired oxidative and contractile pathophysiology following volumetric muscle loss injury. *Scientific reports*, 9(1), 1-17.
- Southern, W. M., Nichenko, A. S., Tehrani, K. F., et al. (2019). PGC-1 $\alpha$  overexpression partially rescues impaired oxidative and contractile pathophysiology following volumetric muscle loss injury. *Scientific reports*, 9(1), 4079-4079. <https://doi.org/10.1038/s41598-019-40606-6>
- Thome, T., Salyers, Z. R., Kumar, R. A., et al. (2019). Uremic metabolites impair skeletal muscle mitochondrial energetics through disruption of the electron transport system and matrix dehydrogenase activity. *Am J Physiol Cell Physiol*, 317(4), C701-C713. <https://doi.org/10.1152/ajpcell.00098.2019>
- Washington, T. A., Perry, R. A., Jr., Kim, J. T., et al. (2021). The effect of autologous repair and voluntary wheel running on force recovery in a rat model of volumetric muscle loss. *Exp Physiol*, 106(4), 994-1004. <https://doi.org/10.1113/ep089207>

## CHAPTER 5

### DISCUSSION AND CONCLUSIONS

The primary goal of my dissertation was to better understand the myriad of contractile and metabolic changes that compose the pathophysiology of volumetric muscle loss in the hopes that this knowledge can inform the development of future therapies. With this goal in mind, my first study characterized the metabolic changes occurring in acute VML injury and how these early changes fed into the characteristic long-term dysfunction. My second study tested whether four FDA-approved drugs that have been successful in other muscle disease models would be able to rescue muscle function following VML injury. My final study was focused on attempting to amplify the effects of formoterol, a drug which offered a partial rescue of contractile and metabolic function after VML injury. The results from these studies helped bridge the knowledge gap concerning the progression of VML pathophysiology and offered several platforms for functional evaluations of potential therapeutic candidates for its treatment. The following is a summary of the questions and main problems and how my research addressed them.

#### **Metabolic inflexibility in VML starts early after injury**

Volumetric muscle loss injuries are characterized by the dampening of mitochondrial metabolism compared to normal, healthy tissue. This metabolic dysfunction is persistent and worsens over time to the point that it affects whole-body metabolism independent of activity (Dalske et al., 2021). However, it is unclear whether this metabolic dysfunction is a direct result of injury or whether there is a systematic breakdown of metabolic processes. To address this question, my first study evaluated the rate of carbohydrate and lipid oxidation early after VML injury up to two weeks

post-injury. Carbohydrate-driven metabolism was significantly affected across timepoints in VML-injured tissue despite there being no difference in lipid-driven metabolism (Figure 2.1). Enzyme activity related to carbohydrate and lipid oxidation prior to oxidative phosphorylation was similarly affected. With the current data it is difficult to conclude whether this change triggers further metabolic deficiency until the pathology reaches whole-body metabolism or if the effect magnifies over time. Still, this addition to the current body of knowledge helps define the severity of VML injury and reinforces the need to early intervention strategies.

### **Calcium ion overload plays a role in VML pathology**

$\text{Ca}^{2+}$  is a ubiquitous signaling molecule within the cell that is tightly regulated through a series of protein chelators, storage within the endoplasmic reticulum, and the mitochondria and with highly monitored channels for its movement. The concentration of  $\text{Ca}^{2+}$  within the cell is several orders of magnitude lower than in the extracellular environment. During VML injury, the internal environment of the cell is exposed to the high concentration of  $\text{Ca}^{2+}$  in the extracellular fluid until the muscle fiber can re-seal. As part of my first study, I delved into the fluctuations of intracellular  $\text{Ca}^{2+}$  concentration shortly following VML injury. VML injured has increased intracellular  $\text{Ca}^{2+}$  that persists for at least a full day after injury (Figure 2.2). Moreover, I was able to recapitulate the metabolic dysfunction seen in early VML injury with an *in vitro* model of  $\text{Ca}^{2+}$  overload (Figure 2.3). Considering the enzyme pyruvate dehydrogenase, an important part of carbohydrate oxidation, is calcium-sensitive and can be regulated by mitochondrial calcium (Gherardi et al., 2019; Lander et al., 2018; Scrima et al., 2020; Zhang et al., 2021), this  $\text{Ca}^{2+}$  overload explains the difference in carbohydrate but not lipid metabolism observed in this study. This study helps clarify the onset of metabolic dysfunction in VML-injured tissue and offers an interesting target for therapeutic development.

### **Formoterol improves contractile-metabolic function after VML injury**

Formoterol is a  $\beta_2$ -adrenergic receptor agonist commonly used as a bronchodilator but with previous history of preventing muscle wasting in models of muscular dystrophy and cancer cachexia. During my second study, I evaluated the effectiveness of four FDA-approved drugs at treating the contractile and metabolic dysfunction associated with VML. Though all the drugs selected had history of improving muscle function in other disease models and could theoretically improve muscle function via the indirect stimulation of PGC-1 $\alpha$ , only formoterol offered any improvement over non-treatment. Overall, the cellular environment after VML is a complicated combination of cytokine dysregulation, inflammation, and loss of contractile units all which contribute to muscle degeneration. The success of only one drug candidate in this study speaks to the difficulty in managing the deterioration of muscle function after VML and the importance of functional testing to determine the effectiveness of a potential therapy rather than qualitative evaluation or recovered tissue volume analysis.

### **Future directions**

There are several directions where research can touch upon next based on the results of these studies. First, metabolic function and flexibility should be evaluated at more timepoints to create a more complete profile of the development of VML pathophysiology. With more data, it could be possible to identify a critical window for intervention that might improve functional rescue after VML. Additional analyses, such as the profiling of active proteases and their interaction with muscle satellite cells across these early timepoints may also offer valuable information for creating therapies.

Skeletal muscle injuries also differ in magnitude and functional outcomes between sexes. The studies shown above were all done in male C57BL/6 mice. It is possible that there are

differences in the effectiveness of our chosen drug candidates between male and females or that a combination of treatments may be necessary to truly affect disease outcome. A truly comprehensive study would include male and female mice of both young and old ages at onset of injury. Injury recovery is one of the processes affected with age, therefore testing these therapies on aging or aged cohorts would offer the most comprehensive understanding of their effect on VML injury.

Lastly, the development of formoterol as a treatment for VML injury should be further explored. In my third study, I combined formoterol administration with rehabilitation and alternative regenerative approaches in an attempt to amplify its effect on VML-injured muscle. The results, though significantly different than untreated VML tissue are still nowhere near the levels of meaningful recovery that would motivate a patient to seek intervention. Therefore, testing different rehabilitation methods and delivery systems to find the best combination of regenerative rehabilitation approach may go a long way in the future of the clinical treatment of VML injury.

## **Conclusion**

In closing, the studies contained herein touched, not only on the physiological exploration of a disease state but on the possible avenues to curtail the devastating long-term effects that typically accompany them. Proper muscle function recovery after injury is paramount for continued homeostasis. Skeletal muscle plays an important role not just in ambulation but in body metabolism, acting as a glucose sink and regulating insulin release. Deficiencies in these processes can lead to the development of comorbidities resulting in an increasingly sickly aging population, decrease in quality of life and financial burden on the healthcare system. Volumetric muscle loss injuries are a devastating ailment, and the healthcare system cannot continue to exist without standardized treatment options to address soft tissue damage after trauma onset. My work has

advanced our understanding of how muscle function is affected after injury and offers many avenues of functional testing to fully evaluate the effectiveness of proposed therapies.

## References

- Dalske, K. A., Raymond-Pope, C. J., McFaline-Figueroa, J., et al. (2021). Independent of physical activity, volumetric muscle loss injury in a murine model impairs whole-body metabolism. *PLoS one*, 16(6), e0253629. <https://doi.org/10.1371/journal.pone.0253629>
- Gherardi, G., Nogara, L., Ciciliot, S., et al. (2019). Loss of mitochondrial calcium uniporter rewires skeletal muscle metabolism and substrate preference. *Cell Death Differ*, 26(2), 362-381. <https://doi.org/10.1038/s41418-018-0191-7>
- Lander, N., Chiurillo, M. A., Bertolini, M. S., et al. (2018). Calcium-sensitive pyruvate dehydrogenase phosphatase is required for energy metabolism, growth, differentiation, and infectivity of *Trypanosoma cruzi*. *J Biol Chem*, 293(45), 17402-17417. <https://doi.org/10.1074/jbc.RA118.004498>
- Scrima, R., Cela, O., Agriesti, F., et al. (2020). Mitochondrial calcium drives clock gene-dependent activation of pyruvate dehydrogenase and of oxidative phosphorylation. *Biochim Biophys Acta Mol Cell Res*, 1867(11), 118815. <https://doi.org/10.1016/j.bbamcr.2020.118815>
- Zhang, J., Zhang, L., Nie, J., et al. (2021). Calcineurin inactivation inhibits pyruvate dehydrogenase complex activity and induces the Warburg effect. *Oncogene*, 40(49), 6692-6702. <https://doi.org/10.1038/s41388-021-02065-0>